

Method Development and Degradation Studies  
to Verify the Stabilization of a Gallium Prodrug of Epinephrine

A Dissertation  
SUBMITTED TO THE FACULTY OF  
UNIVERSITY OF MINNESOTA  
BY

Nicholas M. Livezey

IN PARTIAL FULFILLMENT OF THE REQUIREMENTS  
FOR THE DEGREE OF  
DOCTOR OF PHILOSOPHY

Valérie C. Pierre

September 2021



## Acknowledgements

I would like to thank my advisor, Valérie Pierre, for her constant support and encouragement. She always believed in me even when I did not believe in myself, and for that I will be eternally grateful. I would also like to thank the many incredible scientists in the Pierre Group who has supported me along the way. I am incredibly thankful to Sarah Harris, Sylvie Pailloux, and Heather Brown, who all played a huge role in training me in the lab and helping me grow as a person. I also want to thank Andrey Joaqui, Mark Dresel, Dima Huang, Randy Wilharm, Raju Mandapati, and Fiona Armstrong for their advice and friendship these past 6 years. I would also like to acknowledge the undergraduates who helped me with my work: Sam Ford, Raksha Kandel, Balázs Novotny, Kaitlyn Hubbs, Anqi Lu, and Raima Amin. Their time and effort inside and outside the lab made my work possible and training them was one of the most rewarding experiences I had in graduate school. I would like to thank my collaborators Katherine Muratore and Edgar Arriaga for their advice and guidance as well. I would also like to thank my mentors in teaching, Janie Salmon and Jane Wissinger, for their role in helping me to become a better teacher.

Finally, I would like to thank my friends and family for their emotional and physical support throughout my graduate career. My parents, Doug Livezey and Marianne Livezey, for their undying love and faith in me. My brother, Jesse Livezey, and my sister, Mara Livezey, for their support, advice, and help in the graduate school journey we all shared. My friends Meghan McGreal, Connie Anderson, and Olivia Finster for helping me through some of the hardest times I have ever experienced, both in science and in my personal life. I would like to thank the Pokémon Go community, especially Matthew Luckow, which kept me sane during the stress of graduate school and a global pandemic. There are other unnamed family, friends, and loved ones who have supported me in this journey, and I would like to thank them for their support as well.

## **Dedication**

This dissertation is dedicated to my Baba Millie, vyjko Chris, Dedo Nick, and Grandma Leona. Memory eternal.

## **Abstract**

Utilizing the unique and varied properties of metals, such as their redox activity, lability, and net charge, metal-based prodrugs can be designed and optimized for numerous applications. The most prominent usage of metal-based prodrugs has historically been anti-cancer agents, though there have been more recent efforts in the development of theranostic and antimicrobial agents as well. Gallium has promise for extending the scope of metal-based prodrugs, as it has been FDA approved for the treatment of tumors and hypercalcemia. Epinephrine is a compelling target for a gallium-based prodrug as conventional prodrugs are not suitable for the treatment of anaphylactic shock. This is because the prodrugs are inactive during their long half-lives. Additionally, as should mitigate drug degradation from high pH, light, and heat. The development of a novel gallium prodrug of epinephrine establishes the first prodrug treatment of anaphylactic shock and extends the chemical space of metal-based prodrugs.

## Table of Contents

<b>List of Figures</b> .....	v
<b>List of Schemes</b> .....	vii
<b>List of Abbreviations</b> .....	viii
<b>1. Introduction</b> .....	1
1.1 Metal Based Prodrugs.....	1
1.1.1 Platinum Prodrugs.....	1
1.1.2 Cobalt Prodrugs.....	15
1.1.3 Ruthenium Prodrugs.....	26
1.1.4 Other Metal Prodrugs.....	34
1.2 Gallium in Medicine.....	36
1.2.1 Radioactive Gallium: <sup>67</sup> Ga and <sup>68</sup> Ga.....	36
1.2.2 Non-Radioactive Gallium.....	42
<b>2. Method Development for Studying Catecholamine Degradation</b> .....	45
2.1 Synopsis.....	45
2.2 Background.....	45
2.2.1 Uses of Catechols in Medicine.....	46
2.2.2 Catechol Degradation.....	48
2.2.3 Methods of Studying Catechol Degradation.....	50
2.3 Results and Discussion.....	52
2.3.1 Solvent Systems.....	53
2.3.2 Internal Standards.....	54
2.3.3 Sample Preparation.....	57
2.3.4 Extension to Other Catecholamines.....	57
2.4 Conclusions.....	62
2.5 Experimental.....	62
2.5.1 General Considerations.....	62
2.5.2 Solvent Systems.....	62
2.5.3 Internal Standards.....	64
<b>3. Gallium Mediated Prevention of Epinephrine Degradation</b> .....	67
3.1 Synopsis.....	67
3.2 Background.....	67
3.2.1 Prodrugs.....	70
3.2.2 Metal Based Prodrug Approach.....	72
3.3 Results and Discussion.....	74
3.3.1 Forced Degradation Studies.....	75
3.4 Conclusions.....	82
3.5 Experimental.....	83
3.5.1 General Considerations.....	83
3.5.2 Forced Degradation Studies.....	84
<b>4. Summary and Future Directions</b> .....	85
References.....	87

## List of Figures

<b>Figure 1.1:</b> Chemical structures of platinum ethylene diamine dichloride and clinically used alternatives to cisplatin.....	6
<b>Figure 1.2:</b> Chemical structures of targeted cisplatin analogues.....	10
<b>Figure 1.3:</b> Chemical structures of platinum(IV) prodrugs that have been tested in clinical trials.....	12
<b>Figure 1.4:</b> Chemical structures of platinum(IV) prodrugs with ligands that aid in stability, targeting, and treatment outcomes.....	14
<b>Figure 1.5:</b> Chemical structure of platinum(II) compounds showing promise as antibacterial prodrugs.....	15
<b>Figure 1.6:</b> Chemical structures of cobalt(III) prodrugs with nitrogen mustard cytotoxins.....	18
<b>Figure 1.7:</b> Chemical structures of cobalt(III) prodrugs with minor groove DNA intercalators. *A series of compounds was made by changing these methyl groups to alkyl phosphates, alkyl sulfates, and alkyl carbonates.....	21
<b>Figure 1.8:</b> Chemical structures of cobalt(III) prodrugs with <b>1-33</b> ) an MMP inhibitor and <b>1-34</b> ) an EGFR inhibitor.....	22
<b>Figure 1.9:</b> Chemical structures of cobalt(III) prodrugs with <b>1-35</b> ) naproxen and <b>1-35-1-37</b> ) Schiff bases.....	24
<b>Figure 1.10:</b> Chemical structures of cobalt(III) prodrugs with fluorescent coumarins.....	26
<b>Figure 1.11:</b> Chemical structures of ruthenium photocages with 4-amino pyridine, GABA, and 5-cyanouracil.....	29
<b>Figure 1.12:</b> Chemical structures of ruthenium photocages with various DNA intercalators.....	30
<b>Figure 1.13:</b> Chemical structures of ruthenium photocages with cysteine protease inhibitor.....	31
<b>Figure 1.14:</b> Chemical structures of ruthenium photocages with A) Metyrapone and B) a NAMPT inhibitor.....	32
<b>Figure 1.15:</b> Chemical structure of a ruthenium theranostic agent.....	33
<b>Figure 1.16:</b> Chemical structures of <b>1-52</b> ) a kinetically inert ruthenium prodrug and <b>1-53</b> ) a kinetically labile ruthenium prodrug.....	34
<b>Figure 1.17:</b> Chemical structures of iron, copper, rhodium, osmium, and iridium-based metal prodrugs.....	35
<b>Figure 1.18:</b> Chemical structure of desferrioxamine-B.....	39
<b>Figure 1.19:</b> Chemical structures of NOTA and DOTA chelating agents.....	39
<b>Figure 1.20:</b> Chemical structures of enterobactin mimics used as gallium chelators.....	41
<b>Figure 2.1:</b> Chemical structures of the most prominent catecholamines.....	46
<b>Figure 2.2:</b> Chemical structures of Levodopa and Carbidopa.....	47
<b>Figure 2.3:</b> HPLC traces of heated epinephrine solutions with different mobile phases. T = 30 °C, t = 7 days, $\lambda = 220$ nm, 10 equivalents of Ga(NO <sub>3</sub> ) <sub>3</sub> .....	54
<b>Figure 2.4:</b> Chemical structures of tested internal standards.....	55

**Figure 2.5:** a) HPLC trace of heated epinephrine solution with fluorescein internal standard. b) HPLC trace of heated epinephrine solution with 2,3-dihydroxybenzoic acid internal standard. c) HPLC trace of heated epinephrine solution with phenol internal standard. T = 60 °C, t = 6 days, λ = a) 354 nm b) 314 nm c) 270 nm, 0 equivalents of Ga(NO<sub>3</sub>)<sub>3</sub>.....56

**Figure 2.6:** Relative epinephrine values for epinephrine solutions with a) 0 equivalents of Ga(NO<sub>3</sub>)<sub>3</sub> and b) 1 equivalent of Ga(NO<sub>3</sub>)<sub>3</sub> at various pH values tested with sample preparation method without pH adjustment or a new sample preparation method with pH adjustment. Error bars represent ± one standard deviation, n = 3. \* Indicates a statistically significant difference (2 sample *t*-test, \*: p < 0.05, \*\*: p < 0.03, \*\*\*: p < 0.01).....58

**Figure 2.7:** Relative epinephrine values for epinephrine solutions with a) 0 equivalents of Ga(NO<sub>3</sub>)<sub>3</sub> and b) 1 equivalent of Ga(NO<sub>3</sub>)<sub>3</sub>. All values have been normalized to 1<sup>st</sup> replicate measurements and averages are for all pH values measured.....59

**Figure 2.8:** Overlapping HPLC traces of epinephrine, norepinephrine, and levodopa....60

**Figure 2.9:** a) Relative norepinephrine values of norepinephrine solution with 0 equivalents of Ga(NO<sub>3</sub>)<sub>3</sub>. b) Relative norepinephrine values of norepinephrine solution with 1 equivalent of Ga(NO<sub>3</sub>)<sub>3</sub>. c) Relative levodopa values of levodopa solution with 0 equivalents of Ga(NO<sub>3</sub>)<sub>3</sub>. d) Relative levodopa values of norepinephrine solution with 1 equivalent of Ga(NO<sub>3</sub>)<sub>3</sub>. Each sample was tested at various pH values with the sample preparation method without pH adjustment and the new sample preparation method with pH adjustment. Error bars represent ± one standard deviation, n = 3. \* Indicates a statistically significant difference (2 sample *t*-test, \*: p < 0.05, \*\*: p < 0.03, \*\*\*: p < 0.01).....61

**Figure 3.1:** Degradation pathways of epinephrine and their respective products.....69

**Figure 3.2:** Chemical structure of dipivefrin.....72

**Figure 3.3:** Net charge change with binding of epinephrine to gallium(III).....74

**Figure 3.4:** Relative epinephrine values for pH adjusted solutions of epinephrine in 250 mM pH 7.0 Tris buffer. Forced degradation conditions: a) room temperature, b) 30 °C, c) 40 °C, d) 50 °C, e) 60 °C, f) room temperature with exposure to 365 nm and 254 nm light. Error bars represent ± one standard deviation, n = 3.....78

**Figure 3.5:** Relative epinephrine values for pH adjusted solutions of epinephrine with a) 0 equivalents, b) 1/3 of an equivalent, c) 1 equivalent, and d) 3 equivalents of Ga(NO<sub>3</sub>)<sub>3</sub> in 250 mM pH 7.0 Tris buffer. Error bars represent ± one standard deviation, n = 3.....81

## List of Schemes

<b>Scheme 1.1:</b> Diaquation of cisplatin to the active species.....	2
<b>Scheme 1.2:</b> Mechanism of nucleoside binding of nitrogen mustards. Cyclization (Step 1) and guanine attack (Step 2) are repeated for completion of a DNA crosslink.....	20
<b>Scheme 1.3:</b> Electron capture radioactive decay.....	37
<b>Scheme 1.4:</b> $\beta^+$ decay of $^{68}\text{Ga}$ to $^{68}\text{Zn}$ .....	38
<b>Scheme 2.1:</b> a) Scheme of the degradation of a catecholamine to a semi-quinone in the presence of hydroxyl radical. b) Scheme of the degradation of a catecholamine to a semi-quinone in the presence of superoxide. c) Scheme of the degradation of a semi-quinone to a quinone in the presence of superoxide.....	49

## List of Abbreviations

MOA	mechanism of action
DNA	deoxyribose nucleic acid
UV	ultraviolet
HMG	high mobility group
P53	tumor protein p53
NER	nucleotide excision repair
MMR	mismatch repair
HR	homologous recombination
DACH	1,2-diaminocyclohexane
rRNA	ribosomal ribonucleic acid
ER $\alpha$	estrogen receptor $\alpha$
FDA	food and drug administration
COX	cyclooxygenase
BCE	N,N'-bis(2-chloroethyl)ethylenediamine
DCE	N,N-bis(2-chloroethyl)ethylenediamine
acac	acetylacetone
DCD	N,N-bis(2-chloroethyl)diethylenetriamine
MMP	model matrix metalloproteinase
EGFR	epidermal growth factor receptor
NSAID	nonsteroidal anti-inflammatory drug
NIR	near infrared light
LMCT	ligand to metal charge transfer
bpy	2,2'-bipyridine
GABA	$\gamma$ -amino butyric acid
TPA	tris(2-pyridylmethyl)amine
NAMPT	nicotinamide phosphoribosyltransferase
NAD	nicotinamide adenine dinucleotide
ROS	reactive oxygen species
cyclen	1,3,7,10-tetraazacyclododecane
SPECT	single-photon-emission computer tomography
PET	positron emission tomography
DTPA	diethylenetriaminepentaacetate
DFO	desferrioxamine-B
NOTA	1,4,7-triazacyclononane-N,N',N''-triacetate
DOTA	1,4,7,10-tetraazacyclododecane-1,4,7,10-tetraacetic acid
EDTA	ethylenediaminetetraacetic acid
LC-MS/MS	liquid chromatography with tandem mass spectrometry
HPLC	high-pressure liquid chromatography
PP	polypropylene
Tris	tris(hydroxymethyl)aminomethane

## 1. Introduction

### 1.1 Metal Based Prodrugs

Prodrugs are bio-reversible derivatives of drug molecules that undergo an enzymatic or chemical transformation within the body to release the active drug. Prodrugs can have different properties than their parent compound, such as changed pharmacokinetic properties, increased water solubility, better bioavailability, improved drug delivery, decreased toxicity, a more favorable formulation, or improved compound stability.<sup>1</sup> Though most prodrugs are organic in nature, the sub-set discussed herein will utilize metals as a means to change chemical and pharmaceutical properties.

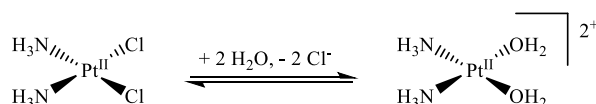
#### 1.1.1 Platinum Prodrugs

Although metals have been used in medicinal applications for nearly 5000 years, their common use in modern medicine can be attributed to the discovery of the first metal-based prodrug developed over 50 years ago.<sup>2-3</sup> Originally used for their ability to inhibit the growth of Gram-negative bacteria, multiple platinum complexes were studied for their anti-tumor activity against sarcoma 180 and leukemia L1210.<sup>4-7</sup> In 1978 the compound now known as cisplatin was FDA approved for clinical use. This discovery was one of the main driving forces for the advancement of medicinal inorganic chemistry, which has resulted in the development of numerous metal-based prodrugs.

Upon discovery of its anti-neoplastic activity, the mechanism of action (MOA) was not well understood. Preliminary studies showed that the platinum complex was aquated intracellularly to form a highly reactive positively charged ionic species that was speculated to be easily attacked by nucleophiles.<sup>8</sup> Ligand exchange is occurs inside the cell

cytoplasm due to 13 times higher concentration of chloride extracellularly.<sup>9</sup> Additionally, the exchange of chloride over ammonia is favored as the chlorides are relatively labile and prone to substitution. This is because ammonia forms more thermodynamically stable bonds with platinum.<sup>10</sup> As a square planar 16 electron species, the aquation occurs through an associative ligand exchange mechanism that results in the retention of stereochemistry. This is crucial as transplatin, the *trans* isomer of cisplatin, is non-toxic. The ligand exchange transformation, which formally classifies cisplatin as a prodrug, is shown in

**Scheme 1.1.**



**Scheme 1.1:** Diaquation of cisplatin to the active species.

The ligand exchange from chlorides to water is important as the platinum complex becomes positively charged. Research has shown that neutral cisplatin predominantly enters cells via passive diffusion. However, the positively charged aqua derivative becomes trapped within the cell as it can no longer permeate the cell membrane.<sup>11</sup> Choice in metal also plays an influential role in ligand exchange. Platinum, as a 3<sup>rd</sup> row transition metal, is the most inert group 10 metal with the largest crystal field splitting. Palladium, while still considered inert, is more labile than platinum. Nickel is significantly more labile than palladium or platinum and undergoes ligand exchange reactions at a moderate rate.<sup>12</sup> Platinum is therefore the metal of choice for creating a prodrug that is stable until it reaches its desired target area.

Purines and pyrimidines of deoxyribose nucleic acid (DNA) inside the cell contain a plethora of nucleophiles. Many studies have confirmed binding of cisplatin to DNA

through the use of ultraviolet (UV) visible spectroscopy, radioisotope labeling, Raman difference spectrophotometry, and various chromatography techniques.<sup>13-18</sup> Specifically, the N(7) sites of guanine and adenosine and the N(3) site of cytosine are prone to binding the platinum.<sup>17, 19-20</sup> Platinum binding to DNA can occur in different ways: as DNA-protein crosslinks, as intrastrand crosslinks, or as interstrand crosslinks.<sup>21-23</sup> DNA-protein crosslinks were noted to occur in bacteriophages, but they were not toxic.<sup>24</sup> Interstrand crosslinks were initially correlated with cell toxicity,<sup>25</sup> though other experiments indicated that interstrand crosslinks were not solely responsible for all platinum binding to DNA – indicating that intrastrand crosslinks existed as well.<sup>26-27</sup> First hypothesized after Stone *et al.* demonstrated that the guanine/cytosine content of DNA was proportional to the platination of the DNA, intrastrand crosslinking was first clearly identified with the confirmation of intrastrand crosslinked oligonucleotide fragments isolated from salmon sperm in 1985.<sup>28</sup> The same adducts were found in Chinese hamster ovary cells treated with cisplatin, indicating that the same DNA crosslinks form in cells as *in vitro*.<sup>29</sup>

With evidence of both interstrand and intrastrand crosslinking being caused by cisplatin, further studies investigated the relative occurrence and toxicity of each type of crosslinking. It was found that interstrand crosslinking only happens at concentrations above the mean lethal dose and occurs infrequently, which means that it cannot be the cause of cell death.<sup>30-31</sup> This indicated that intrastrand crosslinking was the likely cause of cell death. This agrees with the findings that 85-96% of platinum bound to DNA is bound via intrastrand crosslinks and which explains why transplatin, which mainly forms mono-

adducts with DNA, is non-toxic.<sup>32-33</sup> Additional work also showed that there was a linear correlation between the amount of platinum bound to DNA and cytotoxicity.<sup>34</sup>

After forming adducts with DNA, a multitude of events occur that led to cell death. The first and foremost is that DNA synthesis is inhibited, however it has been shown that this inhibition is not the critical step in cisplatin toxicity.<sup>35</sup> Cisplatin crosslinks also cause DNA unwinding, which is recognized by many different proteins.<sup>36</sup> Some of these proteins promote cytotoxicity, for instance high mobility group (HMG)-domain protein HMG1 which binds to the DNA-cisplatin adduct, preventing repair.<sup>37</sup> Another effect of cisplatin on the cell is the activation of cell cycle checkpoints, which allows the cell to stop the cell cycle and examine itself for problems such as DNA damage.<sup>38</sup> This effect likely does not increase toxicity as halting of the cell cycle generally leads to the inhibition of cell death, as quickening the cell cycle in cisplatin treated Chinese hamster ovary cells sped up apoptosis.<sup>39</sup> Perhaps the most important consequence of cisplatin crosslinking is the activation of tumor protein P53 (p53), which functions as a tumor suppressor.<sup>40</sup> After activation, p53 is bound to DNA with the help of HMG1 and HMG2.<sup>41</sup> With extensive damage caused to the DNA through the crosslinks, apoptosis is triggered.<sup>23</sup>

To this day, cisplatin is one of the most common chemotherapeutics for testicular cancer, however it was nearly discarded when phase 1 trials showed gastrointestinal and renal toxicities.<sup>42</sup> In phase 1 trials renal toxicity, toxicity to the kidneys, affected up to 36% of patients and was thought to be the major dose-limiting toxicity of cisplatin.<sup>43</sup> It was found that a single dose of more than 1.95 mg/kg was likely to cause renal impairment and in one case led to patient death through the death of kidney tubule, acute tubular necrosis.<sup>44</sup>

However, renal toxicity was mitigated through slow intravenous infusion of cisplatin with various methods of maintaining patient hydration which limited renal toxicity to less than 5% of patients.<sup>42, 45-47</sup> In addition to the moderate to severe nausea and vomiting that occurs after administration of cisplatin, gastrointestinal toxicity was also prominent in patients. In phase II studies, incidence of gastrointestinal toxicity was found in all patients treated with cisplatin at doses between 30 and 100 mg/m<sup>2</sup>.<sup>48</sup> Other negative side-effects of cisplatin treatment include but are not limited to myelosuppression, which is decrease in bone marrow activity, ototoxicity, which is toxicity to the ear, and neurotoxicity.<sup>44, 47, 49-50</sup>

An additional limitation of cisplatin is that many patients are intrinsically resistant to cisplatin treatment and some originally treatable tumors develop resistance to the prodrug over time.<sup>51</sup> Resistance to cisplatin can occur at many different stages: before binding to DNA, on-target resistance at the DNA crosslinks, post-target resistance on the cascade of events between DNA crosslinking and cell death, or even off-target effects. Mechanisms that occur before cisplatin binds to DNA include reduced uptake,<sup>52-55</sup> increased efflux out of cells,<sup>56-64</sup> and increased inactivation by reduced glutathione or metallothioneins.<sup>65-68</sup> Cisplatin lesions on DNA can be removed by the Nucleotide Excision Repair (NER) system and can be detected by but not repaired by mismatch repair (MMR) proteins.<sup>69-72</sup> Additionally, DNA double-strand breaks can be repaired by homologous recombination (HR) machinery.<sup>73-74</sup> Post-target resistance to cisplatin can be attributed to inactivation of p53,<sup>75</sup> as well as other factors that facilitate apoptosis such as death receptors,<sup>76</sup> cytoplasmic adaptors, BCL-2 proteins,<sup>77-81</sup> caspases,<sup>82</sup> and calpains.<sup>83-84</sup> Off-target resistance mechanisms are pathway alterations that do not directly interact with

cisplatin but their effects counteract the signaling cascade that induces apoptosis. Such mechanisms include upregulation of autophagy,<sup>85-87</sup> overexpression or hyperactivation of conserved kinases,<sup>88-91</sup> and upregulation of specific chaperones.<sup>92-95</sup>

Work has been done to circumvent problems with toxicity and resistance with the development of alternatives to cisplatin. In addition to cisplatin, carboplatin and oxaliplatin have been approved for worldwide usage, while nedaplatin, lobaplatin, and heptaplatin have been approved in various countries (Figure 1.1).<sup>96</sup>

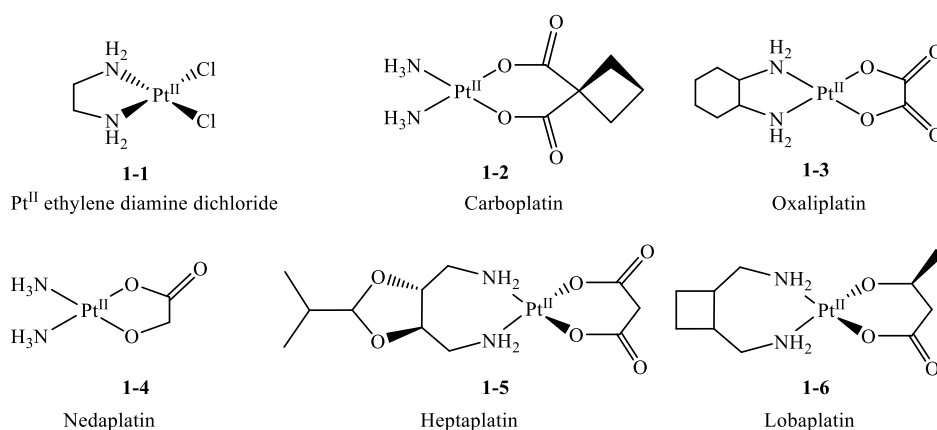


**Figure 1.1:** Chemical structures of platinum ethylene diamine dichloride and clinically used alternatives to cisplatin.

One of the main reasons for the lack of alternatives to cisplatin can be exemplified by platinum ethylenediamine dichloride (**1-1**). Because the ethylene diamine ligand forces the chlorides to remain in the cis conformation, it could be hypothesized that it would have equal or greater biological activity when compared to cisplatin, as the cis conformation is required for biological activity. However, the biological activity of platinum ethylene diamine dichloride is less than cisplatin.<sup>97-98</sup>

Carboplatin (**1-2**) began clinical trials in 1981 as a prodrug analogue to cisplatin.<sup>99</sup> It was noted that carboplatin was significantly less nephrotoxic, ototoxic, and neurotoxic

than cisplatin.<sup>100</sup> However, toxicity to bone marrow in the form of thrombocytopenia, that is having a low blood platelet count, was still present. Despite having different toxicity profiles, carboplatin was shown to have the same MOA as cisplatin. The prodrug is activated upon entering the cell, as the 1,1-cyclobutanedicarboxylic acid ligand is released upon hydration which is required for interaction with DNA.<sup>101</sup> At this point, the active released drug is identical to that of cisplatin, which is corroborated by carboplatin having similar activity in ovarian cancer, small cell carcinoma in lungs, head and neck cancer, and testicular cancer.<sup>102</sup> The likely reason for the difference of noted off-target toxicity is likely explained by the difference in kinetics of their aquation, and therefore their interaction with DNA. The monodentate chlorides of cisplatin have similar rates of aquation, which is about 100 times slower than the first aquation step of carboplatin, which is rate limiting.<sup>103</sup> Under the name Paraplatin®, carboplatin currently is most commonly administered for ovarian cancer, lung cancer, and head and neck cancer.

In the search for prodrugs related to cisplatin, it was determined that platinum compounds with a 1,2-diaminocyclohexane (DACH) ligand have similar therapeutic indexes to that of cisplatin.<sup>104</sup> Later studies found that oxaliplatin (**1-3**) was effective against many cisplatin-resistant cells lines, which led to clinical trials beginning in 1984.<sup>105</sup> Similarly to cisplatin and carboplatin, the activation of the oxaliplatin prodrug begins with aquation of the metal complex with loss of oxalate. However, the platinum complex formed after aquation remains different, due to the DACH ligand which remains attached to the platinum ion. After aquation, oxaliplatin forms intrastrand and interstrand crosslinks with DNA at locations similar to that of cisplatin.<sup>106-109</sup> Despite these similarities, there are still

some crucial differences between oxaliplatin and cisplatin with regards to their targets and biological activity. The most obvious difference stems from the DACH ligand remaining attached upon forming a DNA adduct. The DACH ligand creates a bulkier and more hydrophobic DNA adduct, which has been shown to be more effective at inhibiting DNA synthesis, as well as being more cytotoxic than the DNA adducts of cisplatin.<sup>110-111</sup> However, recent research has shown that oxaliplatin does not kill cells via the DNA damage response. Instead, oxaliplatin induces ribosome biogenesis stress which leads to cell death.<sup>112</sup> This was confirmed by modulating the cellular DNA damage response, which increased sensitivity to cisplatin but not oxaliplatin. Additionally, the synthesis of ribosomal ribonucleic acid (rRNA) was decreased by nearly 50% after treatment with oxaliplatin. Like carboplatin, oxaliplatin showed no nephrotoxicity. The most common acute side effect was peripheral neuropathy in the form of paresthesia, or tingling and numbness, and dysesthesia, or burning and aching, of the hands and feet.<sup>105</sup> Under the name Eloxatin™, the most common usage of oxaliplatin is in the treatment of colorectal cancer. It has also been used in single agent therapy as well as dual agent therapy for ovarian and breast cancer.<sup>113</sup>

Nedaplatin (**1-4**) was developed in 1983 with the hopes of decreasing toxicities caused by cisplatin.<sup>114</sup> Structurally, it is most similar to carboplatin, as aquation removes the bound glycolate to form the released drug identical to cisplatin and carboplatin. Thus, post-aquation, the MOA of nedaplatin is the same as cisplatin and carboplatin.<sup>115</sup> Unsurprisingly, toxicity profiles are similar to carboplatin, with nephrotoxicity and gastrointestinal toxicity no longer being dose-limiting. Like carboplatin, toxicity to bone

marrow production is dose-limiting as thrombocytopenia is the most common, followed by leucopenia, that is decreased white cell count, and anemia.<sup>116</sup> Nedaplatin, marketed under the name Aqupla, is used solely in Japan mainly to treat esophageal cancer, cervical cancer, and head and neck cancer.<sup>114</sup>

Heptaplatin (**1-5**) was developed in South Korea in 1994 with the goal of circumventing cisplatin resistance while decreasing nephrotoxicity and gastrointestinal toxicity.<sup>117</sup> Early studies showed that heptaplatin was indeed more effective than cisplatin against multiple cisplatin resistant cancer cell lines.<sup>118</sup> Additionally, it was shown to be less toxic than cisplatin at similar doses, but toxicity remains as higher doses of heptaplatin have worse toxicity than low doses of cisplatin.<sup>119-120</sup> Structurally, heptaplatin is most similar to oxaliplatin in that the di-amine ligand will remain attached after aquation of the malonic acid ligand. However, heptaplatin does not induce ribosome biogenesis stress like oxaliplatin. Instead, heptaplatin has been shown to interact less frequently with metallothioneins, which leads to its effectiveness against cisplatin-resistant cells.<sup>117</sup> Heptaplatin, marketed as SunPla, is used in South Korea for the treatment of gastric and lung cancer.<sup>121</sup>

Lobaplatin (**1-6**) was developed in Germany but has only been approved for use in China.<sup>96</sup> Structurally, lobaplatin is most similar to heptaplatin, so similar toxicities and MOA is expected. Tested doses induced mild nausea and vomiting, mild leukocytopenia, and thrombocytopenia. No toxicity to the kidneys was found, however doses were well below the level where toxicity was found for heptaplatin.<sup>122</sup> While some studies have found that lobaplatin is able to overcome cisplatin resistance,<sup>123-124</sup> it is not quite certain how.

Lobaplatin is currently used in China for the treatment of leukemia, and inoperable breast and small cell lung cancers.<sup>125</sup>

Additional research has been put into further altering cisplatin to determine changes of efficacy, to create novel mechanisms of cell killing, and to make more targeted prodrugs. These changes were often achieved through the attachment of different biomolecules. Examples of such prodrugs can be seen in Figure 1.2.

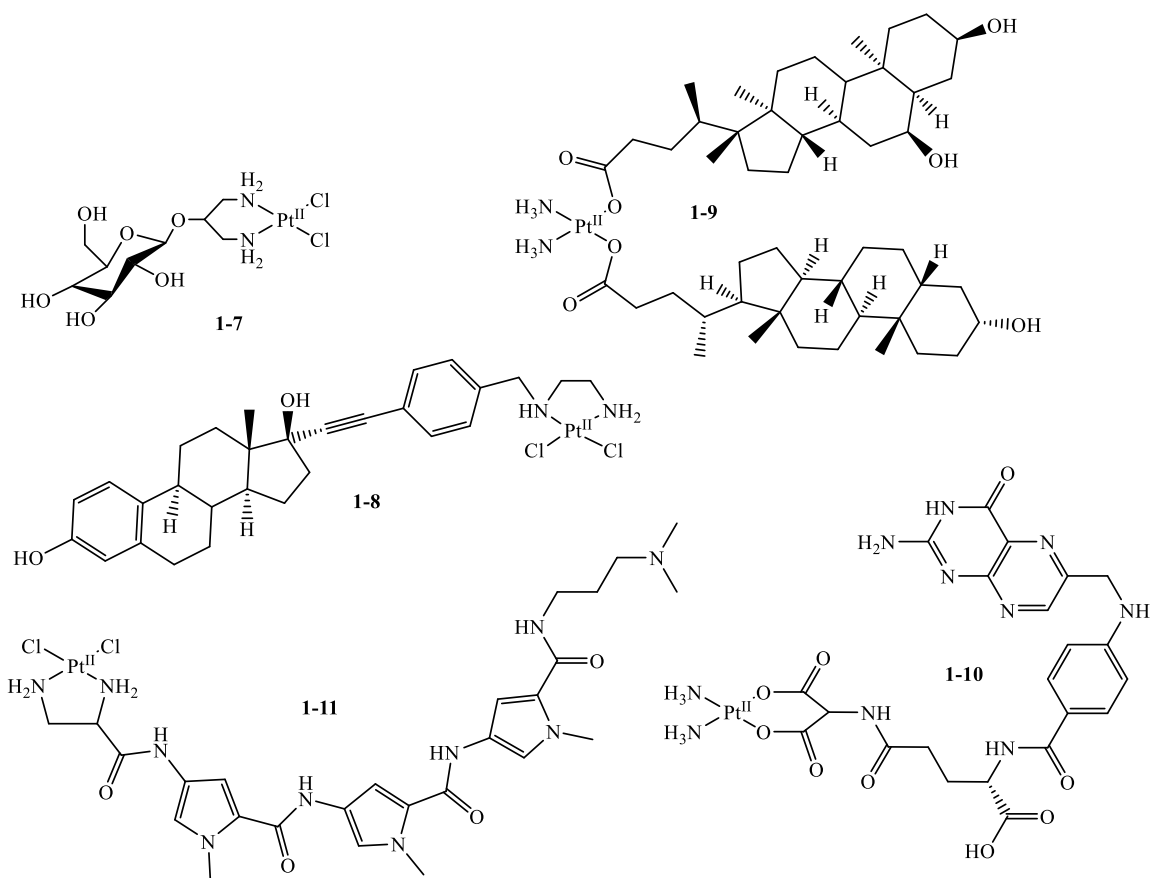


**Figure 1.2:** Chemical structures of targeted cisplatin analogues.

As sugars have been shown to have enhanced uptake in cancer cells, they make promising biomolecules for attachment to platinum to make cisplatin derivatives. The sugar molecules are connected through a linker such as in PtCl<sub>2</sub>(2,3-diamino-2,3-dideoxy-D-glucose) (**1-7**).<sup>126</sup> Early studies showed that such platinum compounds were more effective

than cisplatin, likely due to increased uptake in cancer cells via the glucose receptor, and toxic effects were reduced likely through increased complex solubility in water.<sup>127-128</sup> Another subset of cisplatin derivatives have been created through the attachment of hormones such as *cis*-dichloro[N-(4-(17-ethynylestradiolyl)-benzyl)-ethylenediamine]platinum(II) (**1-8**).<sup>129</sup> With the hormone acting as a vector to bring the platinum-based prodrug to the desired tissues, researchers expected these compounds to be more effective and less toxic than cisplatin. Cisplatin-hormone derivatives were made that successfully bound estrogen receptor  $\alpha$  (ER $\alpha$ ) with high affinity, although they did not show any enhanced toxicity.<sup>130-132</sup> Other derivatives activated their respective receptors at low concentrations, which resulted in increased cancer cell proliferation but caused cell death at higher concentrations.<sup>129</sup> In an effort to target the liver, cisplatin derivatives were synthesized with bile acids such as hyodeoxycholate (**1-9**).<sup>133</sup> Although these compounds had anti-neoplastic effect, they were less effective than cisplatin against cancer cells *in vitro*.<sup>134</sup> Folate receptors have also been found to be overexpressed in different cancer cell lines, making folate an attractive vector for platinum prodrugs.<sup>135</sup> Such prodrugs have been synthesized (**1-10**), however poor water solubility prohibited biological testing.<sup>136</sup> Short peptides have also been attached to platinum through the use of solid-phase synthesis with the aim of altering DNA binding (**1-11**). Ability to bind to DNA was diminished, and this led to reduced potency of these conjugates.<sup>137-140</sup>

In addition to the previously described 4-coordinate platinum(II) prodrugs, there has been recent interest in developing 6-coordinate platinum(IV) prodrugs. There are four platinum(IV) prodrugs that have been tested in clinical trials, however none of them have

been approved by the Food and Drug Administration (FDA) (Figure 1.3).<sup>141</sup> Because of their octahedral structure and their  $d^6$  electronic configuration, it was hypothesized that 6-coordinate platinum(IV) prodrugs will be considerably more stable outside of cancer cells.<sup>142</sup> The low spin  $d^6$  electronic configuration in octahedral geometry completely fills the  $t_{2g}$  orbitals, which results in a more negative crystal field stabilization energy. Platinum(IV) prodrugs are therefore expected to have higher activation energies for ligand exchange and be more inert.<sup>143</sup> The increase in oxidation state also increases the charge of the platinum center, which increases the thermodynamic stability of the complexes. Once inside cancer cells, platinum(IV) prodrugs were hypothesized to undergo a 2-electron reduction by reacting with reducing agents such as ascorbic acid or glutathione. The reduction results in the release of the two axial ligands as well as a 4-coordinate platinum(II) cisplatin derivative. Thus, the axial ligands utilized are typically spectator ligands or ligands that are drugs, typically with a different MOA. Equatorial ligands are usually amine-based or chlorides, resulting in the released 4-coordinate platinum(II) derivative being similar to cisplatin.

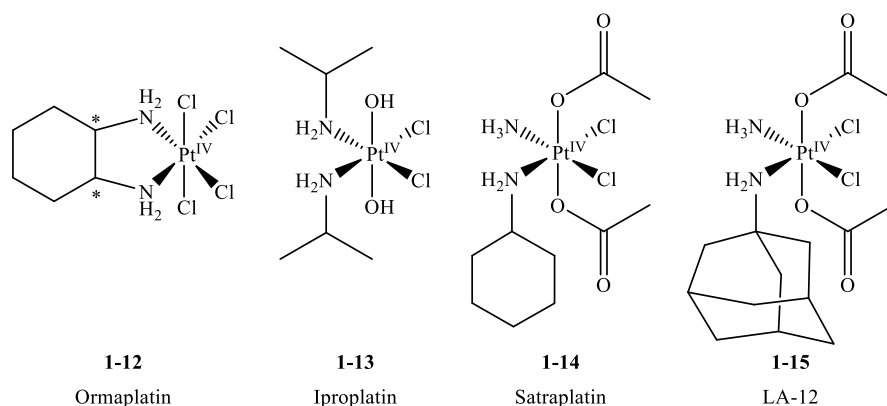


**Figure 1.3:** Chemical structures of platinum(IV) prodrugs that have been tested in clinical trials.

There are three main areas of platinum(IV) prodrug research: altering ligands to aid in stability, altering ligands for targeted delivery, and dual action prodrugs. For improving drug stability over cisplatin, the axial ligands are prominently studied, as they are not required for drug activity after release. One such example is a series of prodrugs made by Dyson *et al.* utilizing axial benzoate ligands (**1-17**).<sup>144</sup> Aromatic ligands were used, as they are known to improve drug uptake through increasing lipophilicity. Functionalization of the benzoate ligands was found to have a strong influence on uptake, and therefore efficacy of the complexes. As with platinum(II), peptide conjugates of platinum(IV) have been made with the hope of creating targeted complexes, as peptide receptors are overexpressed in tumor cells.<sup>145</sup> Both linear and cyclic peptides have been used, with the most promising leads both containing cyclic peptides (**1-17** and **1-18**).<sup>146</sup> In addition to attaching molecules that guide the platinum(IV) prodrug to the desired tissue, targeting has also been attempted by using photoactivatable ligands. Complexes with azido ligands have been frequently studied as photoactivation with 400 nm visible light can lead to similar antineoplastic activities as cisplatin (**1-19**).<sup>147</sup> These compounds have been shown to be stable in the dark, even around cellular reducing agents, such as glutathione.

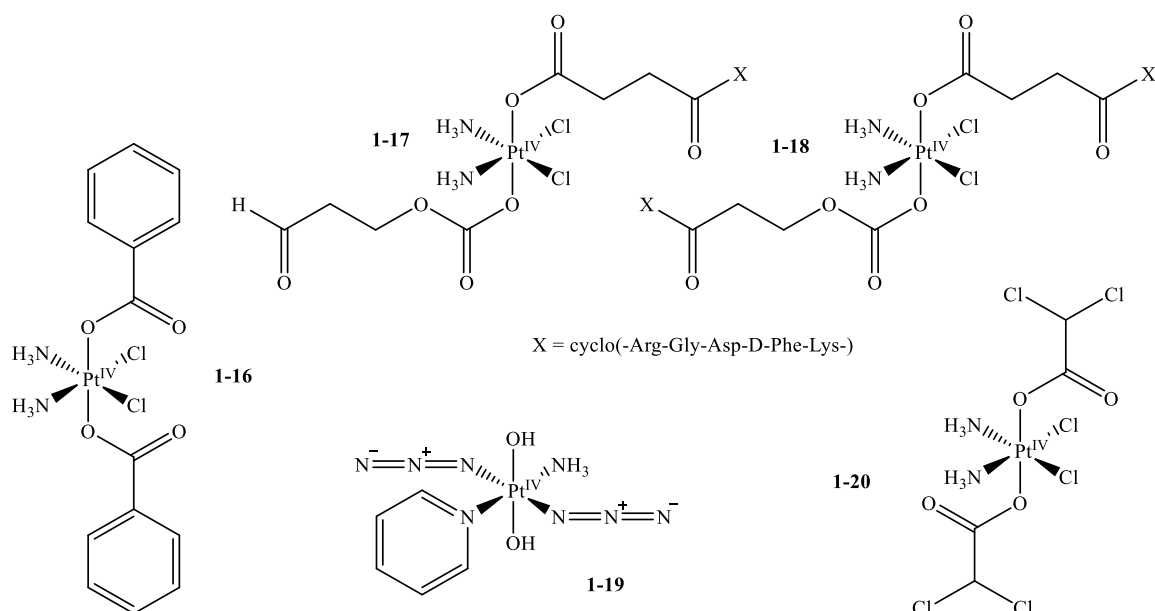


**Figure 1.4:** Chemical structures of platinum(IV) prodrugs with ligands that aid in stability, targeting, and treatment outcomes.

Dual action platinum(IV) prodrugs release additional antineoplastic agents, in addition to a classical platinum(II) drug. Attaching additional antineoplastic agents to a platinum(IV) prodrug that activates primarily inside cancer cells is expected to greatly improve the efficacy of the attached drug. The overall potency of the complex is also expected to improve. Typically, the additional drug's MOA does not involve DNA in order to limit cross-resistance. For example, Mitaplatin contains two dichloroacetate ligands which inhibit glycolysis (**1-20**).<sup>148</sup> Mitaplatin was shown to be more effective at killing lung carcinoma cells than normal cells, and this was attributed to the dual action of the platinum(II) drug and the dichloroacetate ligands.<sup>149</sup> Different enzyme inhibitors, nucleus-targeting cytotoxins, cyclooxygenase (COX) inhibitors, and drugs that target vital organelles have all been studied by numerous research groups.<sup>150-151</sup> Additionally, with two axial positions, two different drugs can be attached, leading to triple-action prodrugs.<sup>152</sup>

Several platinum(II) compounds have shown activity against at least one strain of bacteria.<sup>153</sup>

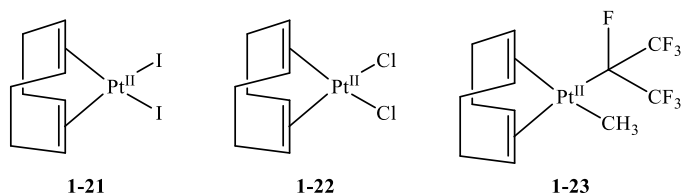


**Figure 1.5:** Chemical structure of platinum(II) compounds showing promise as antibacterial prodrugs.

These compounds are hypothesized to undergo ligand exchange reactions when exposed to solvent and media, resulting in the release of active compounds similar to cisplatin. This indicates that both platinum(II) and platinum(IV) complexes have potential as antibiotic prodrugs.

### 1.1.2 Cobalt Prodrugs

Solid tumors undergoing rapid growth require extensive amounts of oxygen and nutrients. One consequence of their growth is that they often outgrow their vasculature, resulting in hypoxia and malnutrition, which can lead to cell death at the center of the tumor.<sup>154</sup> Solid tumor hypoxia plays a role in platinum(IV) prodrugs, as the lack of oxygen in tumor cells prevents the re-oxidation of the newly 4-coordinate platinum(II) drugs released by the 6-coordinate platinum(IV) prodrug. This allows selective release of the axial ligands of platinum(IV) prodrug in hypoxic tumor environments. Tumor hypoxia preventing metal oxidation has been a main focus of a multitude of metal-based prodrug research, much of it involving the first-row transition metal cobalt.<sup>155-172</sup>

The emergence of cobalt-based prodrugs began with the study of the oxidation of mononuclear cobalt(II) to cobalt(III) by dioxygen in 1987, though the reaction had been

well known for many years prior.<sup>173</sup> Ligand exchange for  $d^7$  cobalt(II) occurs rapidly, as the metal center is labile.<sup>174</sup> However, cobalt(III) complexes primarily exist in a low spin  $d^6$  electron configuration state, meaning ligand exchange happens much more slowly.<sup>175</sup> It is hypothesized that cobalt prodrugs can be made with cytotoxic ligands that are inactivated through coordination. The prodrug that enters the body will remain as an inert cobalt(III) species, as long as it stays in oxygen rich environments. Once the cobalt prodrug reaches its desired target, the hypoxic tumor, the reduction potential of the cell is no longer sufficient to keep the cobalt prodrug oxidized. Inside the tumor cells, the cobalt(II) species will begin to form through reactions with enzymes, or other metabolites. This is expected to cause the loss of the cytotoxic drug ligands, specifically in the hypoxic tumor. In this fashion, cobalt-based prodrugs are expected to be activated specifically in hypoxic tumors. Another draw of cobalt-based prodrugs is that some complexes have been found to be radiosensitizers, or compounds that increase the effectiveness of radiation therapy.<sup>176</sup> Oxygen is extremely electrophilic and is a potent radiosensitizer, since it reacts with free radicals that are generated during radiation therapy. These reactions lead to DNA damage, which cause cell death.<sup>177-178</sup> However, hypoxic tumor cells have lower concentrations of oxygen, which makes them significantly more resistant to radiation therapy than tumor cells in an oxygenated environment.<sup>179</sup> Introducing electrophilic radiosensitizers, that serve the same function as oxygen by binding with DNA free radicals, can help reverse hypoxia induced radiation therapy resistance.<sup>180</sup>

The first cobalt(III) prodrug was synthesized in 1990 with the alkylating mustard bis(2-chloroethyl)amine (**1-24**).<sup>175</sup> Mammary tumor cells EMT6 were forced into a

hypoxic state by putting these cells under a flow of 95% nitrogen and 5% CO<sub>2</sub>. While the prodrugs were efficacious against the tumor cells, it was noted that efficacy decreased in the hypoxic environment. No explanation was provided as to why this experiment did not match the initial hypothesis, that the prodrug would be more effective in a hypoxic environment. A series of cobalt(III) nitrogen mustard complexes were then made and tested in oxygenated and hypoxic environments using either the nitrogen mustards N,N'-bis(2-chloroethyl)ethylenediamine (BCE) or N,N-bis(2-chloroethyl)ethylenediamine (DCE).<sup>181</sup> All four synthesized complexes had toxicity profiles that matched their respective free ligands, which indicated that toxicity was due to release of said ligands. One complex, like the first cobalt(III) prodrug, was more toxic under aerobic conditions, which was attributed to its more facile reduction, with a reduction potential of just -0.13 V. The most promising complex (**1-25**) showed hypoxic selectivity in all tested cell lines, and thus was proven to be the first metal complex that selectively released cytotoxic ligands under hypoxic environments. Further study of this compound was able to describe the relationship between oxygen concentration and cell death, which showed a 25-fold change in potency between hypoxic and oxygenated cells.<sup>182</sup>

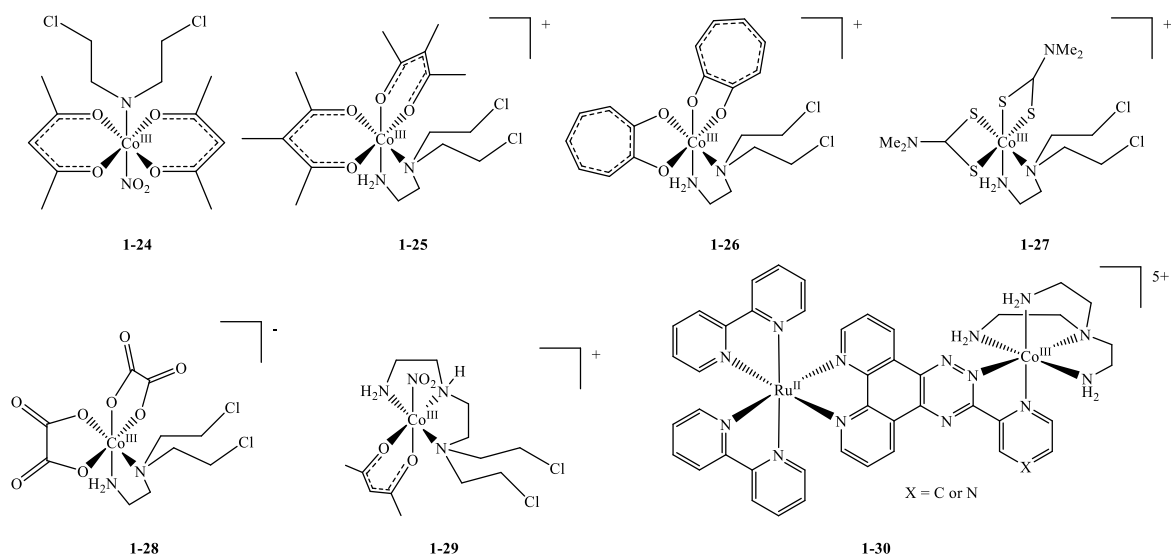


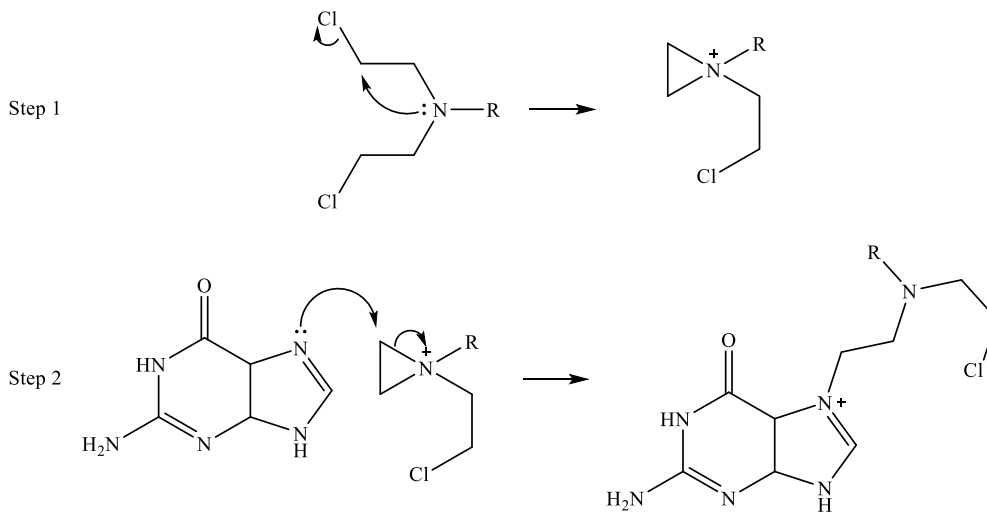
**Figure 1.6:** Chemical structures of cobalt(III) prodrugs with nitrogen mustard cytotoxins.

Work has been done to extend the spectrum of ancillary ligands, beyond that of derivatives of acetylacetonate (acac). One study replaced the acac ligands with tropolonate ligands in the hopes of clarifying the mechanism of selectivity (**1-26**).<sup>183</sup> The tropolonate ligand was chosen because, like acac, it is a bidentate ligand that binds to cobalt through two oxygen atoms, but is more bulky and electron withdrawing. This leads to a more sterically hindered complex with a more positive redox potential. All of the tested complexes showed similar profiles to their mustard ligands, however hypoxic selectivity was lost. Another study replaced the acac ligands with dithiocarbamate ligands (**1-27**).<sup>184</sup> The dithiocarbamate ligands are also bidentate and singly anionic, like the acac ligands. The dithiocarbamate ligands are less sterically hindering than the tropolonate groups, and it was hypothesized that the sulfur donors would increase the rate of electron transfer between cobalt(III) and cobalt(II). Additionally, it was expected that the electrochemistry would be more reversible, allowing for better measurement of redox potentials. Greater reversibility and faster electron transfer were confirmed by cyclic voltammetry.<sup>184</sup>

However, cytotoxicity studies suggested that the dithiocarbamate ligands were responsible for cell death, rather than the release of the nitrogen mustards. The effect of net charge was studied with the synthesis of cobalt(III) complexes with oxalato (**1-28**) and carbonato ligands.<sup>185</sup> Cytotoxicity studies suggested that the nitrogen mustard ligand was responsible for cell death and that the complexes were hypoxia selective. In order to study chelate effects on complex cytotoxicity, a tridentate nitrogen mustard cobalt(III) complex was analyzed (**1-29**).<sup>186</sup> The tridentate mustard, N,N-bis(2-chloroethyl)diethylenetriamine (DCD), by itself is less toxic than DCE. The tridentate cobalt(III) complex of DCD was less toxic than free DCD, indicating inactivation through coordination, and the toxicity of the complex was shown to be caused by DCD release. Additionally, the tridentate cobalt(III) complex was 5 times more efficacious in hypoxic conditions.

Secondary ligand release methods have also been explored through the attachment of a photo-activator (**1-30**).<sup>187</sup> Ruthenium bipyridyl complexes had been extensively studied for their electrochemical and photophysical properties, which makes them ideal candidates for the creation of a photoactivatable cobalt(III) nitrogen mustard heterodinuclear complex.<sup>188-189</sup> Once irradiated, the ruthenium(II) atom is expected to transfer an electron to the cobalt(III) metal center, reducing it to cobalt(II). As with the previous cobalt complexes, this reduction is expected to cause ligand release. The photoactivation studies confirmed that both ethylenediamine and tris(2-aminoethyl)amine were able to be released from the cobalt center, upon irradiation of the heterodinuclear complex. Ligand release was dependent on oxygen concentration, likely due to reoxidation of cobalt(II) to cobalt(III).

Each of the previously mentioned cobalt(III) prodrugs contains a nitrogen mustard as the active drug compound. Nitrogen mustards, or amines with halogenoalkyl groups, have been known to be cytotoxic since their usage in the first world war.<sup>190</sup> After initial studies noted the effect of nitrogen mustards on lymphoid tissue, bone marrow, and epithelial cells in the gastrointestinal tract, Dr. Thomas Dougherty became interested in converting these agents of war into agents of medicine.<sup>191</sup> Nitrogen mustards were first hypothesized to cause DNA crosslinks in 1948 after a study of their reaction with various nucleic acids.<sup>192-193</sup> Further research confirmed that bifunctional nitrogen mustards can form covalent DNA crosslinks, typically on the N(7) site of guanine.<sup>194-195</sup> The mechanism of formation of DNA crosslinks is shown in Scheme 1.2. These DNA crosslinks prevent the separation of DNA strands, preventing DNA replication which leads to cell death.<sup>196</sup>



**Scheme 1.2:** Mechanism of nucleoside binding of nitrogen mustards. Cyclization (Step 1) and guanine attack (Step 2) are repeated for completion of a DNA crosslink.

Cobalt(III) prodrugs have also been made with other DNA alkylating agents, namely DNA minor groove alkylators. In addition to tumor hypoxia preventing re-oxidation, these prodrugs were designed with an alternative method of cytotoxic drug

release. Radiation generates strongly reducing aquated electrons, and the lack of oxygen promotes their longevity. This allows for the radiation activated reduction of cobalt(III) prodrugs, resulting in prodrugs that can be spatially targeted based on the location of radiation therapy. The studied compound (**1-31**) was found to be reduced under hypoxic conditions by ionizing radiation and inside tumor cells, which resulted in the release of the attached DNA minor groove alkylator.<sup>197</sup>

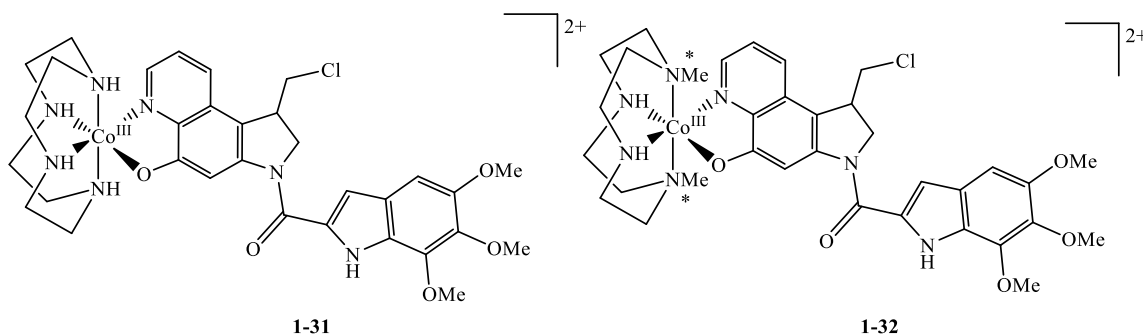


**Figure 1.7:** Chemical structures of cobalt(III) prodrugs with minor groove DNA intercalators. \*A series of compounds was made by changing these methyl groups to alkyl phosphates, alkyl sulfates, and alkyl carbonates.

Later research aimed to elucidate the effect of varying net charge on the biological activity of this cobalt(III) prodrug (**1-32**).<sup>198</sup> The goal was to lower overall lipophilicity, decrease cellular uptake, and therefore decrease off-target cytotoxicity of the metal prodrugs. The different charged complexes showed similar solubilities and stabilities when compared to the parent compound, but unfortunately had slightly worse toxicity profiles, which indicated that cellular uptake was likely uninhibited.

Another class of cobalt(III) prodrugs has been made with inhibitor molecules that target various proteins. Overexpression of Model Matrix Metalloproteinase (MMP) has been shown to be highly correlated with tumor aggressiveness and metastasis, therefore MMP inhibitors have been studied as potential chemotherapeutic agents.<sup>199</sup> Marimastat is

an MMP inhibitor that reached phase III clinical trials, however results indicated that its addition did not produce results significantly better than existing therapies, so further development was stopped. By attaching marimastat to a cobalt(III) center, researchers hoped to improve the efficacy of the drug by providing a vector to cancer cells as well as selective release at cancer cells (**1-33**).<sup>200</sup> The study found that marimastat's IC<sub>50</sub> was greatly increased while bound to the cobalt center. The cobalt(III) complex showed higher growth inhibition than the drug alone, however the complex and marimastat both gave rise to higher levels of tumor metastasis compared to the control.

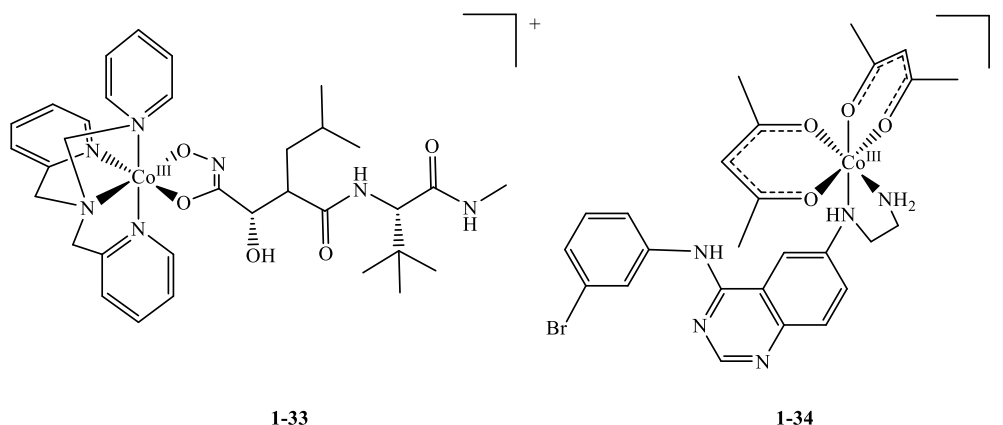


**Figure 1.8:** Chemical structures of cobalt(III) prodrugs with **1-33**) an MMP inhibitor and **1-34**) an EGFR inhibitor.

Epidermal Growth Factor Receptor (EGFR) is a protein that has been found to be overexpressed in a variety of cancers and is correlated with poor prognosis.<sup>201</sup> EGFR inhibitors have been developed and approved for treatment against non-small-cell lung carcinomas with activating mutations in EGFR and metastatic pancreatic cancer. Work has been done to develop an EGFR inhibitor to be used in a cobalt(III) prodrug (**1-34**).<sup>202</sup> The cobalt(III) complex with EGFR inhibitor was found to be inactive while in an oxygenated environment, and activity was significantly increased under hypoxic conditions as

expected. Additionally, it was shown that the cobalt(III) prodrug was distinctly worse than the free ligand at inhibiting EGFR activity, confirming drug inactivation through binding to cobalt(III).

Further research was done to study the attaching of naproxen, a nonsteroidal anti-inflammatory drug (NSAID), to cobalt(III) (**1-35**).<sup>203</sup> As an inhibitor of COX-2, which has been shown to be overexpressed in cancer stem cells, naproxen was an attractive candidate for making a cobalt(III) prodrug.<sup>204</sup> It had also been recently shown that NSAID accumulation suppressed cancer stem cell proliferation.<sup>205</sup> Studies showed that the cobalt(III) complex was capable of selectively killing breast cancer stem cells over bulk breast cancer cells. Additionally, the potency of the cobalt(III) prodrug was enhanced under hypoxia-mimicking conditions, and cytotoxicity was caused by DNA damage, as well as COX-2 inhibition.

Recent attention has been given to developing cobalt(III) prodrugs with Schiff base ligands. Cobalt(III) Schiff base complexes have been shown to inhibit histidine-containing proteins and enzymes. Inhibition occurs through dissociation of axial ligands, which are replaced with the imidazole nitrogens of histidines.<sup>206-207</sup> A series of complexes was made in order to investigate ligand exchange and complex stability (**1-36**).<sup>208</sup> It was found that NH<sub>3</sub> and imidazoles were readily displaced by peptides that contained two histidines, meaning they would be displaced by most target proteins which contain multi-histidine sites. Further work went into synthesizing cobalt(III) complexes with fluorine-containing equatorial ligands (**1-37**).<sup>209</sup> These studies confirmed that ligand exchange is dissociative in nature and the rate of ligand exchange correlates with the reduction potential of the

complexes. Other studies were published on cobalt(III) prodrugs with Schiff base ligands that were successfully able to release the intended ligand upon reduction and prove cytotoxic.<sup>210-211</sup> This includes a series of prodrugs that were targeted at topoisomerase I and II, which are enzymes that play essential functions in DNA repair, replication, and transcription (**1-38**).<sup>212</sup>

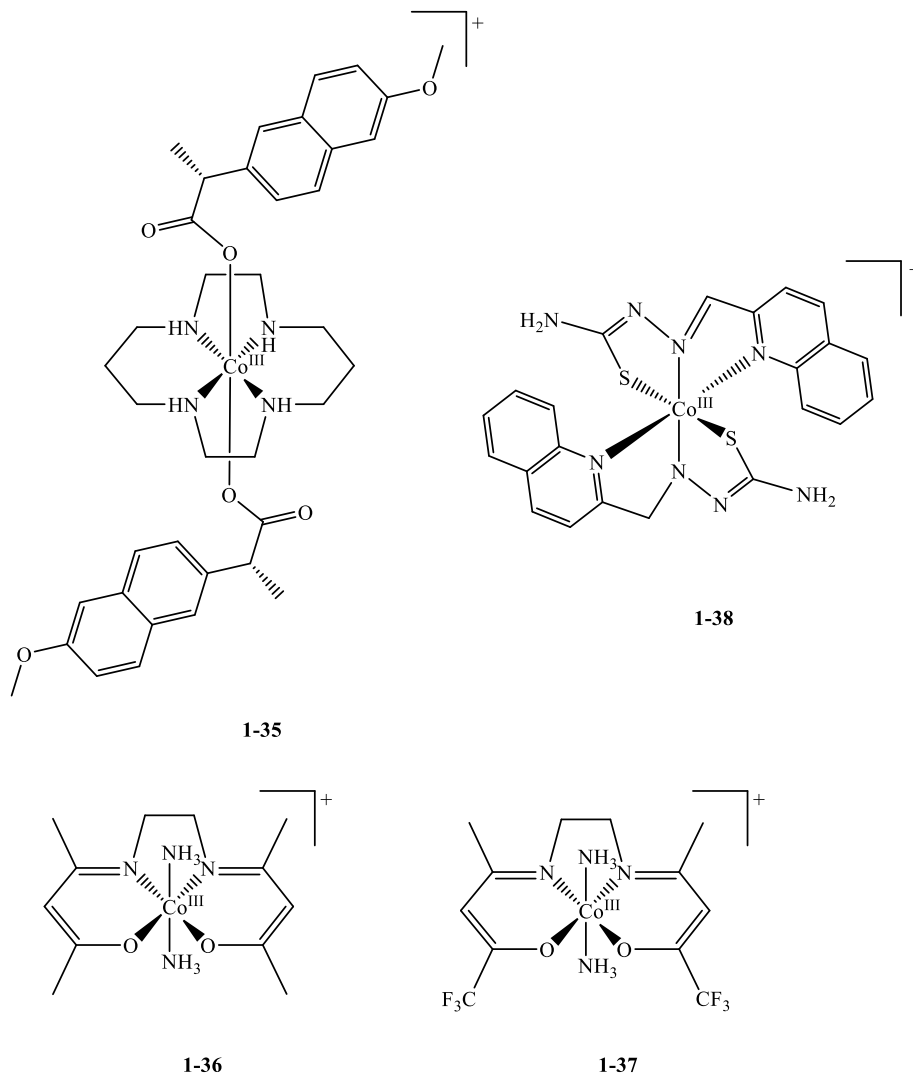


**Figure 1.9:** Chemical structures of cobalt(III) prodrugs with **1-35** naproxen and **1-35-1-37** Schiff bases. Experiments showed that the prodrugs were able to bind to DNA as well as inhibit both enzymes. Cytotoxicity experiments were not performed on these complexes.

Recent work has also gone into developing cobalt(III) prodrugs with fluorescent coumarins. Coumarins are naturally occurring fluorescent organic compounds found in a variety of plants, from essential oils such as cinnamon bark oil and lavender oil, to other plant products, including fruits, berries, and green tea.<sup>213</sup> Coumarins have been implicated in the treatment of high protein edema, chronic infection, blood coagulation and anticoagulation, inflammation, and cancer.<sup>214</sup> Preliminary studies of coumarins showed that not only did coumarins treat cancer but also helped attenuate the side effects of radiation therapy. Esculetin, a coumarin derivative found in traditional Chinese medicine, has been shown to be active against different cancer cell types, including breast cancer and colon cancer.<sup>215-218</sup> Researchers synthesized a cobalt(III) prodrug with esculetin in the hopes of producing a redox-sensitive prodrug that releases the fluorescent coumarin upon being activated in cancer cells (**1-39**). Fluorescent studies confirmed that esculetin's fluorescence was quenched upon coordination to the cobalt(III) center. As the cobalt(III) was reduced to cobalt(II) through the introduction of a hypoxic environment, fluorescence steadily increased with the subsequent dissociation of esculetin. No biological studies were performed with this complex.

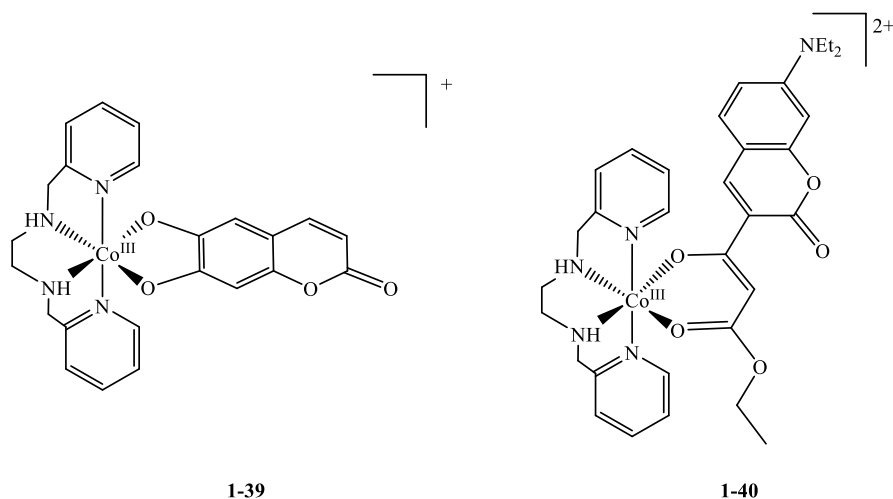


**Figure 1.10:** Chemical structures of cobalt(III) prodrugs with fluorescent coumarins.

Biological studies have been performed on other cobalt(III) prodrugs with fluorescent coumarins. In one such study, both the cobalt(III) and cobalt(II) complexes were synthesized with a coumarin- $\beta$ -keto ester hybrid (**1-40**).<sup>219</sup> Both complexes were found to be cytotoxic to tumor cells and the cobalt(III) complex was found to be significantly more selective against tumor cells. However, cytotoxicity was considerably reduced in both complexes from that of the native ligand, which was attributed to the binding of the coumarin- $\beta$ -keto ester hybrid to the cobalt centers.

### 1.1.3 Ruthenium Prodrugs

In addition to the chemical stimuli above, metal-based prodrugs have been achieved with physical stimuli as well.<sup>220</sup> Photocaging is a technique that has recently been applied to metal-based prodrugs, mainly ruthenium. In general, there are three types of photocaged metal prodrugs: prodrugs in which the released ligands are cytotoxic, prodrugs in which the remaining metal is cytotoxic, and dual action prodrugs in which both the ligands and metal are cytotoxic.<sup>150</sup> Ruthenium complexes with non-toxic ligands, such as amino acids, have been shown to be slightly cytotoxic – meaning ruthenium photocages generally

belong to the latter two categories.<sup>221</sup> The ligands, which can be chosen for either their cytotoxic effect or their ability to stabilize and deactivate the ruthenium metal center, remain attached in the bloodstream and their target tissues, but are released upon irradiation with light. This light usually has a wavelength between 350 and 900 nm. UV-visible light between 350 nm and 650 nm has been shown to work for topical treatments of various conditions and diseases.<sup>222-224</sup> However, this wavelength of light does not penetrate into tissues due to strong scattering, absorption by water, and absorption by other tissue chromophores such as hemoglobin and melanin.<sup>220, 225-226</sup> On the other hand, visible and near infrared light (NIR) with wavelengths from 650 to 900 nm, is able to penetrate less than 10 cm into tissues.<sup>226-228</sup> Compared to shorter wavelength UV-visible light, NIR photons are relatively low in energy meaning they might not provide enough energy to break chemical bonds. Irradiation has been shown to cause a  $\pi^* \rightarrow d$  ligand to metal charge transfer (LMCT), which transitions to a lower energy d-d energy state.<sup>229</sup> This energy decay is important as the d-d transition is Laporte forbidden, meaning direct excitation is difficult due to a small extinction coefficient. The d-d excited state weakens the bond between the ruthenium and the attached ligand(s) of interest, allowing for ligand release.<sup>230</sup>

Photocaged prodrugs have two main benefits: spatial targeting and temporal control. Greater spatial targeting is achieved through location-specific irradiation, which allows for specific release or activation of the drugs at the intended site, while preventing release or activation at off-target locations.<sup>231-232</sup> Changing light intensity and duration allows for control over the amount of prodrug that is activated and how long the prodrug is activated for.<sup>233</sup> Although not applicable to all ruthenium photocages, the lower pH

environment of cancer cells can also improve ligand release. This provides additional selectivity towards cancer cells, leading to fewer off-target effects.<sup>234-235</sup> There are also downsides to photocaging. Phototoxicity can occur with usage of UV-visible light, including, but not limited to, DNA damage, sunburn, premature aging, and immunosuppression.<sup>236</sup> Efforts are being made to reduce these limitations by converting from NIR light to UV-visible *in vivo* through optical upconversion, allowing for the photons to penetrate the necessary tissue and to be energetic enough to photocleave the necessary bonds.<sup>228, 237-238</sup> Light penetration into tissue is also a disadvantage for photocaged prodrugs. This is not a limitation for the treatment of surface cancers, as light penetration is not required in those cases. For treatments that are not on the surface, there is an additional option beyond the previously mentioned conversion of NIR light to UV-visible *in vivo*. Endoscopes and optical fibers can guide the desired UV-visible light directly to its intended site of action, allowing for a more direct irradiation at a controllable depth.<sup>239-240</sup>

The first published example of a ruthenium photocage prodrug is shown below (**1-41**). The neurochemical, 4-aminopyridine, was coordinated to a ruthenium metal center with two 2,2'-bipyridine (bpy) ligands which act as antennae for the irradiated light. The study showed that the prodrug successfully released 4-aminopyridine after irradiation with 473 nm light, and was efficacious in activating neurons, as expected.<sup>241</sup> Subsequently, ruthenium photocage prodrugs were made with a variety of known compounds. This includes neurotransmitters, such as  $\gamma$ -amino butyric acid (GABA) (**1-42**), and anticancer agents such as 5-cyanouracil (**1-43**), an analogue of the neoplastic agent 5-fluorouracil.<sup>242-</sup>

<sup>243</sup> While the GABA prodrug was not tested for its effects on DNA, the 5-cyanouracil prodrug was found to be a potent dual-action anticancer agent, as 5-cyanouracil has been shown to inhibit catabolism, and the remaining ruthenium complex was found to bind DNA.<sup>244</sup>

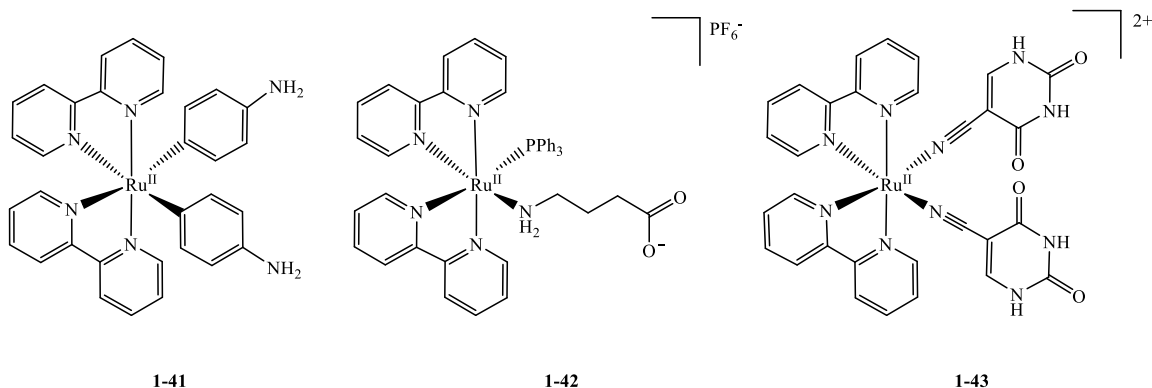


**Figure 1.11:** Chemical structures of ruthenium photocages with 4-amino pyridine, GABA, and 5-cyanouracil.

Ruthenium photocages have also been made with various DNA intercalators (Figure 1.12). A series of complexes were synthesized with increasing structural distortion through methylation of the ligands, with the base compound shown below (**1-44**). It was found that increased methylation resulted in increased rate of ligand ejection, as well as increased light-induced cytotoxicity.<sup>245</sup> This was corroborated by a later study which found that if the complexes were too strained, the complexes were toxic without the need of light irradiation.<sup>246</sup> Tetradentate tris(2-pyridylmethyl)amine (TPA) has been used in a variety of ruthenium photocages as an alternate antenna to bpy.<sup>247-248</sup> A series of bidentate DNA intercalators were tested in combination with TPA to synthesize different ruthenium photocages (**1-45**).<sup>249</sup> The study found that the surface area of the bidentate ligand correlated with DNA binding, the larger the ligand the stronger the complex bound to DNA. There are other mechanisms of ruthenium photocages with DNA intercalators. By

attaching a bipyridyl ligand with a photocleavable ester (**1-46**), researchers were able to create a substitutionally inert ruthenium photocage. Instead of complete ligand release, the ester is cleaved, allowing for the release of 3-(4,5-Dimethoxy-2-nitrophenyl)-2-butyl ester. The native complex was found to be non-toxic at concentrations up to 100  $\mu\text{M}$ , with a significant decrease in  $\text{IC}_{50}$  upon irradiation with 350 nm light.<sup>250</sup>

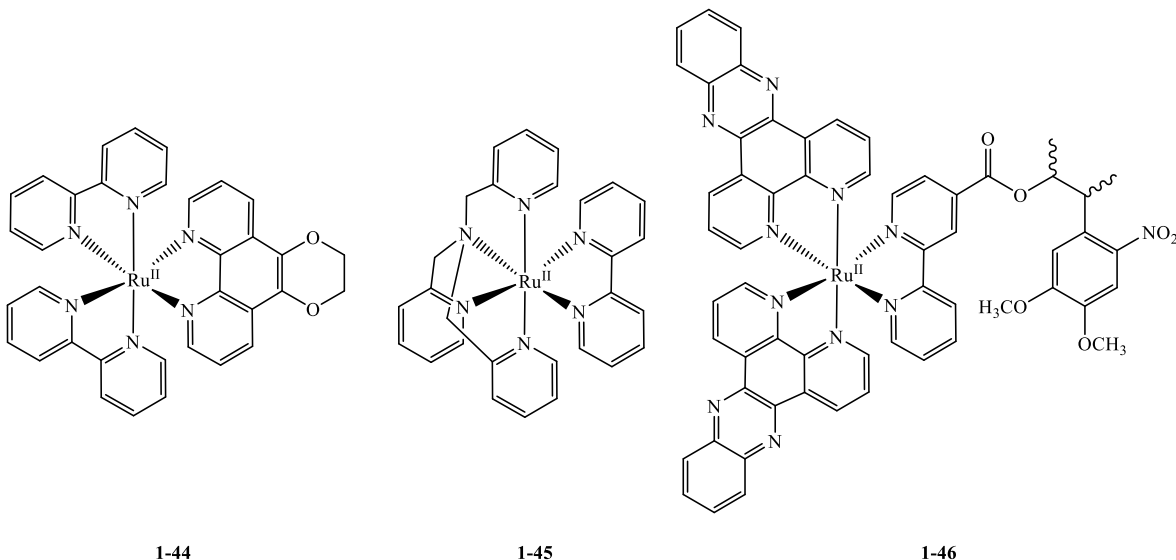


**Figure 1.12:** Chemical structures of ruthenium photocages with various DNA intercalators.

Another class of ruthenium photocages involve the coordination of protein and enzyme inhibitors that have been implicated in cancer. These compounds were initially studied with nitrile ligands, such as the aforementioned 5-cyanouracil prodrug, as nitrile ligands can be exchanged more efficiently than other monodentate ligands upon irradiation.<sup>251</sup> One of the first examples of this are the two ruthenium(II) complexes with attached cysteine protease inhibitors (Figure 1.13).<sup>252-253</sup> Both bpy and TPA ligands were used in separate studies, and each antennae resulted in complexes that were significantly less active than the prodrug without irradiation. Upon irradiation, inhibition of the target cysteine protease was largely restored.

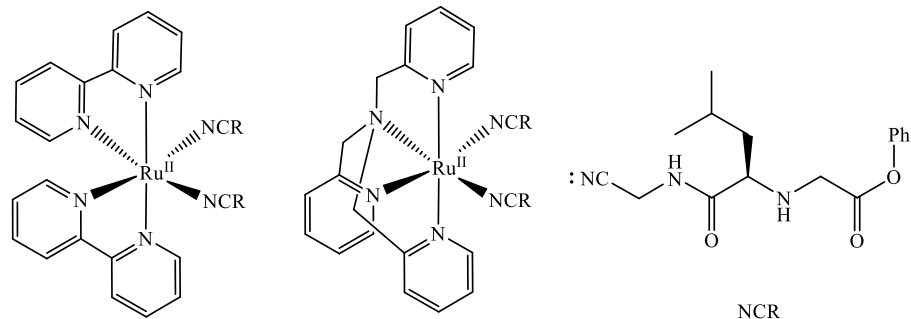


**Figure 1.13:** Chemical structures of ruthenium photocages with cysteine protease inhibitor.

Inhibitors of cytochrome P450s are also attractive prospects for ruthenium photocage prodrugs. Cytochrome P450s are enzymes that catalyze the degradation of foreign synthetic chemicals, such as drugs.<sup>254</sup> Additionally, studies have shown that P450s are over expressed in various cancer cell lines and induce resistance to DNA damaging chemotherapeutics.<sup>255</sup> The synergistic activity of the DNA intercalating ruthenium complex and the cytochrome P450 inhibitor Metyrapone proved potent, with a 136-fold increase in protein inhibition and an  $IC_{50}$  of  $0.05 \mu\text{M}$  upon activation with 470 nm light (**1-49**).<sup>256</sup> A ruthenium photocage has also been made with an inhibitor of the enzyme Nicotinamide Phosphoribosyltransferase (NAMPT) named CHS-828 (**1-50**). NAMPT is responsible for the regulation of intracellular nicotinamide adenine dinucleotide (NAD) and is overexpressed in a number of cancers.<sup>257-258</sup> Clinical trials showed that CHS-828 was active against a number of solid tumors, however, it displayed a number of dose-limiting side effects, had low bioavailability, and had large variation in its pharmacokinetics.<sup>259-260</sup> Thus, CHS-828 was an attractive candidate for incorporating into a ruthenium prodrug. As expected, cytotoxicity of the complex in the dark was diminished

compared to the active drug, and upon irradiation with blue light, the complex displayed a 10-fold increase in toxicity.<sup>261</sup>

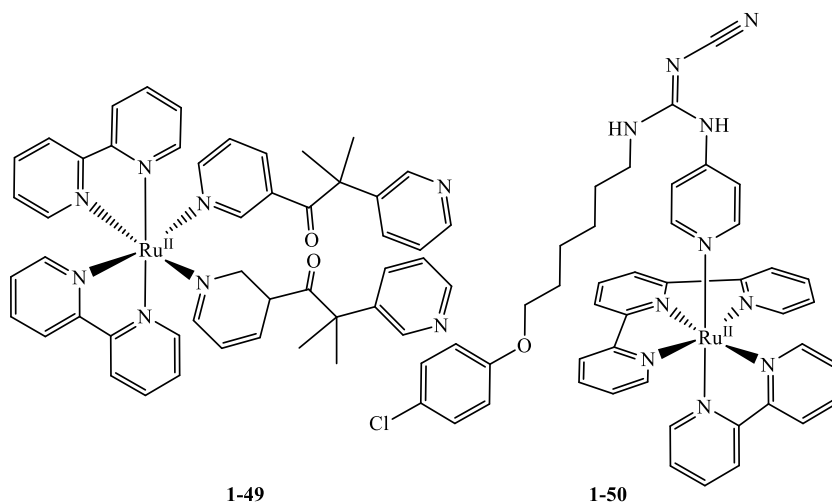
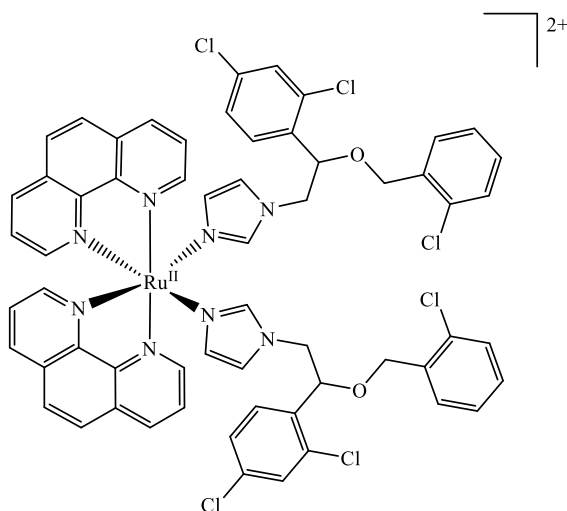


**Figure 1.14:** Chemical structures of ruthenium photocages with A) Metyrapone and B) a NAMPT inhibitor.

A ruthenium photocage with turn-off luminescent properties has also been developed for theranostic applications (Figure 1.15).<sup>262</sup> The complex was made with the potential anti-cancer drug econazole, which is currently approved to treat fungal skin infections.<sup>263</sup> With two equivalents of econazole attached, the ruthenium complex has an intense emission peak at 636 nm. However, once irradiated with 520 nm green light the econazole ligands are released. The di-aqua complex is formed, which is not luminescent. Toxicity studies showed that the complex exhibited low to moderate toxicity in the dark, however, irradiation with green light caused the  $IC_{50}$  values to fall into the nanomolar range. Additional benefits of coordinating econazole to ruthenium included increased solubility and stability.



1-51

**Figure 1.15:** Chemical structure of a ruthenium theranostic agent.

Ruthenium prodrugs have also been investigated for their antimicrobial properties. Early studies demonstrated their activity against Gram-positive and Gram-negative bacteria.<sup>264-265</sup> Generally, ruthenium prodrug antibiotics fall into two categories: kinetically inert and kinetically labile. Kinetically inert ruthenium prodrugs (**1-52**) are unlike previously described prodrugs, in that they do not release their ligands. Instead, the optical excitation leads to either an electron transfer reaction or an energy transfer reaction.<sup>266</sup> Electron transfer reactions result in the generation of reactive oxygen species (ROS). Energy transfer reactions lead to the formation of singlet oxygen. Both of these activation mechanisms result in DNA damage and cytoplasmic membrane damage resulting in bacterial death. Kinetically labile ruthenium prodrugs (**1-53**) require steric strain in order to undergo ligand exchange after optical excitation. The ruthenium complex can then covalently bind to DNA and the released ligand can also have antibiotic properties.

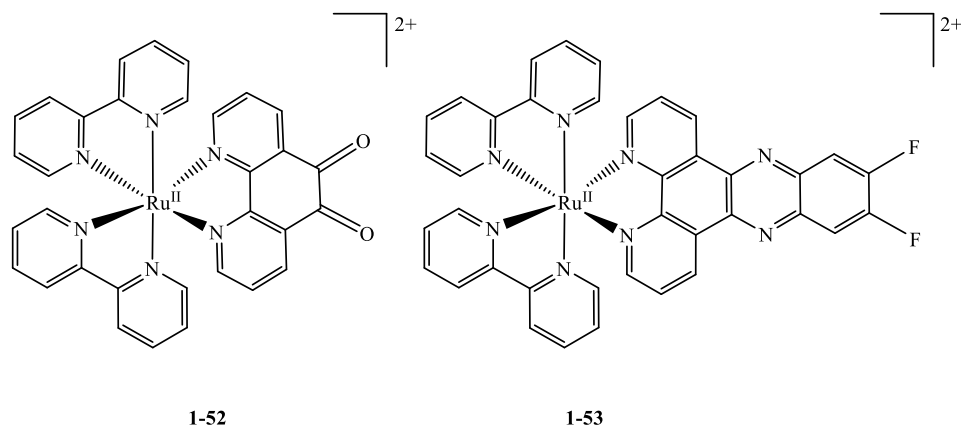


**Figure 1.16:** Chemical structures of **1-52**) a kinetically inert ruthenium prodrug and **1-53**) a kinetically labile ruthenium prodrug.

#### 1.1.4 Other Metal Prodrugs

Beyond platinum, cobalt, and ruthenium, a few other metals have been utilized for metal-based prodrugs. There are surprisingly few iron-based prodrugs, seeing as iron is the most abundant transition metal in the human body. One such prodrug was included in the assembly of a photo-responsive polymer nanoparticle (**1-54**).<sup>267</sup> Upon irradiation with UV light, the iron prodrug is released from the nanoparticle and generates ROS which damages the mitochondria of cancer cells. Another study produced two series of iron complexes (**1-55** and **1-56**), which were shown to cleave DNA under the reducing conditions of cancer cells. The exact mechanism of action is unknown.<sup>268</sup> Copper is also an attractive metal for taking advantage of the hypoxic environment of cancer cells. Nitrogen mustards were attached to copper through various macrocycles, though only 1,3,7,10-tetraazacyclododecane (cyclen) showed promise, as the other complexes released their ligands independent of O<sub>2</sub> concentration (**1-57**).<sup>269</sup> Other first row transition metals include vanadium, which has been used as an antidiabetic, and manganese, which has been used as a delivery system for carbon monoxide.<sup>270-271</sup>

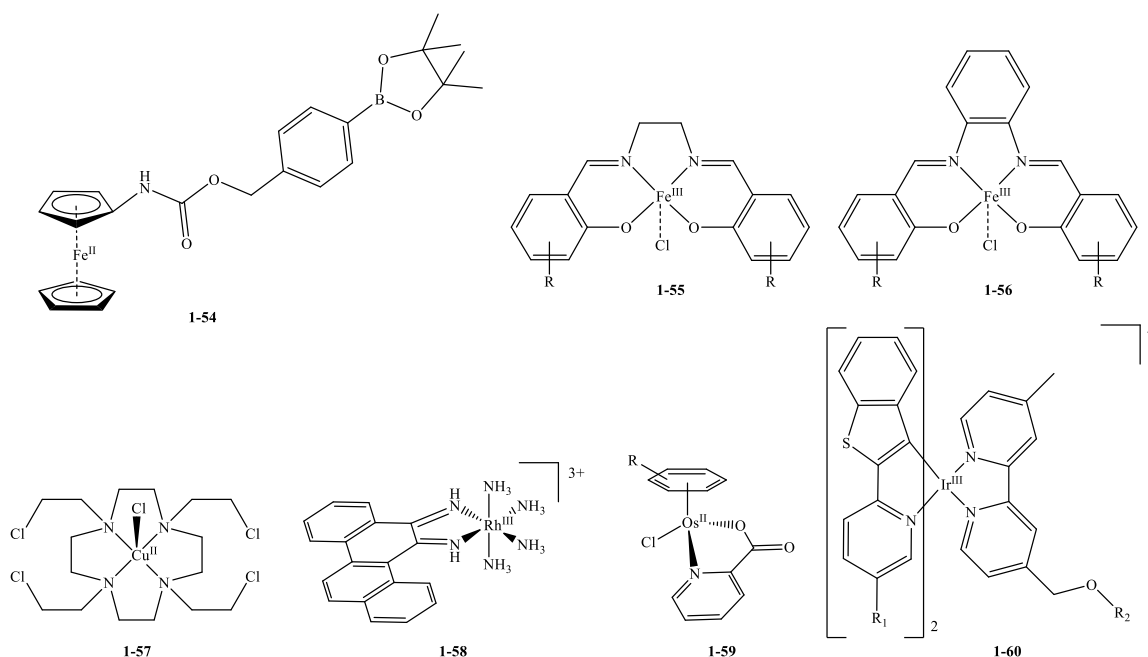


**Figure 1.17:** Chemical structures of iron, copper, rhodium, osmium, and iridium-based metal prodrugs.

Like ruthenium, a series of rhodium(III) complex were synthesized with the aim of utilizing photo-activation (**1-58**). The study found that, upon irradiation, the complexes bound DNA more strongly and also cleaved DNA with a high specificity for base-pair mismatch regions.<sup>272</sup> Several osmium half-sandwich prodrugs have been synthesized (**1-59**). Bidentate *O,O*, *N,N*, and *O,N* anticancer agents are coordinated and are hydrolyzed in aqueous media.<sup>273</sup> A series of iridium complexes have been made as pH activated radiosensitizers (**1-60**). Once inside the mildly acidic environment of cancer cells, the quenching moiety is cleaved, and the prodrug is activated. Irradiation with x-rays produces ROS in mitochondria which was found to cause DNA damage.<sup>274</sup>

Reviewing the uses of metal-based prodrugs, one thing is obvious – cell death is a common goal. This is logical, as many transition metal ions are toxic to the human body. Platinum, which has been shown to be non-toxic in the form of nanoparticles,<sup>275</sup> has an LD<sub>50</sub> of roughly 30 mg/kg as K<sub>2</sub>PtCl<sub>4</sub> in rats.<sup>276</sup> Cobalt also shows variability in toxicity as

insoluble  $\text{Co}_3\text{O}_4$  has an  $\text{LD}_{50}$  of 3.7 g cobalt/kg, but  $\text{CoCl}_2$  has an  $\text{LD}_{50}$  of just 42.4 mg/kg.<sup>277</sup> The same trend is seen with ruthenium as well;  $\text{RuO}_2$  has an  $\text{LD}_{50}$  of 4.6 g/kg in rats, whereas  $\text{RuCl}_3$  has an  $\text{LD}_{50}$  of 3.2 mg/kg.<sup>278</sup> These values show that solubility, oxidation state, and ligands all play important roles in the toxicity of transition metals. Designing a vector to target desired tissues, sequestering the metal in a stabilizing ligand framework, and utilizing changes in oxidation state, are all essential tools in limiting the toxicity of metal-based prodrugs.

## 1.2 Gallium in Medicine

Gallium is a group 13 p-block metal. With an oxidation state of +3, gallium's electronic configuration becomes  $[\text{Ar}]3d^{10}$ . Having a full valence shell of electrons, gallium is not redox active.<sup>279</sup> Gallium(III) has an octahedral ionic radius of 0.620 Å.<sup>280</sup> This value closely matches the most abundant metal in the human body, iron. Iron(III) has an octahedral ionic radius of 0.645 Å when high spin and 0.55 Å when low spin.<sup>281</sup> Iron(III) and gallium(III) also have matching net charge values and are both hard Lewis acids. Altogether, this makes gallium(III) an excellent mimic of iron(III), while the lack of redox activity and an oral  $\text{LD}_{50}$  value of 0.48 g/kg make it an attractive candidate for usage in medicine.<sup>282</sup>

### 1.2.1 Radioactive Gallium: $^{67}\text{Ga}$ and $^{68}\text{Ga}$

Gallium exists in two natural stable isotopes:  $^{69}\text{Ga}$  and  $^{71}\text{Ga}$ . The unstable  $^{67}\text{Ga}$  and  $^{68}\text{Ga}$  are both radioisotopes with medicinal uses.  $^{67}\text{Ga}$  has a half-life of three days and decays through electron capture, which is a process in which the nucleus absorbs an

electron which converts a proton to a neutron and emits an electron neutrino as well as a gamma ray (Scheme 1.3).



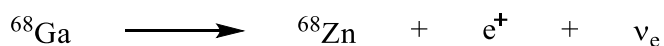
**Scheme 1.3:** Electron capture radioactive decay.

Gallium was first studied as a radioemitter in 1950, in which a study found that  $^{72}\text{Ga}$  was deposited in bones and proliferating tissues.<sup>283</sup> This led to the first study of  $^{67}\text{Ga}$  in 1969, in which the ability of [ $^{67}\text{Ga}$ ]gallium citrate to image cancerous tumors was first tested on a patient with stage IV Hodgkin's lymphoma.<sup>284</sup> This study was corroborated by additional studies that vastly increased case number and proved its usefulness in the identification and management of Hodgkin's disease.<sup>285-287</sup> Since then, [ $^{67}\text{Ga}$ ]gallium citrate has also shown to be effective at imaging inflammatory and septic lesions.<sup>288-289</sup>

Gallium scanning is a fairly simple process. Once radioactive  $^{67}\text{Ga}$  is injected into the patient, time is required for the isotope to localize in the cancerous tissue. Radioactivity is measured by a gamma camera, usually in the form of single-photon-emission computer tomography (SPECT). The images generated by SPECT show the localization of  $^{67}\text{Ga}$  in the patient's body. Gallium scanning was not widely adopted and has recently been replaced by positron emission tomography (PET) imaging due to the long wait times after  $^{67}\text{Ga}$  injection, poor spatial resolution, lack of specificity between cancer and inflammation, and poor sensitivity to slow-growing lymphomas.<sup>290</sup>

The first PET agents utilized  $^{18}\text{F}$  and  $^{11}\text{C}$ , two positron emitting radioisotopes.<sup>291-</sup>  
<sup>292</sup> While  $^{18}\text{F}$  is still the most commonly used isotope for PET, both  $^{18}\text{F}$  and  $^{11}\text{C}$  have the drawback of having half-lives of 110 minutes and 20 minutes respectively and are only able to be generated at cyclotrons.  $^{68}\text{Ga}$  has a similar half-life of 68 minutes but is able to

be generated through the decay of  $^{68}\text{Ge}$ .  $^{68}\text{Ge}$  can be produced at particle accelerators and with its half-life of 271 days, can be safely transported wherever  $^{68}\text{Ga}$  is needed.<sup>293</sup> However,  $^{68}\text{Ga}$  generators are expensive and their yield decreases considerably over time.<sup>294</sup>  $^{68}\text{Ga}$  PET agents are taken orally or injected into the patient's body, where they are directed to tissue of interest, usually cancerous tumors, by aid of an attached vector. After 30-60 minutes, the agent has been absorbed into the tissue of interest.  $^{68}\text{Ga}$  usually decays through  $\beta^+$  decay, or the emission of a positron and an electron neutrino (Scheme 1.4).



**Scheme 1.4:**  $\beta^+$  decay of  $^{68}\text{Ga}$  to  $^{68}\text{Zn}$ .

During the emission of positrons, gamma rays are also emitted which, like in SPECT imaging, are measured through the use of gamma cameras.<sup>295</sup> Much work has gone into designing appropriate ligands for  $^{68}\text{Ga}$ . The ligand can provide a vector for the  $^{68}\text{Ga}$  to be delivered to the tissue of interest, however, it needs to bind  $^{68}\text{Ga}$  strongly enough so that the complex is stable. Diethylenetriaminepentaacetate (DTPA) is a commonly used chelator for radiopharmaceuticals that is sufficiently stable with other radioisotopes, but not stable enough with gallium for *in vivo* work.<sup>296</sup> Therefore, desferrioxamine-B (DFO) was proposed as an alternative which was shown to be significantly more stable in human serum (Figure 1.18).<sup>297</sup> DFO also has a terminal amine, on which various biological vectors can be attached, making it an attractive chelating agent for radioactive metals. However, DFO bound gallium(III) is not stable enough to prevent leaching *in vivo*.<sup>298</sup>

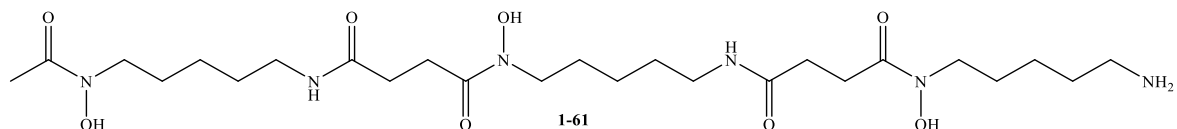


**Figure 1.18:** Chemical structure of desferrioxamine-B.

Many additional linear chelators have been studied, such as HBED and THP, and when combined with different vectors such as folate, provide specificity to the radiopharmaceutical agents.<sup>299-302</sup>

Recent studies have focused on macrocyclic ligands due to their significantly increased stability. Of particular interest for  $^{68}\text{Ga}$  are 1,4,7-triazacyclononane- $\text{N,N',N''}$ -triacetate (NOTA) and 1,4,7,10-tetraazacyclododecane-1,4,7,10-tetraacetic acid (DOTA) (Figure 1.19).

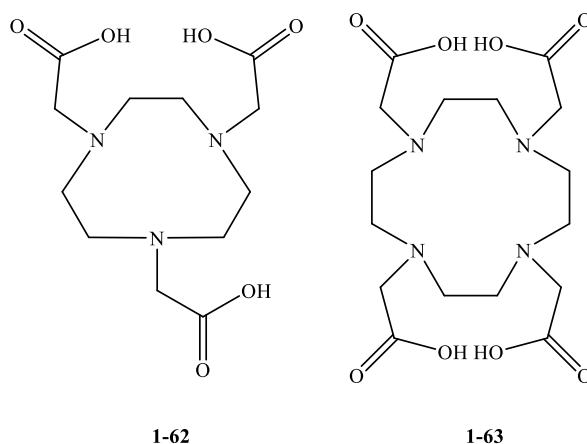


**Figure 1.19:** Chemical structures of NOTA and DOTA chelating agents.

Both of these ligands form complexes with gallium with extremely high stability constants – where  $\log[K_{\text{ML}}]$  is 30.98 for Ga-NOTA and 26.05 for Ga-DOTA.<sup>303-304</sup> Many derivatives of NOTA have been synthesized, tested, and have shown promise as PET agents, but have yet to be FDA approved.<sup>305-310</sup> This is possibly due to the increased difficulty of the synthesis of NOTA analogues, as each carboxylate coordinates to the gallium center. Functionalization of DOTA is significantly more facile, as only two of the four available

carboxylates coordinate to the gallium center, leaving the remaining two available for the attachment of biological vectors. Many derivatives of DOTA have been synthesized and tested, and have shown promise as PET agents.<sup>311-314</sup> Since 2019, the FDA approved the first <sup>69</sup>Ga radiopharmaceutical [<sup>68</sup>Ga]Ga-DOTA-TOC and the second [<sup>68</sup>Ga]Ga-DOTA-TATE, both being Ga-DOTA conjugates with targeting peptides.<sup>315-316</sup> Since their approval, both radiopharmaceuticals have proved their worth in the identification and imaging of various cancers. In addition to NOTA and DOTA derivatives, many other cyclic chelating agents have been studied, such as PCTA.<sup>302, 317</sup>

<sup>68</sup>Ga PET has recently been extended to imaging fungal and bacterial infections. Taking advantage of the previously mentioned similarities between Ga<sup>3+</sup> and Fe<sup>3+</sup>, researchers utilized siderophores, small molecules synthesized by fungi and bacteria in order to sequester iron, to target fungal and bacterial infection. This was first demonstrated by radiolabeling the siderophores of the fungus *Aspergillus fumigatus*, desferri-triacetylfusarine C and desferri-ferricrocin, and then using them to image *A. fumigatus in vitro* and *in vivo*.<sup>318</sup> A similar study was performed on the siderophore pyoverdine, which is native to the bacteria *Pseudomonas aeruginosa*.<sup>319</sup> However, the limitation of both of these studies is that the natural siderophores produced by *A. fumigatus* and *P. aeruginosa* both lack a chemical handle onto which a targeting vector can be attached. This was done in a recent study by the Pierre group, in which synthetic mimics of the natural *Enterobacteriaceae* siderophore enterobactin were made with pendant carboxylic acids, onto which targeting vectors could be attached (Figure 1.20).<sup>320</sup> The thermodynamic stabilities of the complexes were studied through competition titrations with DFO. The

lead compound, TREN-CAM (**1-64**), formed a complex that was significantly more stable than DFO and the other ligands. The observed pGa values also indicated that a smaller ligand cap since was preferred. Radiolabeling yields for were determined for the ligands with ten-minute reactions. All ligands, except 3,3-Glu-CAM (**1-67**), exhibited radiolabeling yields greater than or equal to 90%, which is typical for kinetically rapid chelators. Together, this demonstrates that catechol binding of gallium is kinetically labile while being thermodynamically stable.

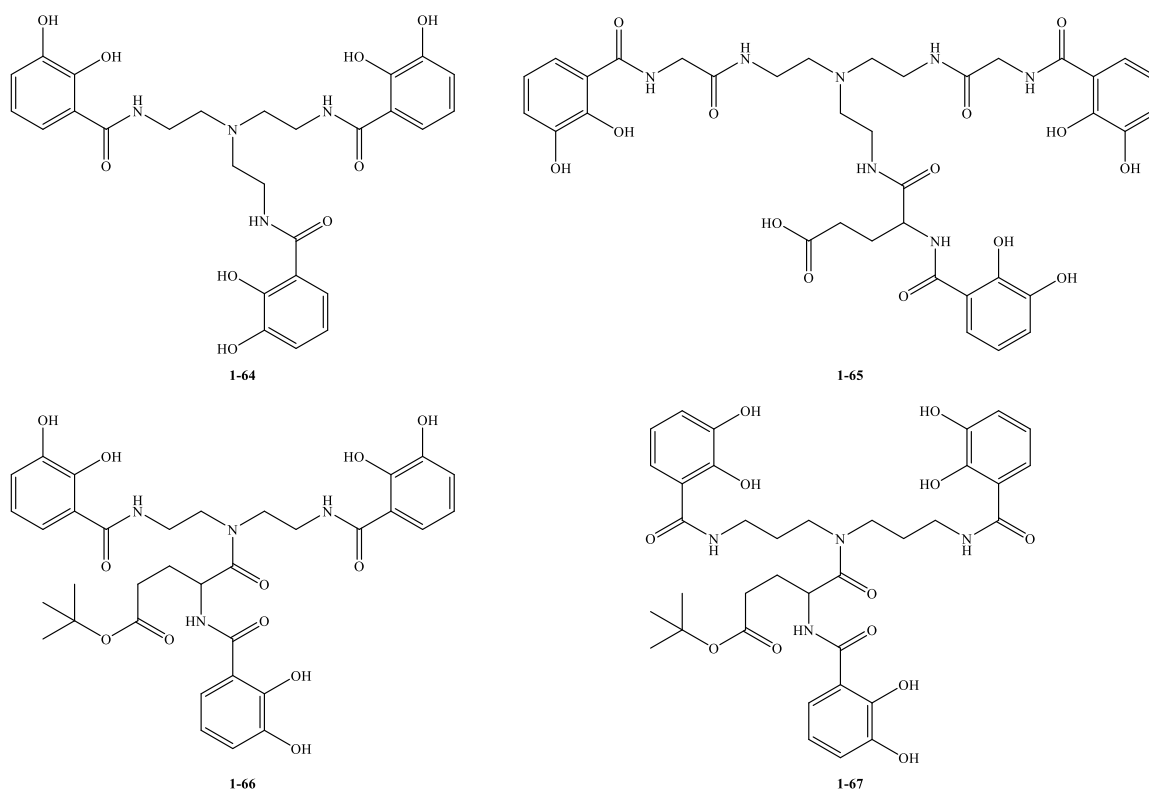


**Figure 1.20:** Chemical structures of enterobactin mimics used as gallium chelators.

The synthetic mimics remained at least as stable as Ga-DFO in buffer and no de-chelation in human serum was observed for Ga-TREN-CAM and Ga-TREN-bis-GlyGluCAM (**1-65**) within 2 hours. The *in vivo* studies in mice indicated that the Ga-TREN-CAM radiotracer was cleared rapidly from mice in under 15 minutes.

### 1.2.2 Non-Radioactive Gallium

In addition to imaging, gallium has also been utilized for its antineoplastic activity in the form of gallium nitrate. Initial studies showed that of the group 13 metals gallium was less toxic than indium and thallium, and was the most effective at suppressing tumor growth.<sup>321</sup> Further studies showed that gallium was able to bind to the phosphate backbone of DNA, but no interaction was found between gallium and nucleotides.<sup>322</sup> This binding led to the inhibition of DNA synthesis, with an  $IC_{50}$  of 120  $\mu$ M for T cell lymphocytes.<sup>323</sup> Incubating cells in 300  $\mu$ M gallium has also been associated with the disruption of protein synthesis, however overt cell injury was not identified.<sup>324</sup> Additionally, it has been shown that gallium inhibits certain enzymes as well as tubulin polymerization, which has been largely attributed to its competition with magnesium.<sup>325-329</sup>

Early clinical trials consisted of a gallium nitrate administered through intravenous infusion.<sup>330-331</sup> Tumor regression and disease stabilization was observed, however renal toxicity was dose-limiting and was cumulative. Renal toxicity can be mitigated through extended infusion and hydration. Later clinical trials administered gallium chloride and gallium maltolate orally.<sup>332-334</sup> Gallium chloride and gallium maltolate each showed promising results, warranting further study.<sup>282</sup>

In 1984, researchers identified that two-thirds of patients who were receiving gallium nitrate as an anticancer drug were also developing hypocalcemia.<sup>335</sup> As hypercalcemia is a common, life-threatening disorder that can be associated with cancer, treatment with gallium nitrate was compelling.<sup>336-337</sup> Early clinical trials gave patients gallium nitrate at a dose of 700 mg/m<sup>2</sup> by rapid intravenous infusion over a 15 to 30 minute

period.<sup>338</sup> This high of a dose resulted in high peak plasma levels, which led to nephrotoxicity, which was dose-limiting. A second infusion schedule was tested at a dose of 200 to 400 mg/m<sup>2</sup> per day over the course of 5 to 7 days, which resulted in a greater amount of gallium nitrate infused, while being better tolerated by patients. Additional studies demonstrated that gallium nitrate was more effective than calcitonin, a hormone produced by humans that regulates the levels of calcium in the blood, for controlling hypercalcemia. Shortly after, gallium nitrate was FDA approved for the treatment of hypercalcemia.<sup>339-340</sup> Hypocalcemia may also develop in patients with normal blood calcium levels, but this can be managed through oral supplementation of calcium carbonate.<sup>341</sup> Gallium nitrate has since been withdrawn from sale for the treatment of hypercalcemia, however, the FDA states that the reasons were not due to safety or efficacy.

Gallium has also been used in combination with siderophores as a modality for the creation of antimicrobial agents. One approach, known as the Trojan-horse approach, involves the attachment of a gallium chelating siderophore to an already known antibiotic agent. Since the siderophores are natural iron chelating agents produced by bacteria and fungi in order to scavenge for iron within their environment, increased uptake of the siderophore attached antibiotic is expected. This methodology has been shown to be effective in the creation of theranostic and therapeutic antibiotic compounds.<sup>342-344</sup> The second approach to gallium-siderophore based antibiotics is through the trafficking of gallium to bacteria and fungi. Since Ga<sup>3+</sup> and Fe<sup>3+</sup> are so similar, the introduction of excess gallium to bacteria and fungi disrupts their iron metabolism, often leading to cell death. This methodology has also been shown to be effective in treating infections.<sup>345-349</sup> Though

both methodologies have shown incredible promise, no gallium-based antibiotics have been FDA approved.

## 2. Method Development for Studying Catecholamine Degradation

### 2.1 Synopsis

Catecholamines are important drugs that can be used to treat anaphylactic shock, Parkinson's disease, and mitigate sepsis. Unfortunately, catecholamines are prone to degradation. Therefore, it is important to develop methods that are able to accurately monitor and identify this degradation. Current methods do exist but have been limited to the analysis of a singular catecholamine. There is no consensus between current methods as they utilize multiple different solvent systems. Additionally, many current methods do not use internal standards which increase the accuracy of measurements and current methods do not use sample preparation methods that aim to ensure catecholamine solubility and sample stability. This is important as catecholamine solubility is variable in water depending on the pH, and catecholamines undergo degradation which can be exacerbated by pH, heat, and light. A method was developed that utilized a solvent system of 0.02 M pH 2.5 phosphate buffer with 0.25 g/L ethylenediaminetetraacetic acid (EDTA), and 0.06 g/L sodium octyl sulfate with acetonitrile, an internal standard of phenol, and a sample preparation method that utilized the addition of 100  $\mu$ L of 1 M HCl in order to lower sample pH. This method was able to successfully separate different catecholamines from each other and other UV-visible absorbing additives, accurately monitor catecholamine solubility and degradation, and increased sample solubility and stability.

### 2.2 Background

Catecholamines are a group of neurotransmitters and hormones derived mainly from the amino acid tyrosine. Dopamine, norepinephrine, and epinephrine (Figure 2.1) are

primarily synthesized in the adrenal medulla and in adrenergic neurons in the central nervous system.<sup>350</sup> Each of these catecholamines plays an important role in the sympathetic nervous system, specifically with the fight-or-flight response.

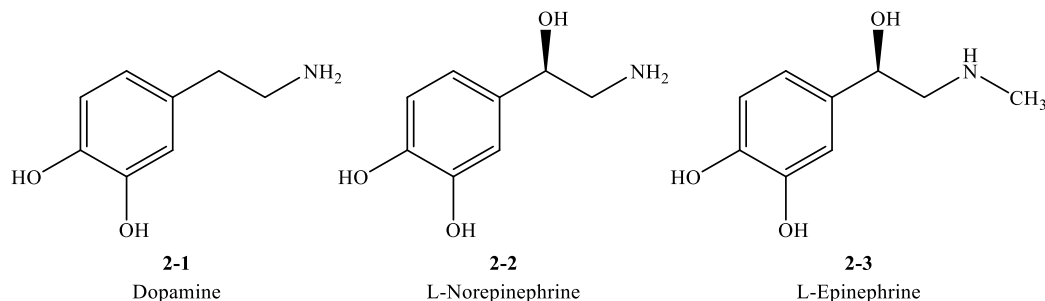


**Figure 2.1:** Chemical structures of the most prominent catecholamines.

Dopamine (**2-1**), the most prevalent catecholamine in the brain, is most commonly known as the chemical of pleasure, as it is released by environmental stimuli associated with reward. It has also been linked to motor and motivational functions, addiction, and other mental disorders.<sup>351-353</sup> Norepinephrine (**2-2**) is associated with the brain's response to stressful stimuli. It increases heart rate, blood pressure, and triggers the release of glucose in order to prepare the body to respond to said stimuli. It has also been linked to depression and post-traumatic stress disorder.<sup>354-355</sup> Epinephrine (**2-3**) is associated most closely with strong emotions such as fear or anger. Once released, epinephrine causes increased heart rate, blood pressure, and triggers the release of glucose.

### 2.2.1 Uses of Catechols in Medicine

In addition to their natural functions within the human body, catecholamines have been used in medicine. In 1960, dopamine deficiency in the striatum was first reported in connection with Parkinson's disease. This led to the usage of levodopa (**2-4**), a natural precursor to dopamine, as a treatment for Parkinson's disease (Figure 2.2).<sup>356</sup>

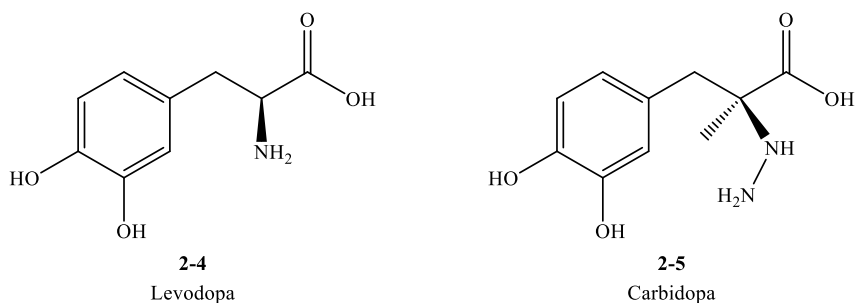


**Figure 2.2:** Chemical structures of Levodopa and Carbidopa.

Research into improving the effectiveness of Parkinson's treatment has included the synthesis of levodopa derivatives with the aim to increase treatment efficacy and searching for other analogues of dopamine that are more effective than levodopa.<sup>357-358</sup> Other research has gone into the creation of additional formulations that increase the efficacy of levodopa and the development of novel delivery systems, such as inhalation and transdermal patches.<sup>359</sup> Levodopa combined with carbidopa (**2-5**) is to this day the most frequently used treatment of Parkinson's disease.<sup>360</sup> Carbidopa is an aromatic amino acid decarboxylase inhibitor that helps prevent the decarboxylation of levodopa to dopamine outside the brain.<sup>361</sup> The addition of carbidopa to levodopa reduces the infusion rate required to produce a clinical response, as well as the time required for plasma clearance of levodopa. Additionally, dopamine has been implicated in the pathology of dementia, however its exact role in Alzheimer's disease remains unclear.<sup>362</sup> Recent studies validated the positive effects of dopamine derivatives on indicators of Alzheimer's disease such as metal ions, metal-free amyloid- $\beta$ , metal-bound amyloid- $\beta$ , and ROS.<sup>363</sup>

The most frequent usage of catecholamines in medicine is the utilization of epinephrine in the treatment of anaphylactic shock. First synthesized in 1906, it was primarily used in the treatment of asthma, croup, which is the infection of the upper airway,

and during surgery to prolong the duration of simultaneously administered local anesthetics.<sup>364-365</sup> In the 1960s, syringes prefilled with epinephrine were introduced to counteract anaphylaxis triggered by foods, medication, and insect venoms. The first epinephrine auto-injectors were introduced in 1980. To this day, epinephrine is the first drug to be administered in the treatment of anaphylactic shock as it is able to completely reverse most if not all symptoms in a matter of seconds.<sup>366</sup>

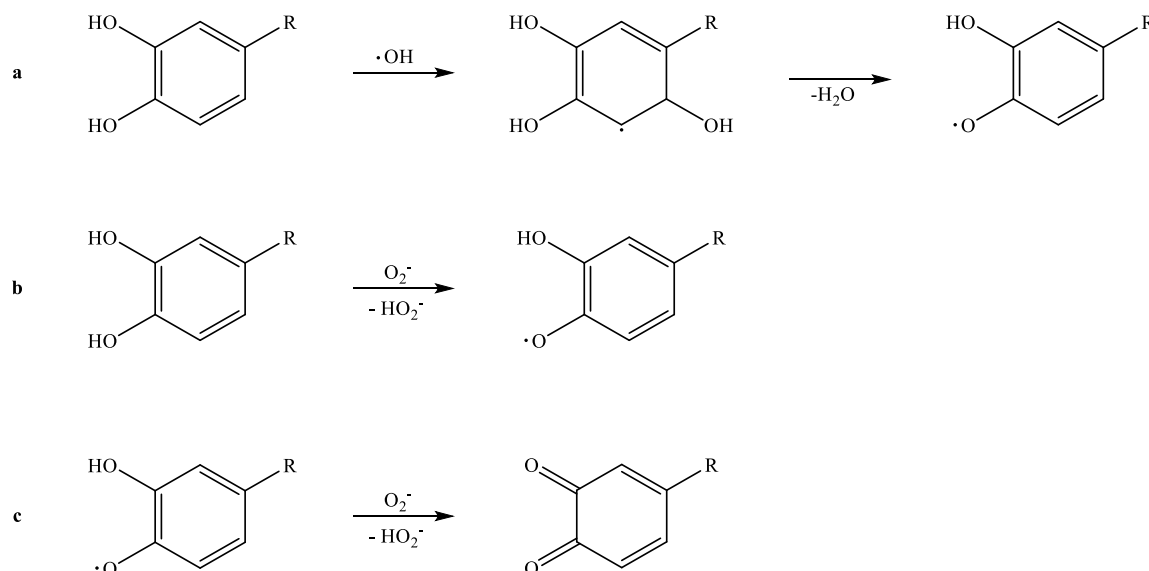
High doses of dopamine, norepinephrine, and epinephrine have also been studied as vasopressors in the mitigation of sepsis. However, studies have been inconclusive as some studies showed catecholamines caused no increase of blood flow in the desired locations, whereas other studies showed that catecholamines caused increased or decreased blood flow in the desired locations. No greater effect of metabolism, function, or survival rate was found.<sup>367-369</sup>

### 2.2.2 Catechol Degradation

Drug stability and degradation is an important part of ensuring the quality, efficacy, and safety of formulated drug products. Research has been done to study the effect of light and heat on drugs such as lovastatin, riboflavin, aztreonam, and chloroquine.<sup>370-371</sup> Studies have also implicated drug formulation, specifically comparing aqueous and solid state, and drug concentration in water also plays a role in drug decomposition.<sup>372-373</sup> The stability of catecholamines before their usage in the human body is therefore of concern. Understanding drug degradation is especially important in the treatment of life-threatening conditions, such as anaphylaxis, where catecholamines are stored in aqueous solution. The degradation mechanism of catecholamines has been extensively studied under pulse-

radiolysis and in the presence of enzymes such as superoxide dismutase.<sup>374-376</sup>

Catecholamines were found to undergo single electron oxidation that formed semi-quinones, which then underwent an additional single electron oxidation to form quinones (Scheme 2.1). The initial oxidation from catechol to semi-quinones could be caused by both hydroxyl radical and superoxide, whereas the second oxidation from semi-quinone to quinone can only occur with the assistance of superoxide.



**Scheme 2.1:** a) Scheme of the degradation of a catecholamine to a semi-quinone in the presence of hydroxyl radical. b) Scheme of the degradation of a catecholamine to a semi-quinone in the presence of superoxide. c) Scheme of the degradation of a semi-quinone to a quinone in the presence of superoxide.

A variety of external factors can increase the rate of auto-oxidation of catecholamines. The most obvious factor is the pH of the surrounding solution, as the first mechanistic step of the oxidation of catecholamines is the deprotonation of a single hydroxyl group. It is therefore unsurprising that studies have found that the rate of catecholamine degradation increases as pH increases.<sup>377-378</sup> Another factor is light, especially UV-visible light, which can photoactivate catecholamines in order to induce oxidation.<sup>379-380</sup> The absorbance of light causes a  $\pi \rightarrow \pi^*$  transition, which in turn can lead to the generation of a free radical

intermediate.<sup>379</sup> This intermediate has been hypothesized to then react with oxygen in order to form adrenochrome and H<sub>2</sub>O<sub>2</sub>. The last major external promoter of catecholamine degradation is heat. Studies have found that temperatures below room temperature aid in preventing degradation of catecholamines.<sup>381-382</sup> It follows that temperatures above room temperature would increase the rate of degradation of catecholamines.

### 2.2.3 Methods of Studying Catechol Degradation

Many methods have been utilized in the past to study the degradation of catecholamines. Early studies utilized UV-visible spectroscopy to determine the rate and amount of degradation occurring.<sup>379-380, 383</sup> This is done by monitoring the change in optical density or absorbance at wavelengths corresponding to the starting catecholamines and the expected degradation products. UV-visible spectroscopic analysis is the most facile method but typically does not work for more complex systems, where the catecholamine and any degradant may absorb in the same range of wavelengths. Liquid chromatography with tandem mass spectrometry (LC-MS/MS) is another powerful technique that has been used to analyze catecholamines and various metabolites.<sup>384-385</sup> Different catecholamine degradants are separated and quantified through the use of liquid chromatography and are then analyzed and identified through the attached tandem mass spectrometer. The most commonly used tool for analyzing catecholamine degradation is high-pressure liquid chromatography (HPLC) in tandem with either UV-visible spectroscopy or electrochemical detectors.<sup>381, 386-389</sup> Reverse phase chromatography separate catecholamines and their degradants, and the attached spectrometer or detector identifies or quantifies each compound. This separation is the major benefit of LC-MS/MS and

HPLC over conventional UV-visible analysis. The separation of analytes allows for clearer quantification and identification. However, this usually involves much optimization and troubleshooting in order to prevent coelution.

Each analytical method and catecholamine have different conditions for running and analyzing samples. Work has been done by the Sogorb group to make an analytical method for the simultaneous determination of multiple catecholamines, however this method was not tested on samples that underwent forced degradation.<sup>390</sup> To the best of my knowledge, no report has been made of a method that is able to analytically determine the amount of every catecholamine and its corresponding degradation. In order to do so, a starting point must be established. Current epinephrine analytical methods are an attractive starting point, as epinephrine is used in expensive auto-injectors which experience degradation and need to be replaced. However, even amongst methods solely for the purpose of analyzing epinephrine, there is no consensus. For instance, solvent systems used to analyze epinephrine vary from single solvent systems consisting of aqueous buffers, to mixed solvent systems with water and acidified organic solvents, to single solvent systems consisting of methanol with dilute aqueous acid.<sup>386, 390-397</sup> Another drawback with most currently published methods is the choice of internal standard. The most frequently used internal standard, 3,4-dihydroxybenzylamine,<sup>394, 397-398</sup> has the disadvantages of eluting closely to epinephrine and degrading through the same mechanisms as epinephrine.

The final incompatibility with current methodologies of epinephrine degradation analysis, and what is required for this planned study, is that previous methodologies have no intentional control for epinephrine solubility and shelf stability of samples. This is

especially important for methods that use harsh conditions, as initial experiments performed indicated that not all compounds were soluble after forced degradation. Catecholamine solubility, including epinephrine, is highly dependent on the pH of the solution that it is in – with minimal solubility reported at pH 9.4.<sup>399</sup> The pH of the solution also plays a role in catecholamine degradation, with higher pH values causing more degradation. This is important for this study, as samples will be sitting at room temperature for nearly 20 hours before analysis by HPLC, due to the large number of samples being analyzed in triplicate. Therefore, an ideal methodology would also ensure that the pH values of prepared samples were low in order to optimize the solubility of the samples as well as the stability of the samples. Herein, I describe the development of a sample preparation and analytical HPLC method to be used in the study of the degradation of any catecholamine, aiming to tackle the current limitations of existing methods.

### 2.3 Results and Discussion

Epinephrine was chosen as the model compound for this study because it is a life-saving drug and because epinephrine in auto-injectors undergo degradation and are expensive to replace. In order to successfully develop a complete analytical method to determine the degradation of any catecholamine, a set of experimental conditions must be determined. This includes determining a solvent system and HPLC method that adequately separates catecholamines from each other, determining an internal standard that is stable and elutes at a time that will not interfere with catecholamines nor their degradants, and a sample preparation method that ensures sample solubility and stability. These conditions

were first determined with epinephrine and were then extended to a number of other catecholamines in order to demonstrate the method's versatility.

Additionally, the experiments performed to validate this method will utilize partially degraded epinephrine, to verify that the method will work for analyzing degradation of catecholamines, and gallium nitrate to confirm separation of analytes from UV-visible absorbing additives.

### 2.3.1 Solvent Systems

The first step to developing the analytical method was to determine the solvent system. Identifying which solvents to use was critical for the separation of analytes in order to accurately identify total concentration and degradation. Typical HPLC mobile phases combine an aqueous mobile phase, typically water or a buffer solution, and a hydrophilic organic solvent, such as acetonitrile or methanol. Methods that have been previously utilized to study epinephrine degradation were then tested. Two HPLC methods were chosen. The first had been used to study the sulfonation and racemization pathways of epinephrine utilizing a flow rate of 0.7 mL/min and a mobile phase of 89.93% 5 mM pH 7.0 ammonium acetate buffer, 10% acetonitrile, and 0.07% formic acid.<sup>392</sup> The second method tested was previously used to study the thermal degradation of epinephrine auto-injectors. This HPLC method utilized a flow rate of 0.5 mL/min and a mobile phase of 0.02 M pH 2.5 phosphate buffer with 0.25 g/L EDTA and 0.06 g/L sodium octyl sulfate.<sup>386</sup> These two methods were then tested on samples of epinephrine that had been treated with 10 equivalents of gallium nitrate and placed into 30 °C water baths for 7 days to induce degradation (Figure 2.3).

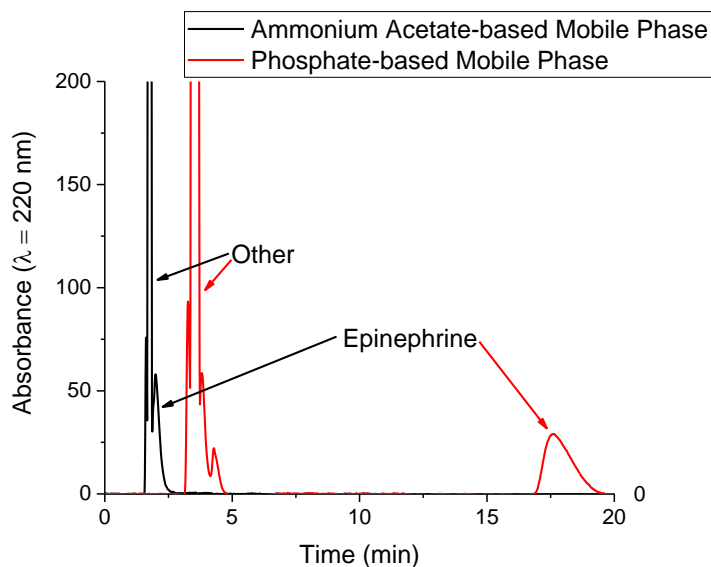


**Figure 2.3:** HPLC traces of heated epinephrine solutions with different mobile phases. T = 30 °C, t = 7 days,  $\lambda = 220$  nm, 10 equivalents of  $\text{Ga}(\text{NO}_3)_3$ .

Both methods were able to separate epinephrine from other UV-visible absorbing species, however the ammonium acetate-based solvent system produced retention times of 2.7 minutes for epinephrine and 2.1 minutes for other UV-visible absorbing species, which were too close together to prevent overlapping peaks. The phosphate-based mobile phase produced retention times of 17.6 minutes for epinephrine and 3.8 minutes for other UV-visible absorbing species, which were far enough apart to prevent peak overlap. Therefore, the phosphate-based mobile phase was chosen for further study.

### 2.3.2 Internal Standards

After selecting the solvent system to be used, the next step for developing the analytical method was to determine the optimal internal standard. Internal standards are utilized in order to correct analyte absorbance values for any errors in sample preparation, inconsistencies in sample injection volume, or errors in UV-visible absorption. Typically, HPLC internal standards are compounds that have similar structures and properties to the

analyte of interest, such as 3,4-dihydroxybenzylamine. To overcome the previously mentioned issues of degradation and similar retention times, different internal standards were tested. 2,3-Dihydroxybenzoic (2-6) acid was selected as a compound with a very similar structure to epinephrine, as it contains a catechol. Phenol (2-7), containing a singular aromatic hydroxyl group, was selected as a compound with a moderate similarity to epinephrine. Fluorescein was the final tested internal standard, which has the least similar chemical structure to epinephrine (2-8).

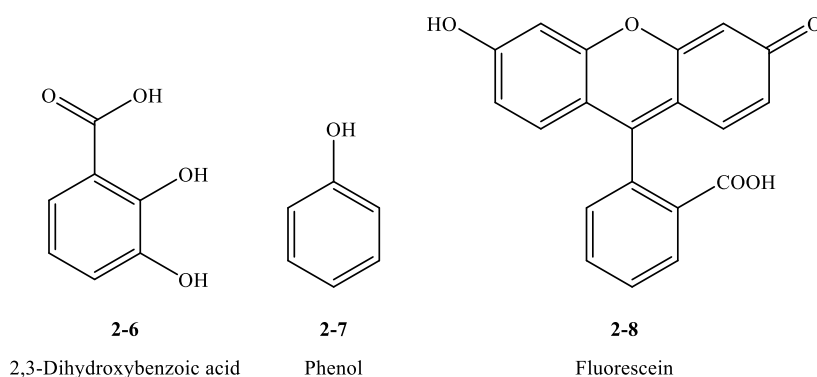


**Figure 2.4:** Chemical structures of tested internal standards.

Initial tests were performed with these internal standards using the phosphate-based method, but even with 60 minutes of elution time, the internal standards were never observed. Therefore, alterations to the original literature method were necessary in order to continue with these internal standards. The elution conditions were changed to include a linear gradient of acetonitrile, with final return to the phosphate-based mobile phase. These new elution conditions retained the ability to separate epinephrine from other UV-visible absorbing species, while now eluting each of the prospective internal standards (Figure 2.5). Additionally, the retention time of epinephrine became 6.6 minutes.

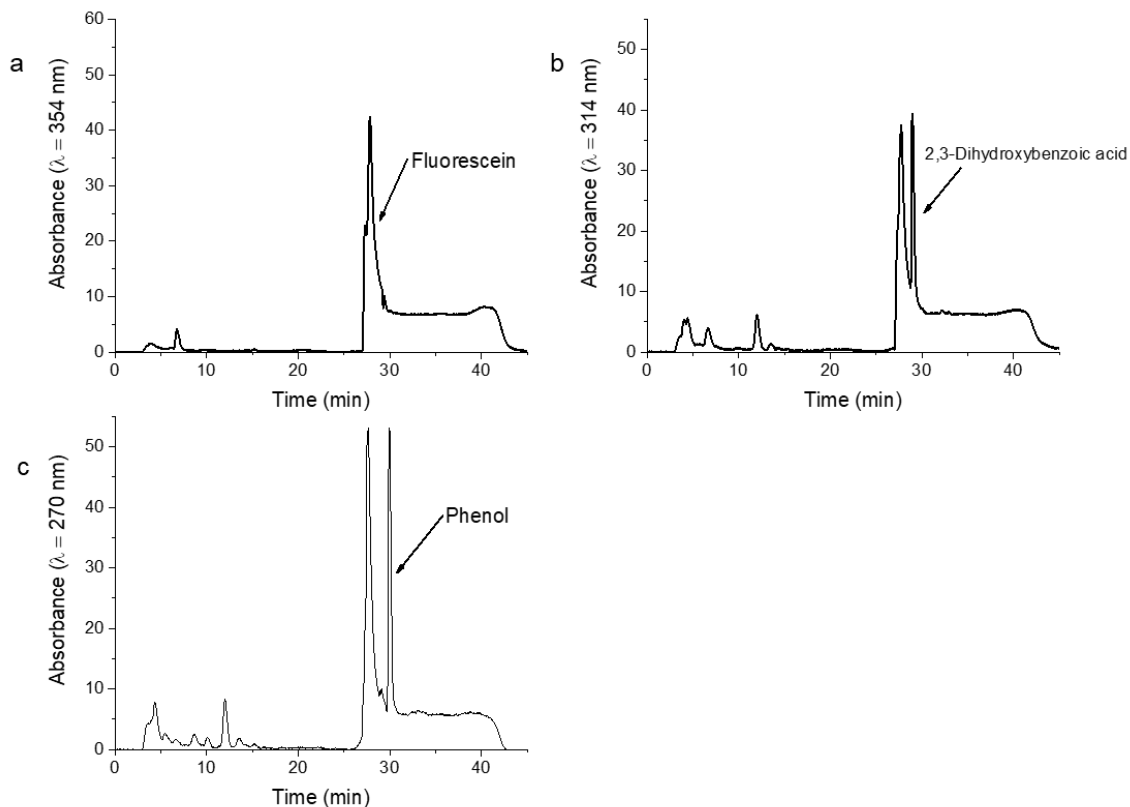


**Figure 2.5:** a) HPLC trace of heated epinephrine solution with fluorescein internal standard. b) HPLC trace of heated epinephrine solution with 2,3-dihydroxybenzoic acid internal standard. c) HPLC trace of heated epinephrine solution with phenol internal standard. T = 60 °C, t = 6 days,  $\lambda$  = a) 354 nm b) 314 nm c) 270 nm, 0 equivalents of  $\text{Ga}(\text{NO}_3)_3$ .

The downsides to this new set of elution conditions includes the creation of a new solvent front peak in the UV-visible spectra, as well as an increase in the background absorbance. However, both issues are easily resolved through subtraction of a blank. The elution of fluorescein coincides with the solvent front peak at 27 minutes and the elution of 2,3-dihydroxybenzoic acid occurs 29 minutes, which are both too close to the solvent front peak. On the other hand, phenol eluted at 31 minutes, which allowed for a clean integration of the peak. Therefore, phenol was selected as the internal standard for further study.

### 2.3.3 Sample Preparation

The final step of method development was optimizing HPLC sample preparation in order to ensure complete sample solubility as well as stability. This was necessary as sample degradation can create insolubilities, and samples that recently underwent degradation are unlikely to be stable. This was especially important when running experiments in triplicate, as the run time of one set of samples with 45-minute run times can last many hours. Two HPLC sample preparation methods were tested: a more traditional sample preparation method without pH adjustment and a novel method that utilized the addition of 100  $\mu\text{L}$  of 1 M HCl to considerably reduce the pH in order to ensure sample solubility and stability. Both sets of HPLC samples were made immediately after thawing the previously frozen aliquots in order to prevent degradation before HPLC sample preparation. Additionally, both sample preparation methods were tested without (Figure 2.6a) and with (Figure 2.6b) gallium nitrate at basic and acidic pHs to validate epinephrine sample solubility over a wide pH range.

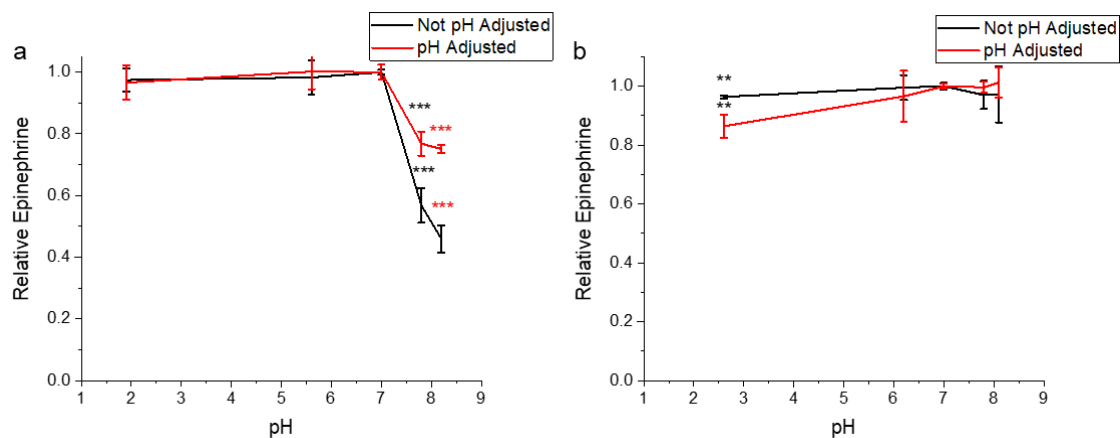


**Figure 2.6:** Relative epinephrine values for epinephrine solutions with a) 0 equivalents of  $\text{Ga}(\text{NO}_3)_3$  and b) 1 equivalent of  $\text{Ga}(\text{NO}_3)_3$  at various pH values tested with sample preparation method without pH adjustment or a new sample preparation method with pH adjustment. Error bars represent  $\pm$  one standard deviation,  $n = 3$ . \* Indicates a statistically significant difference (2 sample  $t$ -test, \*:  $p < 0.05$ , \*\*:  $p < 0.03$ , \*\*\*:  $p < 0.01$ ).

Sample epinephrine ( $E_S$ ) values are found by taking the integrated absorbance of the epinephrine peak ( $A_E$ ) at 280 nm and dividing by the integrated absorbance of the internal standard peak ( $A_{IS}$ ) at 270 nm (Eq. 2.1).

$$E_S = (A_E) / (A_{IS}) \quad (\text{Eq. 2.1})$$

The relative epinephrine ( $E_R$ ) of each sample is then calculated by dividing by the value of the sample at pH 7 (Eq. 2.2).

$$E_R = E_S / (E_S \text{ at pH7}) \quad (\text{Eq. 2.2})$$

$E_R$  values for samples without gallium were unchanged for pH values more acidic than 7, which is unsurprising given that epinephrine is soluble at acidic pHs. However, for the two basic pH values of 7.8 and 8.2, there is a significant increase in  $E_R$  between the sample preparation method without pH adjustment and the newer method that reduced pH values, indicating that the newer method was better at maintaining sample solubility. This benefit is lost in the samples with 1 equivalent of gallium nitrate, which is hypothesized to be due

to coordination between gallium and epinephrine (Figure 2.6b). This coordination complex would have a higher net charge, and therefore have better water solubility at basic pHs.

Additionally, sample stability over time was measured. This was done by dividing the sample epinephrine values of the second and third replicate of each measurement by the sample epinephrine value of the first replicate (Figure 2.7). On average, the values of samples prepared with the new sample preparation method retained 1% more of their initial epinephrine concentration per 5 hours than the samples prepared without pH adjustment. This effect is greatly magnified in samples that are unstable, as relative epinephrine values dropped by 10% for samples without added HCl. Again, this effect is somewhat lost with the introduction of 1 equivalent of gallium nitrate, likely caused by the binding of epinephrine to gallium.

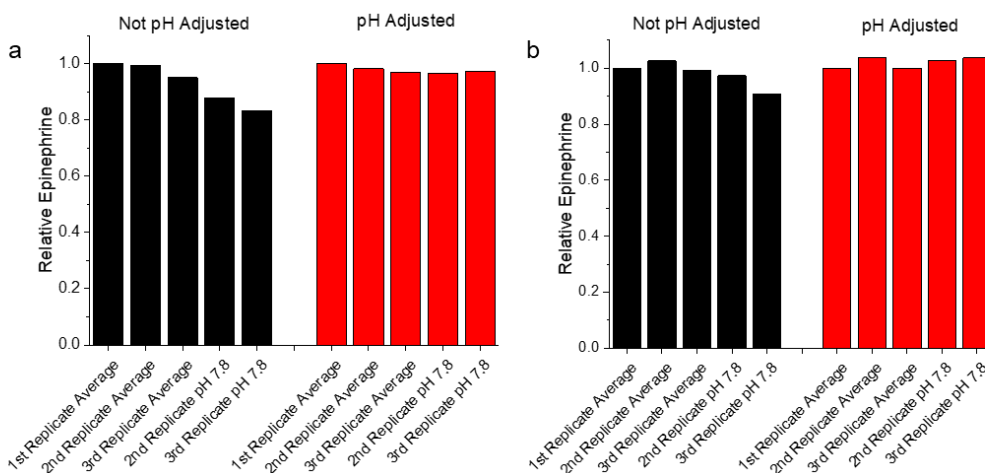


**Figure 2.7:** Relative epinephrine values for epinephrine solutions with a) 0 equivalents of Ga(NO<sub>3</sub>)<sub>3</sub> and b) 1 equivalent of Ga(NO<sub>3</sub>)<sub>3</sub>. All values have been normalized to 1<sup>st</sup> replicate measurements and averages are for all pH values measured.

### 2.3.4 Extension to Other Catecholamines

The solvent system, internal standard, and sample preparation method were then tested on levodopa and norepinephrine in order to confirm reproducibility with other

catecholamines. Levodopa and norepinephrine were chosen because they are both drugs that are used within the field of medicine and are prone to the same oxidative degradation as epinephrine. Under the chosen solvent system and elution method, levodopa had a retention time of 10.5 minutes and norepinephrine had a retention time of 4.7 minutes, which are both significantly separated from epinephrine at 6.6 minutes (Figure 2.8).

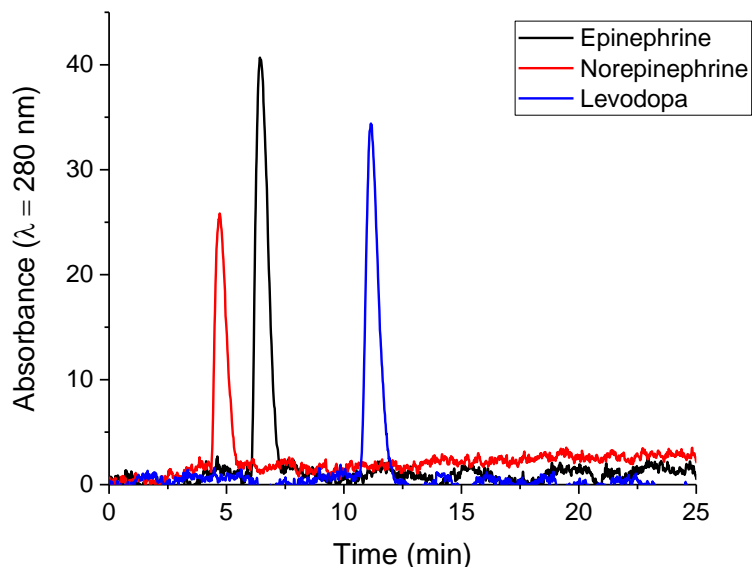


**Figure 2.8:** Overlapping HPLC traces of epinephrine, norepinephrine, and levodopa.

Sample solubility and stability was measured for levodopa and norepinephrine in the same manner as epinephrine. Both levodopa and norepinephrine exhibited increased sample solubility with the new sample preparation method at basic pHs without gallium nitrate (Figure 2.9).

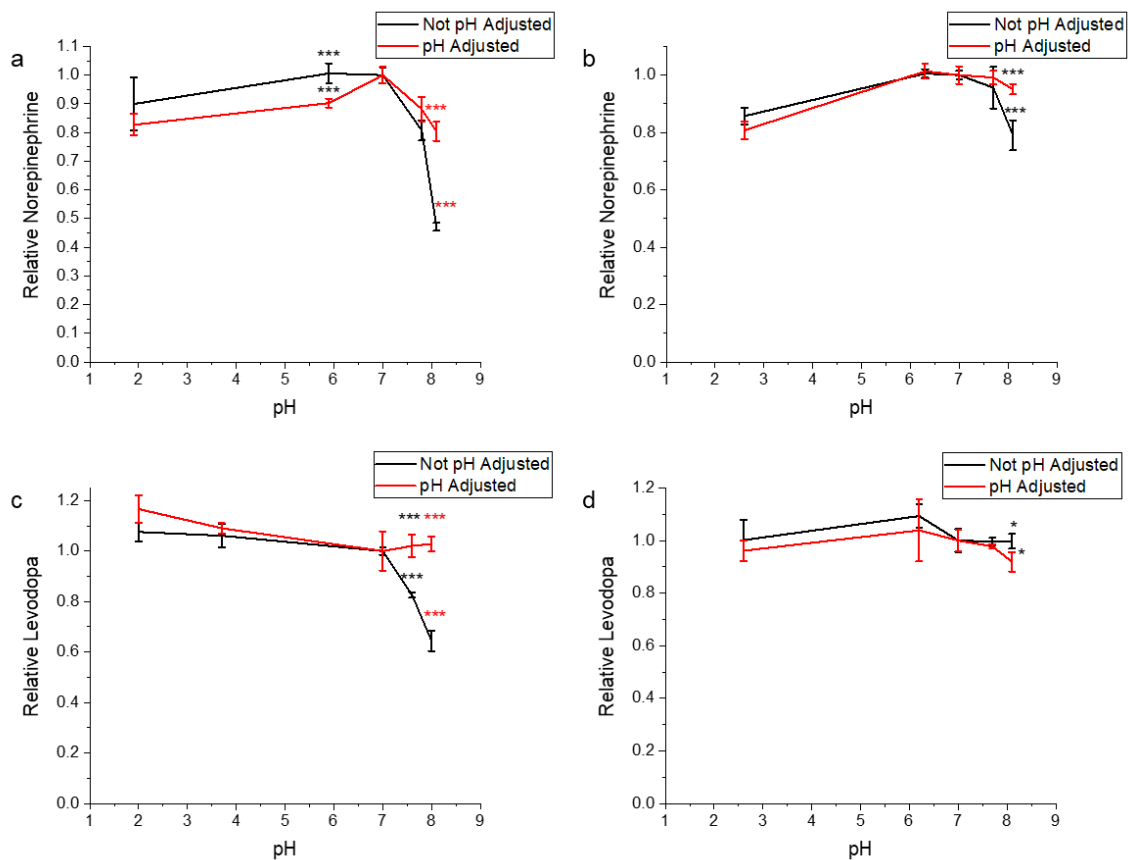


**Figure 2.9:** a) Relative norepinephrine values of norepinephrine solution with 0 equivalents of Ga(NO<sub>3</sub>)<sub>3</sub>. b) Relative norepinephrine values of norepinephrine solution with 1 equivalent of Ga(NO<sub>3</sub>)<sub>3</sub>. c) Relative levodopa values of levodopa solution with 0 equivalents of Ga(NO<sub>3</sub>)<sub>3</sub>. d) Relative levodopa values of norepinephrine solution with 1 equivalent of Ga(NO<sub>3</sub>)<sub>3</sub>. Each sample was tested at various pH values with the sample preparation method without pH adjustment and the new sample preparation method with pH adjustment. Error bars represent ± one standard deviation, n = 3. \* Indicates a statistically significant difference (2 sample *t*-test, \*: p < 0.05, \*\*: p < 0.03, \*\*\*: p < 0.01).

With the addition of gallium nitrate, only the most basic sample of norepinephrine remained more soluble while both sample preparation methods were equivalent for the rest. Stability tests were less conclusive, with the only significant difference between the two sample preparation methods being norepinephrine with 1 equivalent of gallium at basic pH values.

## 2.4 Conclusions

A new method of analyzing catecholamine degradation was developed. Through the selection of a solvent system and the optimization of an elution method, the differentiation of epinephrine, levodopa, norepinephrine, and added UV-visible absorbing compounds was possible. The addition of an internal standard allowed for more accurate measurements of degradation and solubility. This in turn allowed for the improvement of sample preparation methods with regards to compound solubility and shelf stability. In combination, these improvements will allow for the study of catecholamines under any conditions that have undergone different types of forced degradation.

## 2.5 Experimental

### 2.5.1 General Considerations

Unless otherwise noted, reagents were purchased from commercial suppliers and used without further purification. All water is distilled water that was further purified by a Millipore cartridge system (resistivity 18 M $\Omega$ ). Analytical HPLC was performed with a Varian Prostar 210 HPLC instrument (Agilent, Santa Clara, CA) equipped with a Varian ProStar 335 diode array detector and an Agilent Zorbax Eclipse XDB-C18 column (5  $\mu$ m pore size, 4.6  $\times$  150 mm). All pH measurements were performed using a Thermo Scientific Ag /AgCl refillable probe and a Thermo Orion 3 Benchtop pH meter.

### 2.5.2 Solvent Systems

**Water and Acetonitrile HPLC** Two 5-dram scintillation vials were prepared with NaCl (60. mg, 1.0 mmol) and Na<sub>2</sub>S<sub>2</sub>O<sub>5</sub> (17 mg, 0.089 mmol) in 9 mL of water. To one vial Ga(NO<sub>3</sub>)<sub>3</sub> (14 mg, 0.055 mmol) was added. To each vial epinephrine (10. mg, 0.055 mmol)

in 1 mL of water was added. Each vial was then shaken thoroughly, and pH adjusted until the pH was between 2 and 5. The vials were then placed in a 30 °C bath for 48 hours. Samples were prepared for HPLC by mixing 170  $\mu$ L of the sample with 30  $\mu$ L of acetonitrile. The samples were then filtered through 0.2  $\mu$ m polypropylene (PP) syringe filters and loaded onto the HPLC and analyzed with a flow rate of 1.0 mL/min with the following elution conditions: 15% CH<sub>3</sub>CN / 85% water from 0 to 2 minutes, a linear gradient to 100% CH<sub>3</sub>CN until 23 minutes, 100% CH<sub>3</sub>CN until 26 minutes, followed by a linear gradient back to 15% CH<sub>3</sub>CN / 85% water at 30 minutes which was held until 32 minutes.

**Ammonium Acetate-Based Mobile Phase** Formic acid (0.35 mL, 9.3 mmol) and ammonium acetate (190 mg, 2.5 mmol) were dissolved into 450 mL of water and 50 mL of acetonitrile. This solution was then pH titrated to a final volume of 500 mL and a pH of 7.0.

**Phosphate-Based Mobile Phase** Disodium EDTA (0.500 g, 1.49 mmol), sodium phosphate monobasic (5.52 g, 4.60 mmol), and sodium octyl sulfate (0.120g, 0.517 mmol) was dissolved in 1.95 L of water. This solution was then pH titrated to a final volume of 2.00 L and a pH of 2.50.

**Ammonium Acetate and Phosphate HPLC** Three 5-dram scintillation vials were prepared with NaCl (60. mg, 1.0 mmol). No Ga(NO<sub>3</sub>)<sub>3</sub> was added to the first vial, 1 equivalent of Ga(NO<sub>3</sub>)<sub>3</sub> (14 mg, 0.055 mmol) was added to another, and 10 equivalents of Ga(NO<sub>3</sub>)<sub>3</sub> (140 mg, 0.55 mmol) was added to the last. Epinephrine (10. mg, 0.055 mmol) and 10 mL of water were then added to each vial, which was then shaken and heated in a

water bath at 30 °C for 48 hours. HPLC samples of each vial were then prepared by filtering 200 µL through 0.2 µm PP syringe filters. Each sample was then analyzed by both solvent systems, the ammonium acetate-based mobile phase and the phosphate-based mobile phase, with a flow rate of 0.5 mL/min from 0 to 30 minutes.

### 2.5.3 Internal Standards

**Internal Standards** Stock solutions of phenol, fluorescein, and 2,3 dihydroxybenzoic acid were prepared by dissolving 2 mg of each solid into 2 mL of water.

**Internal Standards HPLC Old Elution Method** A 5-dram scintillation vial was prepared with NaCl (60. mg, 1.0 mmol) and epinephrine (10. mg, 0.055 mmol). The solids were then dissolved into 10 mL of water and heated in a water bath at 60 °C for 6 days. Three HPLC samples were prepared by taking 200 µL of the degraded epinephrine solution and mixing in 50 µL of each internal standard stock solution, one sample per internal standard. Each sample was then analyzed with a flow rate of 0.5 mL/min of the phosphate-based mobile phase from 0 to 30 minutes.

**Internal Standards HPLC New Elution Method** A 5-dram scintillation vial was prepared with NaCl (60. mg, 1.0 mmol) and epinephrine (10. mg, 0.055 mmol). The solids were then dissolved into 10 mL of water and heated in a water bath at 60 °C for 6 days. Three HPLC samples were prepared by taking 200 µL of the degraded epinephrine solution and mixing in 50 µL of each internal standard stock solution, one sample per internal standard. Each sample was then analyzed with a flow rate of 0.5 mL/min with the following elution conditions: 100% of the phosphate-based mobile phase from 0 to 20 minutes, a linear gradient to 50% phosphate-based mobile phase and 50% CH<sub>3</sub>CN from 20 to 22.5

minutes, 50% phosphate-based mobile phase and 50% CH<sub>3</sub>CN from 22 to 32 minutes, a linear gradient to 100% phosphate-based mobile phase from 32.5 to 35 minutes, and 100% phosphate-based mobile phase from 35 to 45 minutes.

#### 2.5.4 Sample Preparation

**General Sample Preparation Procedure** A 5-dram scintillation vial was prepared with NaCl (60. mg, 1.0 mmol), the catecholamine (epinephrine, 10. mg, 0.055 mmol; norepinephrine, 10. mg, 0.059 mmol; levodopa, 10. mg, 0.051 mmol), and Ga(NO<sub>3</sub>)<sub>3</sub> (0 equivalents, 0 mg, 0 mmol; 1 equivalent, 14 mg, 0.055 mmol). Then 9 mL of 250 mM pH 7.0 tris(hydroxymethyl)aminomethane (Tris) buffer was added to the vial which was then sonicated to aid in the dissolution of epinephrine. The solution was then pH adjusted back to 7.0 and taken to a final volume of 10 mL with the addition of more 250 mM pH 7.0 Tris. A 500 µL aliquot of the sample was taken and then 20 µL of 6M HCl was added. The pH was measured, another 500 µL aliquot of the sample was taken for the first acidic sample, and then 20 µL of 6M HCl was added. The pH was measured again, another 500 µL aliquot was taken for the second acidic sample, and 40 µL of 50% NaOH was added. The pH was measured again, another 500 µL aliquot was taken for the first basic sample, and 20 µL of 50% NaOH was added. The pH was measured and a final 500 µL aliquot was taken for the second basic sample. To prepare the HPLC samples without pH adjustment, 200 µL of each aliquot was mixed with 100 µL of internal standard. These mixtures were vortexed and then pushed through 0.22 µm nylon syringe filters before being loaded onto the HPLC. To make the HPLC samples with pH adjustment, 200 µL of each aliquot was mixed with 100 µL of internal standard and 100 µL of 1M HCl. These mixtures were vortexed and

then pushed through 0.22  $\mu\text{m}$  nylon syringe filters before being analyzed by the new elution method.

### **3. Gallium Mediated Prevention of Epinephrine Degradation**

#### **3.1 Synopsis**

Epinephrine auto-injectors are commonly used to treat anaphylactic shock. Epinephrine experiences degradation caused by high pH, heat, and light which can make the auto-injectors unsafe to use. Additionally, the formulation of epinephrine auto-injectors is quite acidic, which causes the injection to be more painful than it needs to be. The creation of an epinephrine prodrug could solve both of these problems; however, conventional prodrugs of epinephrine cannot be used to treat anaphylactic shock due to their long half-lives. A metal-based prodrug of gallium-bound epinephrine provides an attractive alternative. Gallium complexes with catecholamines are known to be stable and gallium is known to be kinetically labile, redox inactive, and non-toxic at concentrations necessary for an epinephrine auto-injector. Multiple forced degradation studies were performed on epinephrine solutions with varying equivalents of gallium which were then analyzed by the previously described analytical method. Optimal gallium concentration was found to be between 1 and 3 equivalents and stabilization of epinephrine solutions was seen in conditions up to 50 °C and under UV-visible light.

#### **3.2 Background**

Epinephrine is a lifesaving catecholamine that is used in the treatment of anaphylactic shock. The most common method of administering epinephrine in response to anaphylactic shock is through the use of an auto-injector. Epinephrine auto-injectors contain a solution of epinephrine, usually at a concentration of 1 mg/mL, with added sodium chloride, sodium metabisulfite, and hydrochloric acid. For those that cannot afford

or do not have access to auto-injectors, epinephrine solutions are typically provided in an ampule or a prefilled syringe.<sup>400</sup> These solutions are typically injected into the skin or muscle, where the epinephrine is then absorbed into the bloodstream.<sup>401</sup> Once in the bloodstream, epinephrine is delivered throughout the body where it is able to counteract the effects of anaphylactic shock as an  $\alpha$ - and  $\beta$ -adrenergic receptor agonist.<sup>402</sup>

When an antigen enters the body, the body typically responds in one of two ways. The first is an antibody-antigen response, in which the immunoglobulin IgE is produced.<sup>403</sup> IgE attaches to mast cells, where it is able to recognize the antigen and facilitate the release of inflammatory mediators such as histamine. The second is the direct activation of mast cells without the aid of IgE, which typically occurs on the first encounter with an antigen. Both responses lead to anaphylactic shock, which is marked by a drop in blood pressure, vasodilation, bronchoconstriction, and general swelling caused by increased capillary permeability. As an  $\alpha$ -adrenergic receptor agonist, epinephrine activates blood vessel constriction, resulting in increased blood pressure and decreased angioedema.<sup>402</sup> As a  $\beta$ -adrenergic receptor agonist, epinephrine induces faster and harder heartbeats and bronchodilation. The activation of  $\beta$ -adrenergic receptor also results in the increase of cyclic adenosine monophosphate in mast cells and basophiles, which inhibits the release of additional inflammatory mediator. These effects combined make epinephrine an excellent treatment for anaphylactic shock.

Solutions of epinephrine have been shown to be prone to degradation which causes concentrations to go below recommended levels after just two years under optimal storage conditions.<sup>392</sup> This is problematic as maintaining epinephrine concentration is critical for

ensuring the efficacy of injectable epinephrine. Another concern is the production of adrenochrome, one of the oxidative degradation products of epinephrine (**3-3**).<sup>404</sup> At one point adrenochrome was thought to be a hallucinogenic, however it is now classified as a psychoactive substance – which would be detrimental to give to someone undergoing anaphylactic shock.<sup>405</sup> Additionally, the replacement of an epinephrine auto-injector can cost over \$300, which is a high cost for a lifesaving drug.<sup>406</sup> In the current formulation of epinephrine auto-injectors, steps have been taken in the effort to prevent epinephrine degradation. Sodium metabisulfite ( $\text{Na}_2\text{S}_2\text{O}_5$ ) is an inorganic salt that is added to the formulation as an antioxidant and preservative.<sup>393, 407</sup> In addition to increasing stability, the addition of  $\text{Na}_2\text{S}_2\text{O}_5$  also results in the formation of an additional sulfonated degradation product (**3-4**).<sup>392</sup>

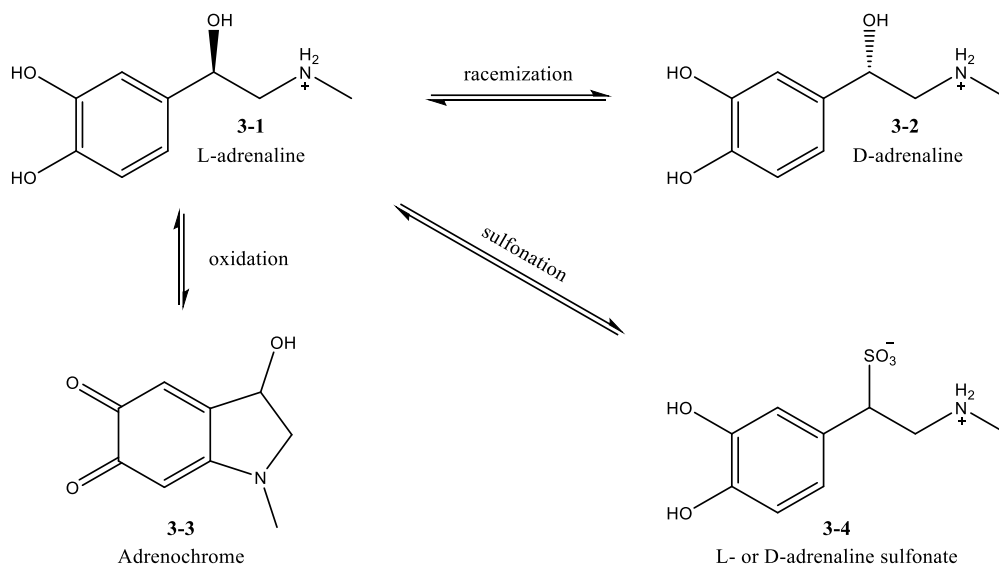


**Figure 3.1:** Degradation pathways of epinephrine and their respective products.

Epinephrine auto-injectors have also been formulated at a pH of 2.2 to 5, which helps prevent the oxidation of epinephrine by ensuring the protonation of the catechol.<sup>408</sup> It is also recommended to keep the epinephrine between 20 to 25 °C and protected from light,

as these exposures can lead to degradation. Even with these preventative measures, epinephrine degradation in auto-injectors still occurs at ambient temperatures.<sup>392</sup> Another drawback to this formulation is that studies have found that pH values of solutions that are not close to physiological pH cause additional pain upon injection.<sup>409</sup> Therefore, additional methods of stabilization that improve epinephrine stability and allow for a more neutral pH formulation are necessary.

### 3.2.1 Prodrugs

One potential method to stabilize epinephrine is through the use of a prodrug. In order to be effective, the prodrug would need to be stable in solution and able to rapidly release the active drug, epinephrine, in the order of seconds upon entering a human body. This is critical, as immediate response to anaphylactic shock is necessary to prevent symptom progression and the need for multiple doses.<sup>410</sup> Prodrugs of catecholamines have been studied since the late 1960's, with the research of lipophilic derivatives of norepinephrine that were capable of crossing the blood-brain barrier.<sup>411</sup> Subsequent work involved the synthesis of apomorphine diester prodrugs with the goal of prolonged biological activity,<sup>412-413</sup> and methyldopa prodrugs with the goal of increased gastrointestinal uptake.<sup>414-416</sup> Additionally, prodrugs of dopamine and levodopa have sparked interest for the treatment of Parkinson's disease. Research has shown that the therapeutic response to levodopa depends on the efficiency of absorption, therefore initial ester-based prodrugs of levodopa aimed to increase bio-availability.<sup>417</sup> By esterifying the catechol, the lipophilicity of the prodrugs can be increased up to 20,000 times that of the original drug, resulting in between 2.5 and 10 times greater concentration of the active drug

in the brain.<sup>418-422</sup> Newer generations of catecholamine prodrugs have been synthesized and studied for their effect on absorptivity, lipophilicity, half-life, blood brain barrier penetration, and overall efficacy. These prodrugs included derivatives of the native catecholamines with added amide functional groups,<sup>423-425</sup> amino acid functional groups,<sup>426-428</sup> and various heterocycles.<sup>429-430</sup>

In contrast to levodopa and dopamine, there has been significantly less work done to investigate prodrugs of epinephrine. The first reported usage of an epinephrine derivative for medicinal usage was the study of the two mono-methoxy derivatives and the dimethoxy derivative of epinephrine for their catatonic effects, however there was no indication that these compounds acted as a prodrug.<sup>431</sup> The first and only clinically used prodrug of epinephrine was first reported in 1976.<sup>432</sup> In addition to its typical usage as a treatment for anaphylactic shock, epinephrine has also been FDA approved to treat glaucoma. A concentrated solution of epinephrine is instilled directly into the eye, but due to its high polarity, epinephrine is poorly absorbed through the eye's lipoidal membrane. Therefore, a prodrug of epinephrine was necessary in order to improve lipoidal absorptivity, which was done through the addition of two pivaloyl groups to epinephrine to make dipivefrin (**3-5**).

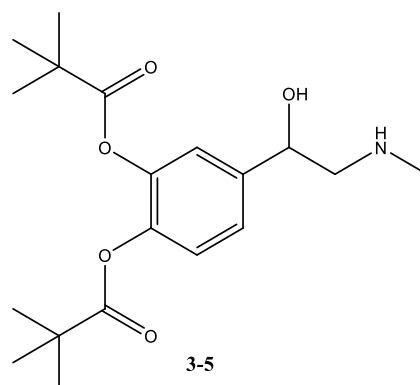


**Figure 3.2:** Chemical structure of dipivefrin.

Improved lipoidal absorptivity was confirmed because dipivefrin was about 100 times more effective than epinephrine in the management of glaucoma. Additionally, the prodrug had fewer side effects than epinephrine as expected since the hydrolysis of the pivaloyl groups had a half-life of nearly 2 hours in rabbit eye homogenate. This led to the prodrug being 100 to 400 times less effective than epinephrine on the cardiovascular system of cats and dogs. While dipivefrin had success in the treatment of glaucoma in humans, the half-life of nearly 2 hours would exclude dipivefrin from being efficacious in the treatment of anaphylactic shock. In order for a prodrug to be viable in the treatment of anaphylactic shock, the half-life would need to be in the order of seconds. The rate of most hydrolysis for esters is typically in the order of minutes, meaning that a non-covalent approach might be best for an epinephrine prodrug that is to be used for the treatment of anaphylactic shock.<sup>433-434</sup>

### 3.2.2 Metal Based Prodrug Approach

One approach to the creation of an epinephrine prodrug that can be used for the treatment of anaphylactic shock is that of a metal-based prodrug. Similar to that of previously described metal-based prodrugs, the coordination of epinephrine to a metal

center would deactivate and stabilize epinephrine. Care must be given to the metal of choice, given the various constraints of the system. As the metal would be injected into the human body, it is of utmost importance that it is non-toxic at the required concentrations. Catecholamines have two hydroxylate groups that act as hard bases and can coordinate to a metal center in a bidentate fashion. Therefore, the ideal metal would be hard as well in order to promote effective binding. The binding between epinephrine and the metal of choice would need to be thermodynamically stable in order to ensure the longevity of epinephrine auto-injectors, but not too stable as to prevent the dissociation of epinephrine once inside the body. The ideal metal would also be redox inactive in order to deter the oxidation of bound epinephrine. Lastly, the metal of choice needs to be labile as epinephrine dissociation needs to be rapid once the complex has entered the human body.

Gallium(III) is an excellent choice for this metal-based prodrug since it fulfills all the above requirements. Gallium nitrate has been previously FDA approved for the treatment of hypercalcemia at concentrations that far exceed the concentration required for an epinephrine auto-injector.<sup>340</sup> Gallium is a hard metal and has also been previously used to bind catechols, primarily in the form of siderophores and siderophore mimics.<sup>320, 343, 435</sup> Gallium(III) is unable to perform redox chemistry as it is a  $d^{10}$  metal.<sup>436</sup> Additionally, gallium is regarded as a labile metal meaning that rapid decomplexation of epinephrine should be achievable.<sup>437</sup> Once inside the body, gallium has been shown to hydrolyze to  $\text{Ga}(\text{OH})_3$  and bind to phosphate to form  $\text{HGaPO}_4^+$  which has a  $K_{\text{sp}}$  of  $10^{-21}$ .<sup>438</sup> With overall formation constants for binding gallium by tri-catecholate ligands being previously reported between 41.9 and 36.6, it is hypothesized that epinephrine will be released from

gallium upon entering the bloodstream.<sup>439</sup> The equilibrium constant for the exchange of gallium(III) from epinephrine to phosphate can be estimated from these values as  $2.3 \times 10^{19}$ , which heavily favors the formation of gallium phosphate. The coordination of epinephrine to gallium(III) has the added benefit of increasing the net charge on epinephrine (Figure 3.3).

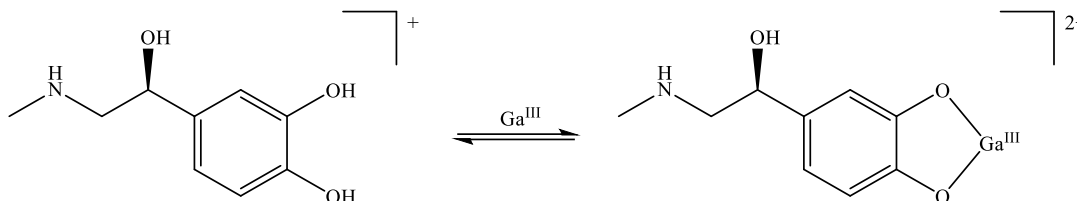


**Figure 3.3:** Net charge change with binding of epinephrine to gallium(III).

This is hypothesized to increase epinephrine's solubility in neutral pH ranges, allowing for a formulation to be made at a neutral pH. Therefore, it is hypothesized that the usage of gallium nitrate to create a metal-based prodrug should improve epinephrine stability and allow for a more neutral pH formulation. Herein, I describe the results of forced degradation studies in order to determine the best formulation of a gallium-based prodrug for epinephrine and provide future directions for continued work.

### 3.3 Results and Discussion

Gallium nitrate was chosen for the formation of a metal-based prodrug for epinephrine as it has been previously FDA approved for the treatment of hypercalcemia.<sup>339-340</sup> Gallium nitrate was administered through a continuous intravenous infusion at a dose of  $200 \text{ mg/m}^2$  per day at a concentration of  $25 \text{ mg/mL}$ .<sup>440</sup> Renal toxicity was dose-limiting, with a maximum tolerated dose of  $400 \text{ mg/m}^2$  per day.<sup>330-331, 441</sup> Additionally, the no-observed-adverse-effect level for gallium nitrate was found to be  $12.5 \text{ mg/kg}$  with an oral  $\text{LD}_{50}$  of  $1.75 \text{ g/kg}$  and an intraperitoneal injection  $\text{LD}_{50}$  of  $80 \text{ mg/kg}$  per day in mice.<sup>282, 442</sup>

These values are all multiple orders of magnitude larger than the amount used in this study. In order to test the ability of gallium nitrate to stabilize and prevent the degradation of epinephrine, various forced degradation studies were performed. Forcing conditions used were heat and UV-visible light, which are common factors responsible for the degradation of epinephrine in auto-injectors. Optimizations of sample preparation were necessary in order to properly account for pH changes caused by both the addition of gallium nitrate and the degradation of epinephrine. These optimizations and the resulting forced degradation studies are discussed below. Additionally, ideal gallium concentration was determined by comparing the degradation of epinephrine solutions with 1/3 of an equivalent, 1 equivalent, and 3 equivalents of gallium nitrate. The 1/3 of an equivalent concentration was chosen because epinephrine is expected to coordinate to gallium in a bidentate manner, which would lead to the formation of a six-coordinate complex based on literature precedence. Concentrations of 1 and 3 equivalents were tested because higher concentrations would shift the binding equilibrium towards epinephrine being bound by gallium.

### 3.3.1 Forced Degradation Studies

Forced degradation studies were performed on samples that contained the same concentration of epinephrine and salt as auto-injectors but were dissolved in 250 mM Tris buffer and pH adjusted back to 7.0 to determine gallium's efficacy at neutral pH. Buffer was necessary to prevent epinephrine degradation from lowering the pH of the solution, as this prevents degradation. Additionally, pH adjustment was shown to be necessary as the pH of samples with 1 and 3 equivalents of gallium nitrate in previous experiments were

lowered to 6.0 and 2.5 respectively. Although gallium nitrate is a Lewis acid, the change in pH was surprising due to the high concentration of buffer used. The change in pH is likely caused by two factors. First, the conjugate acid of Tris has a  $pK_a$  of 8.1 at 25 °C, which implies an effective buffer range of 7.1 to 9.1.<sup>443</sup> The result of being outside the effective buffer range is that the epinephrine samples at pH 7.0 have disproportionate amounts of Tris and its conjugate acid. Through the use of the Henderson-Hasselbalch equation, the theoretical concentrations of Tris and its conjugate acid are 18.4 mM and 231.6 mM respectively. The second factor is the dissolution of gallium nitrate. The samples with 1 and 3 equivalents of gallium nitrate contain 5 mM and 16 mM of gallium nitrate respectively. This is less than the concentration of basic Tris, which would suggest a minimal change in pH. However, previous studies have found that gallium(III) typically forms  $Ga(OH)_3$  in aqueous solution.<sup>444</sup> This implies that the dissolution of  $Ga(NO_3)_3$  into water could generate up to 3 protons per molecule of gallium nitrate. Therefore, the concentration of protons generated by gallium nitrate could be up to 16 mM and 49 mM for the samples with 1 and 3 equivalents of gallium nitrate respectively. The estimated pH value for the epinephrine solution with 1 equivalent of gallium nitrate, as calculated by the Henderson-Hasselbalch equation, is 6.08 which closely matches the experimental value. The samples with 3 equivalents of gallium nitrate would generate a higher concentration of protons than basic Tris, which corroborates the drastic changes in pH observed. The estimated pH value for the epinephrine solution with 3 equivalents of gallium nitrate is 1.5, which is significantly smaller than the experimental value of 2.5. This is likely caused by gallium nitrate generating fewer than 3 full equivalents of protons. An additional alteration

was that the antioxidant sodium metabisulfite, which is present in auto-injector formulations, was removed to allow increased epinephrine degradation. The degradation conditions tested were room temperature, heating at 30 °C, 40 °C, 50 °C, 60 °C, and room temperature under UV-visible light with a wavelength of 365 nm and 254 nm. Results from forced degradation studies can be seen below (Figure 3.4).

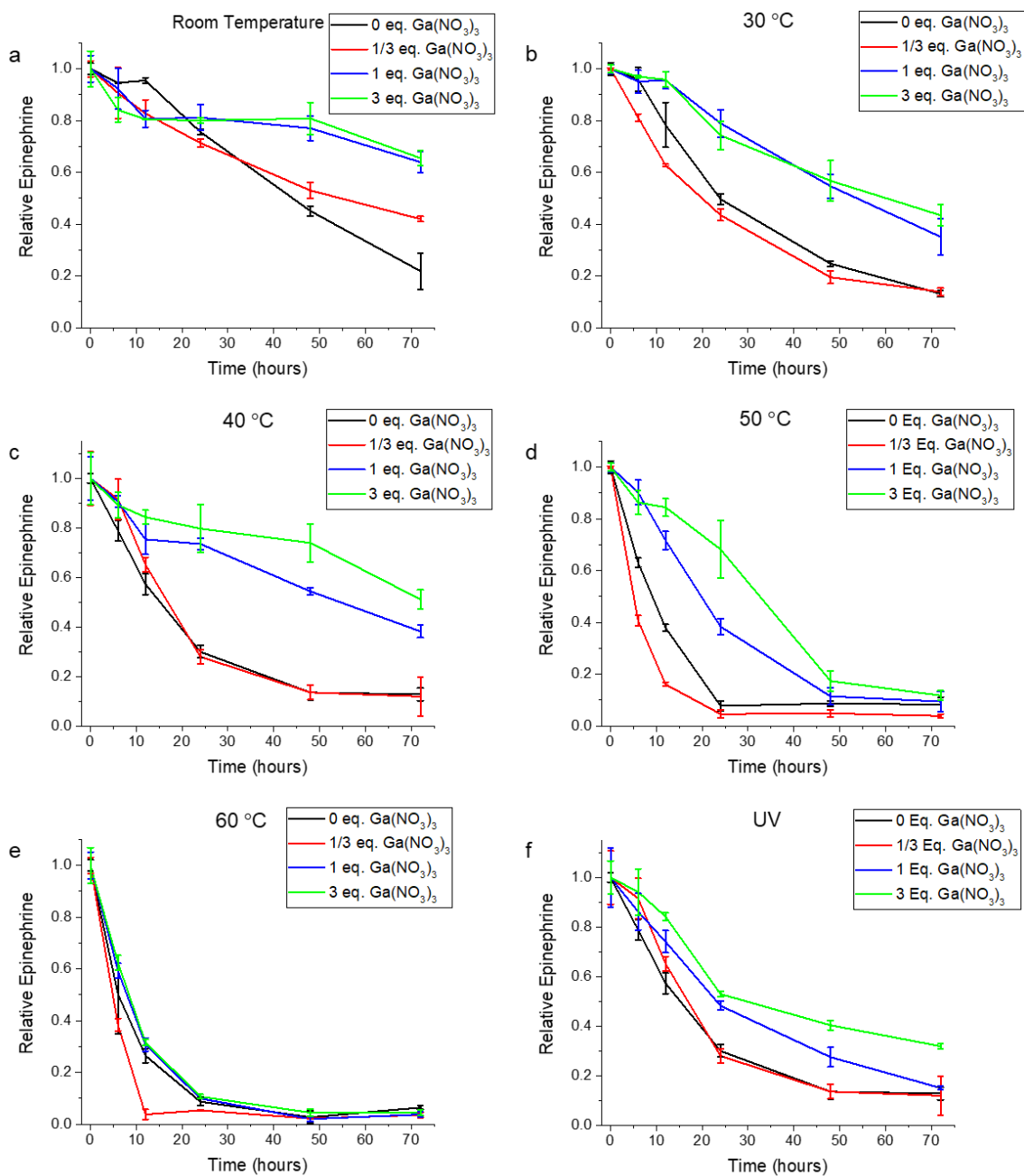


**Figure 3.4:** Relative epinephrine values for pH adjusted solutions of epinephrine in 250 mM pH 7.0 Tris buffer. Forced degradation conditions: a) room temperature, b) 30 °C, c) 40 °C, d) 50 °C, e) 60 °C, f) room temperature with exposure to 365 nm and 254 nm light. Error bars represent  $\pm$  one standard deviation,  $n = 3$ .

Statistical significance of relative epinephrine between samples was determined by a two samples *t*-test with *p* values less than 0.05.

At room temperature, the samples with 1/3, 1, and 3 equivalents of gallium nitrate experienced statistically equivalent epinephrine degradation until 24 hours. The sample with no gallium nitrate was an outlier with less degradation than the other samples up until 24 hours. After 24 hours the samples with 1 equivalent and 3 equivalents of gallium nitrate were statistically equivalent, with 65% of the initial epinephrine concentration remaining after 72 hours. One third of an equivalent of gallium nitrate to epinephrine reduced degradation, as 42% of the initial concentration remained after 72 hours, as compared to 22% in the control without gallium nitrate.

At 30 °C, differentiation in epinephrine degradation between the samples with 0 equivalents and 1 and 3 equivalents of gallium nitrate began at 12 hours. Statistically significant prevention of degradation was seen up until 72 hours where 0 and 1/3 of an equivalent of gallium nitrate retained 13% of their original epinephrine concentration and 1 equivalent and 3 equivalents of gallium nitrate retained 35% and 43% of their original epinephrine concentration, respectively. The sample with 1/3 of an equivalent of gallium nitrate experienced more degradation than the control until 72 hours of degradation.

At 40 °C, the difference in epinephrine degradation between the samples with 0 and 1/3 of an equivalent and the samples with 1 equivalent and 3 equivalents of gallium nitrate is most pronounced, especially after 24 and 48 hours. The difference in epinephrine degradation between the samples with 3 equivalents and 0 equivalents of gallium nitrate after 48 hours of 40 °C heating is 41%, whereas after the samples subject to 48 hours of 30 °C heating had a difference in epinephrine degradation of only 20%. This difference is caused by increased degradation in the samples with no gallium nitrate, as the samples with

1 and 3 equivalents of gallium nitrate experience similar degradation at 30 °C and 40 °C. Additionally, the sample with 3 equivalents of gallium nitrate experienced statistically significantly less degradation of epinephrine than the sample with 1 equivalent at 48 and 72 hours.

At 50 °C, the rate of degradation of each sample increases drastically. The samples with 1 equivalent and 3 equivalents of gallium nitrate still experienced significantly less degradation of epinephrine than the samples with 1/3 of an equivalent and no equivalents of gallium nitrate up until 48 hours. After 48 hours of heating at 50 °C, only the sample with 3 equivalents of gallium nitrate has a statistically significantly higher relative epinephrine value than the control. After 72 hours, all samples have equivalent or lesser relative epinephrine values than the control.

At 60 °C, the measured relative epinephrine values for the samples with 0, 1, and 3 equivalents of gallium nitrate are statistically equivalent for the entire experiment. These values being equivalent is likely due to the high temperatures causing the dissociation of epinephrine from gallium, preventing gallium from providing any stabilization to epinephrine in this experiment. The effect of temperature on epinephrine stabilization with gallium nitrate can also be seen by comparing the relative epinephrine values of samples with the same equivalents of gallium nitrate that have been heated at various temperatures (Figure 3.5). As the temperature increases, the amount of coordination that occurs between gallium(III) and epinephrine decreases, which in turn causes an increase in the degradation of epinephrine.

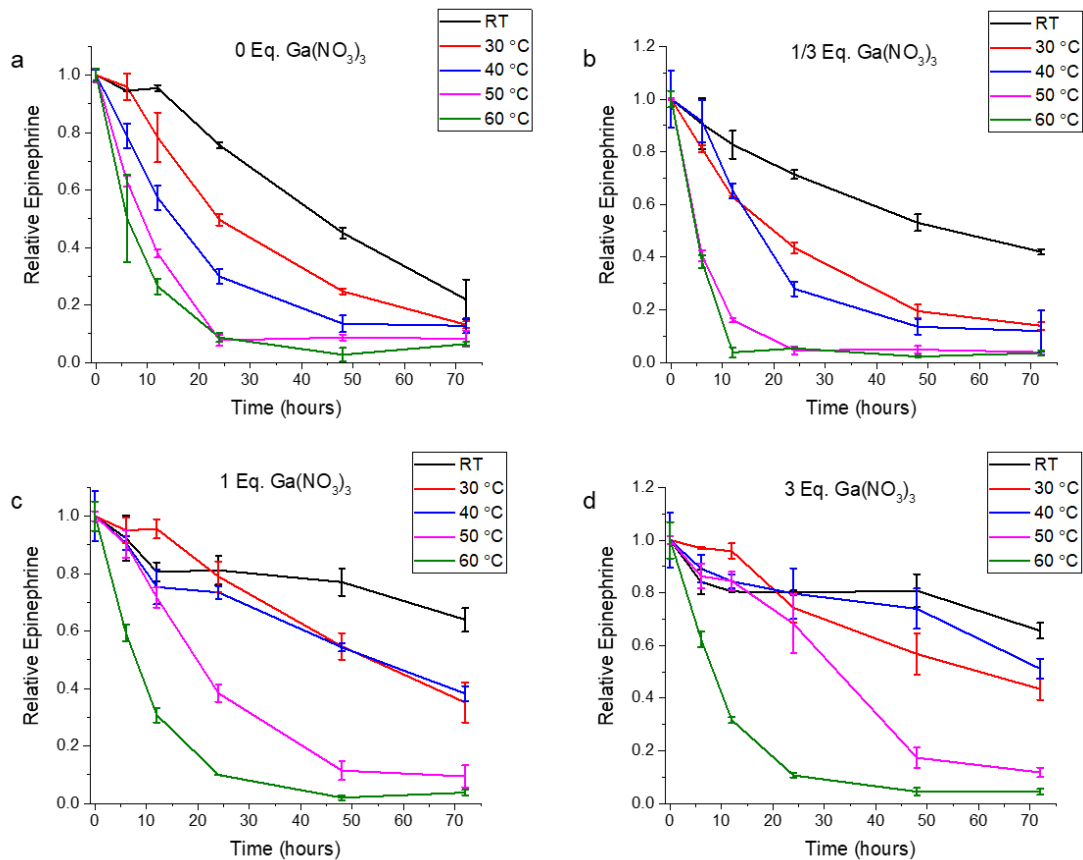


**Figure 3.5:** Relative epinephrine values for pH adjusted solutions of epinephrine with a) 0 equivalents, b) 1/3 of an equivalent, c) 1 equivalent, and d) 3 equivalents of  $\text{Ga}(\text{NO}_3)_3$  in 250 mM pH 7.0 Tris buffer. Error bars represent  $\pm$  one standard deviation, n = 3.

In addition to temperature-based forced degradation studies, forced degradation studies with UV-visible light were also performed (Figure 3.4f). The epinephrine sample with 1/3 of an equivalent of gallium nitrate experienced no stabilization when compared to the control with no gallium nitrate. The samples with both 3 equivalents and 1 equivalent of gallium nitrate both were stabilized, as the amount of epinephrine remaining after 48 hours of exposure to UV-visible light was 40% and 27% respectively. This was significantly more than that remaining in the samples with 1/3 of an equivalent and no equivalents of gallium nitrate, which had only 13% of their initial concentration of epinephrine remaining.

The forced degradation data demonstrates that the addition of gallium nitrate to solutions of epinephrine was able to reduce the amount of degradation that epinephrine undergoes. This supports the initial hypothesis that a gallium-based prodrug of epinephrine will help prevent degradation. The data also suggests that gallium nitrate was able to reduce degradation caused by both heat and light. This is compelling, as reducing degradation from all sources will decrease the necessity of needing to replace an epinephrine auto-injector. These results also suggest that a neutral formulation of an epinephrine auto-injector might be possible, however no direct comparison was made between current epinephrine auto-injector formulation and the formulations presented here. Additionally, the scope of gallium nitrate as an epinephrine prodrug is limited by temperature, as stabilization of epinephrine by the presence of gallium nitrate was not detected at 60 °C. However, it is unlikely that an epinephrine auto-injector will experience the extreme heat of 60 °C for an extended period of time.

### 3.4 Conclusions

The addition of gallium nitrate to solutions of epinephrine as a metal-based prodrug was successful at stabilizing solutions of epinephrine and preventing degradation. Prevention of degradation caused by the addition of gallium nitrate was maximized at 40 °C. At 60 °C the addition of gallium nitrate no longer decreased epinephrine degradation, likely due to the high temperatures favoring the dissociation of epinephrine from gallium. Stabilization of epinephrine was also seen in samples exposed to UV-visible light. Epinephrine in the presence of 1/3 an equivalent of gallium nitrate typically experienced more degradation than the control and the samples with 1 or 3 equivalents of gallium

nitrate. This indicates that a gallium(III) bound to three molecules of epinephrine to form a six-coordinate complex is not likely the mechanism responsible for epinephrine stabilization. One possible explanation is the coordination of three epinephrine molecules to gallium increases the local concentration of epinephrine and therefore increases the rate of degradation. The samples with 1 equivalent and 3 equivalents of gallium nitrate were typically similar in their ability to prevent degradation, with 3 equivalents slightly outperforming those with only 1 equivalent. However, the samples with 3 equivalents typically contained a white precipitate, possibly gallium(III) hydroxide. The presence of an insolubility is not ideal for an epinephrine auto-injector. Therefore, the ideal concentration for usage in epinephrine auto-injectors is likely between 1 and 3 equivalents.

### 3.5 Experimental

#### 3.5.1 General Considerations

Unless otherwise noted, reagents were purchased from commercial suppliers and used without further purification. All water is distilled water that was further purified by a Millipore cartridge system (resistivity 18 M $\Omega$ ). Analytical HPLC was performed with a Varian Prostar 210 HPLC instrument (Agilent, Santa Clara, CA) equipped with a Varian ProStar 335 diode array detector and an Agilent Zorbax Eclipse XDB-C18 column (5  $\mu$ m pore size, 4.6  $\times$  150 mm). Unless otherwise specified, HPLC measurements were performed at a flow rate of 0.5 ml/min with follow following elution conditions: 100% of the phosphate-based mobile phase from 0 to 20 minutes, a linear gradient to 50% phosphate-based mobile phase and 50% CH<sub>3</sub>CN from 20 to 22.5 minutes, 50% phosphate-based mobile phase and 50% CH<sub>3</sub>CN from 22 to 32 minutes, a linear gradient to 100%

phosphate-based mobile phase from 32.5 to 35 minutes, and 100% phosphate-based mobile phase from 35 to 45 minutes. All pH measurements were performed using a Thermo Scientific Ag /AgCl refillable probe and a Thermo Orion 3 Benchtop pH meter.

### 3.5.2 Forced Degradation Studies

**Forced Degradation with Buffer and pH adjustment** 5-Dram scintillation vials were prepared with NaCl (60 mg, 1.0 mmol) and epinephrine (10 mg, 0.05 mmol). Ga(NO<sub>3</sub>)<sub>3</sub> was then added into vials labeled as 0 equivalents (0 mg, 0 mmol), 1/3 of an equivalent (4.2 mg, 0.02 mmol), 1 equivalent (14 mg, 0.05 mmol), or 3 equivalents (42 mg, 0.16 mmol). Then 9 mL of 250 mM pH 7.0 Tris was added to each vial, which were sonicated to aid in the dissolution of epinephrine. Each vial was then pH adjusted back to 7.0 and taken to a final volume of 10 mL with the addition of more 250 mM pH 7.0 Tris buffer. A vial of each gallium concentration was then placed under the following degradation conditions: room temperature, room temperature with a UV-visible lamp directly above, 30 °C, 40 °C, 50 °C, and 60 °C. The pH of each sample was measured and 500 µL aliquots were taken of each sample at 0 hours, 6 hours, 12 hours, 24 hours, 48 hours, and 72 hours of stirring under each degradation condition. Samples were immediately frozen until they were ready to be loaded onto the HPLC. Once ready, the samples were defrosted and 200 µL of each sample was mixed with 100 µL of internal standard and 100 µL of 1 M HCl. These mixtures were vortexed and then pushed through 0.22 µm nylon syringe filters before being run on the HPLC.

#### 4. Summary and Future Directions

The above research was guided by previously reported analytical methods for the analysis of catecholamines and the requirements of designing a metal-based prodrug for the treatment of anaphylactic shock. An analytical method was developed to enable the simultaneous analysis of the degradation of multiple catecholamines. A solvent system and solvent mixing method were made that was able to successfully differentiate epinephrine, levodopa, and norepinephrine from each other and other added UV-visible absorbing compounds. An internal standard was chosen that was not a catecholamine and allowed for more accurate measurements of degradation and solubility. The method was completed with a sample preparation method that allowed for better catecholamine solubility and shelf stability. The development of this analytical method aided in the creation of a metal-based prodrug of epinephrine. Gallium nitrate was chosen as the metal salt for this metal-based prodrug because it was previously FDA approved for the treatment of hypercalcemia.<sup>339</sup> Additionally gallium(III) is redox-inactive,<sup>279</sup> has been shown to form thermodynamically stable complexes with catechols,<sup>349</sup> and is known to be labile.<sup>437</sup> The addition of gallium nitrate to solutions similar to epinephrine auto-injectors was successful at preventing degradation of epinephrine caused by heat and UV-visible light. Optimal gallium concentration is between 1 and 3 equivalents of gallium nitrate to epinephrine and reduction of degradation is temperature dependent, as no benefit is observed at 60 °C.

Future directions should focus on the study and optimization of the usage of gallium as a metal-based prodrug for epinephrine. The ability of gallium to bind and unbind epinephrine needs to be better understood. Many methods can be utilized in order to do

this. UV-visible spectroscopy can be used to monitor changes in the  $\pi - \pi^*$  transition of the catechol that are caused by gallium binding.<sup>445</sup>  $^1\text{H}$  and  $^{13}\text{C}$  nuclear magnetic resonance spectroscopy can be utilized to monitor the change in chemical environment of the catechol due to gallium binding.<sup>446-447</sup> Cyclic voltammetry can also be utilized to monitor electrochemical changes that are caused by the binding of gallium.<sup>448</sup> Both UV-visible spectroscopy and cyclic voltammetry were attempted for this study, however both attempts were unsuccessful. UV-visible spectroscopy was not sensitive enough to detect any unbinding of gallium from epinephrine, and epinephrine without the addition of gallium nitrate was not soluble in the organic solvents tested for cyclic voltammetry. Exploring additional experimental conditions might increase the sensitivity of UV-visible spectroscopy and utilizing aqueous cyclic voltammetry might allow for the study of epinephrine without the addition of gallium.

Forced degradation studies indicated that a three to one ratio of epinephrine to gallium was not ideal for stabilization, therefore, the addition of ancillary ligands is possible. Focus should be on the effect of adding antioxidant ligands, such as ascorbic acid, on the stabilization of epinephrine. Other ligand effects, such as using electron donating ligands, electron withdrawing ligands, or sterically bulky ligands. Testing a wide variety of suitable ligands would be ideal in order to optimize parameters such as epinephrine degradation, stability of epinephrine binding, and lability of epinephrine release.

Finally, the work discussed here can be extended through the creation of metal-based prodrugs for other catecholamines, such as levodopa, norepinephrine, or dopamine.

## References

1. Rautio, J.; Kumpulainen, H.; Heimbach, T.; Oliyai, R.; Oh, D.; Järvinen, T.; Savolainen, J., Prodrugs: design and clinical applications. *Nat. Rev. Drug Discovery* **2008**, *7* (3), 255-270.
2. Sadler, P. J., Inorganic Chemistry and Drug Design. In *Adv. Inorg. Chem.*, Sykes, A. G., Ed. Academic Press: 1991; Vol. 36, pp 1-48.
3. Orvig, C.; Abrams, M. J., Medicinal Inorganic Chemistry: Introduction. *Chem. Rev.* **1999**, *99* (9), 2201-2204.
4. Rosenberg, B.; Vancamp, L.; Trosko, J. E.; Mansour, V. H., Platinum Compounds: a New Class of Potent Antitumour Agents. *Nature* **1969**, *222* (5191), 385-386.
5. Rosenberg, B.; Vancamp, L.; Krigas, T., Inhibition of Cell Division in Escherichia Coli by Electrolysis Products from a Platinum Electrode. *Nature* **1965**, *205*, 698-9.
6. Rosenberg, B.; Renshaw, E.; Vancamp, L.; Hartwick, J.; Drobnik, J., Platinum-induced filamentous growth in Escherichia coli. *J. Bacteriol.* **1967**, *93* (2), 716-21.
7. Renshaw, E.; Thomson, A. J., Tracer studies to locate the site of platinum ions within filamentous and inhibited cells of Escherichia coli. *J. Bacteriol.* **1967**, *94* (6), 1915-8.
8. Zwelling, L. A.; Kohn, K. W., Mechanism of action of cis-dichlorodiammineplatinum(II). *Cancer Treat. Rep.* **1979**, *63* (9-10), 1439-44.
9. Walker, W. F.; Johnston, I. D. A., 2 - Water and Electrolyte Metabolism. In *The Metabolic Basis of Surgical Care*, Walker, W. F.; Johnston, I. D. A., Eds. Butterworth-Heinemann: 1971; pp 13-47.
10. Martinho, N.; Santos, T. C. B.; Florindo, H. F.; Silva, L. C., Cisplatin-Membrane Interactions and Their Influence on Platinum Complexes Activity and Toxicity. *Front. Physiol.* **2019**, *9*, 1898-1898.
11. Eljack, N. D.; Ma, H.-Y. M.; Drucker, J.; Shen, C.; Hambley, T. W.; New, E. J.; Friedrich, T.; Clarke, R. J., Mechanisms of cell uptake and toxicity of the anticancer drug cisplatin. *Metallomics* **2014**, *6* (11), 2126-2133.
12. Miessler, G. L.; Tarr, D., Inorganic Chemistry, 2013. Pearson Education, Inc.
13. Stone, P. J.; Kelman, A. D.; Sinex, F. M., Specific binding of antitumour drug cis-Pt(NH<sub>3</sub>)<sub>2</sub>Cl<sub>2</sub> to DNA rich in guanine and cytosine. *Nature* **1974**, *251* (5477), 736-737.
14. Stone, P. J.; Kelman, A. D.; Stnex, F. M.; Bhargava, M. M.; Halvorson, H. O., Resolution of  $\alpha$ ,  $\beta$  and  $\gamma$  DNA of *Saccharomyces cerevisiae* with the antitumor drug cis-Pt(NH<sub>3</sub>)<sub>2</sub>Cl<sub>2</sub>. Evidence for preferential drug binding by GpG sequences of DNA. *J. Mol. Biol.* **1976**, *104* (4), 793-801.
15. Munchausen, L. L.; Rahn, R. O., Physical studies on the binding of cis-dichlorodiamine platinum(II) to DNA and homopolynucleotides. *Biochim. Biophys. Acta* **1975**, *414* (3), 242-255.
16. Mansy, S.; Rosenberg, B.; Thomson, A., Binding of cis- and trans-dichlorodiammineplatinum (II) to nucleosides. I. Location of the binding sites. *J. Am. Chem. Soc.* **1973**, *95* (5), 1633-1640.
17. Mansy, S.; Chu, G. Y. H.; Duncan, R. E.; Tobias, R. S., Heavy metal nucleotide interactions. 12. Competitive reactions in systems of four nucleotides with cis- or trans-

- diammineplatinum(II). Raman difference spectrophotometry of the relative nucleophilicity of guanosine, cytidine, adenosine, and uridine monophosphates and analogous DNA bases. *J. Am. Chem. Soc.* **1978**, *100* (2), 607-616.
18. Rahn, R. O., Chromatographic analysis of the adducts formed in DNA complexed with cis-diamminedichloroplatinum(II). *J. Inorg. Biochem.* **1984**, *21* (4), 311-321.
  19. Chottard, J. C.; Girault, J. P.; Chottard, G.; Lallemand, J. Y.; Mansuy, D., Interaction of cis-diaquodiammineplatinum dinitrate with ribose dinucleoside monophosphates. *J. Am. Chem. Soc.* **1980**, *102* (17), 5565-5572.
  20. Eastman, A., Separation and characterization of products resulting from the reaction of cis-diamminedichloroplatinum (II) with deoxyribonucleosides. *Biochemistry* **1982**, *21* (26), 6732-6736.
  21. Eastman, A., The formation, isolation and characterization of DNA adducts produced by anticancer platinum complexes. *Pharmacol. Ther.* **1987**, *34* (2), 155-166.
  22. Roberts, J. J.; Thomson, A. J., The Mechanism of Action of Antitumor Platinum Compounds. In *Prog. Nucleic Acid Res. Mol. Biol.*, Cohn, W. E., Ed. Academic Press: 1979; Vol. 22, pp 71-133.
  23. Siddik, Z. H., Cisplatin: mode of cytotoxic action and molecular basis of resistance. *Oncogene* **2003**, *22* (47), 7265-7279.
  24. Shooter, K.; Howse, R.; Merrifield, R.; Robins, A., The interaction of platinum II compounds with bacteriophages T7 and R17. *Chem. Biol. Interact.* **1972**, *5* (5), 289-307.
  25. Zwelling, L. A.; Anderson, T.; Kohn, K. W., DNA-Protein and DNA Interstrand Cross-linking by *cis*- and *trans*- Platinum(II) Diamminedichloride in L1210 Mouse Leukemia Cells and Relation to Cytotoxicity. *Cancer Res.* **1979**, *39* (2 Part 1), 365-369.
  26. Filipinski, J.; Kohn, K. W.; Bonner, W. M., The nature of inactivating lesions produced by platinum (II) complexes in phage  $\lambda$  DNA. *Chem. Biol. Interact.* **1980**, *32* (3), 321-330.
  27. Roberts, J. J.; Friedlos, F., Quantitative aspects of the formation and loss of DNA interstrand crosslinks in Chinese hamster cells following treatment with cis-diamminedichloroplatinum(II) (cisplatin) I. Proportion of DNA-platinum reactions involved in DNA crosslinking. *Biochim. Biophys. Acta* **1981**, *655* (2), 146-151.
  28. Fichtinger-Schepman, A. M. J.; Van der Veer, J. L.; Den Hartog, J. H.; Lohman, P. H.; Reedijk, J., Adducts of the antitumor drug cis-diamminedichloroplatinum (II) with DNA: formation, identification, and quantitation. *Biochemistry* **1985**, *24* (3), 707-713.
  29. Plooy, A. C. M.; Fichtinger-Schepman, A. M. J.; Schutte, H. H.; van Dijk, M.; Lohman, P. H. M., The quantitative detection of various Pt-DNA-adducts in Chinese hamster ovary cells treated with cisplatin: application of immunochemical techniques. *Carcinogenesis* **1985**, *6* (4), 561-566.
  30. Munchausen, L. L., The Chemical and Biological Effects of *cis*-Dichlorodiammineplatinum (II), an Antitumor Agent, on DNA. *Proc. Natl. Acad. Sci.* **1974**, *71* (11), 4519-4522.
  31. Pinto, A. L.; Lippard, S. J., Binding of the antitumor drug cis-diamminedichloroplatinum (II)(cisplatin) to DNA. *Biochim. Biophys. Acta* **1985**, *780* (3), 167-180.

32. Kelland, L. R., New platinum antitumor complexes. *Crit. Rev. Oncol.* **1993**, *15* (3), 191-219.
33. Eastman, A.; Barry, M. A., Interaction of trans-diamminedichloroplatinum(II) with DNA: formation of monofunctional adducts and their reaction with glutathione. *Biochemistry* **1987**, *26* (12), 3303-3307.
34. Fraval, H. N. A.; Roberts, J. J., Excision Repair of *cis*-Diamminedichloroplatinum(II)-induced Damage to DNA of Chinese Hamster Cells. *Cancer Res.* **1979**, *39* (5), 1793-1797.
35. Sorenson, C. M.; Eastman, A., Influence of *cis*-Diamminedichloroplatinum(II) on DNA Synthesis and Cell Cycle Progression in Excision Repair Proficient and Deficient Chinese Hamster Ovary Cells. *Cancer Res.* **1988**, *48* (23), 6703-6707.
36. Bellon, S. F.; Coleman, J. H.; Lippard, S. J., DNA unwinding produced by site-specific intrastrand crosslinks of the antitumor drug *cis*-diamminedichloroplatinum (II). *Biochemistry* **1991**, *30* (32), 8026-8035.
37. Huang, J. C.; Zamble, D. B.; Reardon, J. T.; Lippard, S. J.; Sancar, A., HMG-domain proteins specifically inhibit the repair of the major DNA adduct of the anticancer drug cisplatin by human excision nuclease. *Proc. Natl. Acad. Sci.* **1994**, *91* (22), 10394-10398.
38. Shapiro, G. I.; Harper, J. W., Anticancer drug targets: cell cycle and checkpoint control. *J. Clin. Invest.* **1999**, *104* (12), 1645-1653.
39. Demarcq, C.; Bunch, R. T.; Creswell, D.; Eastman, A., The role of cell cycle progression in cisplatin-induced apoptosis in Chinese hamster ovary cells. *Cell Growth Differ.* **1994**, *5* (9), 983-994.
40. Appella, E.; Anderson, C. W., Post-translational modifications and activation of p53 by genotoxic stresses. *Eur. J. Biochem.* **2001**, *268* (10), 2764-2772.
41. Jayaraman, L.; Moorthy, N. C.; Murthy, K. G. K.; Manley, J. L.; Bustin, M.; Prives, C., High mobility group protein-1 (HMG-1) is a unique activator of p53. *Genes Dev.* **1998**, *12* (4), 462-472.
42. Cisplatin. *Ann. Intern. Med.* **1984**, *100* (5), 704-713.
43. Prestayko, A. W.; D'Aoust, J. C.; Issell, B. F.; Croke, S. T., Cisplatin (*cis*-diamminedichloroplatinum II). *Cancer Treat. Rev.* **1979**, *6* (1), 17-39.
44. DeConti, R. C.; Toftness, B. R.; Lange, R. C.; Creasey, W. A., Clinical and Pharmacological Studies with *cis*-Diamminedichloroplatinum(II). *Cancer Res.* **1973**, *33* (6), 1310-1315.
45. Al-Sarraf, M.; Fletcher, W.; Oishi, N.; Pugh, R.; Hewlett, J. S.; Balducci, L.; McCracken, J.; Padilla, F., Cisplatin hydration with and without mannitol diuresis in refractory disseminated malignant melanoma: a southwest oncology group study. *Cancer Treat. Rep.* **1982**, *66* (1), 31-35.
46. Hayes, D. M.; Cvitkovic, E.; Golbey, R. B.; Scheiner, E.; Helson, L.; Krakoff, I. H., High dose *Cis*-platinum diammine dichloride. Amelioration of renal toxicity by mannitol diuresis. *Cancer* **1977**, *39* (4), 1372-1381.
47. Merrin, C., Treatment of Advanced Bladder Cancer with *Cis*-Diamminedichloroplatinum (II NSC 119875): A Pilot Study. *J. Urol.* **1978**, *119* (4), 493-495.

48. Higby, D. J.; Wallace, H. J.; Albert, D.; Holland, J. F., Diamminodichloroplatinum in the Chemotherapy of Testicular Tumors. *J. Urol.* **1974**, *112* (1), 100-104.
49. Higby, D. J.; Higby, D. J.; Wallace Jr., H. J.; Albert, D. J.; Holland, J. F., Diamminodichloroplatinum: A phase I study showing responses in testicular and other tumors. *Cancer* **1974**, *33* (5), 1219-1225.
50. Rossof, A. H.; Slayton, R. E.; Perlia, C. P., Preliminary clinical experience with cis-diamminedichloroplatinum (II) (NSC 119875, CACP). *Cancer* **1972**, *30* (6), 1451-1456.
51. Giaccone, G., Clinical perspectives on platinum resistance. *Drugs* **2000**, *59* (4), 9-17.
52. Ishida, S.; Lee, J.; Thiele, D. J.; Herskowitz, I., Uptake of the anticancer drug cisplatin mediated by the copper transporter Ctr1 in yeast and mammals. *Proc. Natl. Acad. Sci.* **2002**, *99* (22), 14298-14302.
53. Katano, K.; Kondo, A.; Safaei, R.; Holzer, A.; Samimi, G.; Mishima, M.; Kuo, Y.-M.; Rochdi, M.; Howell, S. B., Acquisition of Resistance to Cisplatin Is Accompanied by Changes in the Cellular Pharmacology of Copper. *Cancer Res.* **2002**, *62* (22), 6559-6565.
54. Holzer, A. K.; Manorek, G. H.; Howell, S. B., Contribution of the Major Copper Influx Transporter CTR1 to the Cellular Accumulation of Cisplatin, Carboplatin, and Oxaliplatin. *Mol. Pharmacol.* **2006**, *70* (4), 1390-1394.
55. Ishida, S.; McCormick, F.; Smith-McCune, K.; Hanahan, D., Enhancing Tumor-Specific Uptake of the Anticancer Drug Cisplatin with a Copper Chelator. *Cancer Cell* **2010**, *17* (6), 574-583.
56. Nakayama, K.; Kanzaki, A.; Ogawa, K.; Miyazaki, K.; Neamati, N.; Takebayashi, Y., Copper-transporting P-type adenosine triphosphatase (ATP7B) as a cisplatin based chemoresistance marker in ovarian carcinoma: Comparative analysis with expression of MDR1, MRP1, MRP2, LRP and BCRP. *Int. J. Cancer* **2002**, *101* (5), 488-495.
57. Nakayama, K.; Kanzaki, A.; Terada, K.; Mutoh, M.; Ogawa, K.; Sugiyama, T.; Takenoshita, S.; Itoh, K.; Yaegashi, N.; Miyazaki, K.; Neamati, N.; Takebayashi, Y., Prognostic Value of the Cu-Transporting ATPase in Ovarian Carcinoma Patients Receiving Cisplatin-Based Chemotherapy. *Clin. Cancer Res.* **2004**, *10* (8), 2804-2811.
58. Safaei, R.; Holzer, A. K.; Katano, K.; Samimi, G.; Howell, S. B., The role of copper transporters in the development of resistance to Pt drugs. *J. Inorg. Biochem.* **2004**, *98* (10), 1607-1613.
59. Aida, T.; Takebayashi, Y.; Shimizu, T.; Okamura, C.; Higasimoto, M.; Kanzaki, A.; Nakayama, K.; Terada, K.; Sugiyama, T.; Miyazaki, K.; Ito, K.; Takenoshita, S.; Yaegashi, N., Expression of copper-transporting P-type adenosine triphosphatase (ATP7B) as a prognostic factor in human endometrial carcinoma. *Gynecol. Oncol.* **2005**, *97* (1), 41-45.
60. Koike, K.; Kawabe, T.; Tanaka, T.; Toh, S.; Uchiumi, T.; Wada, M.; Akiyama, S.-i.; Ono, M.; Kuwano, M., A Canalicular Multispecific Organic Anion Transporter (cMOAT) Antisense cDNA Enhances Drug Sensitivity in Human Hepatic Cancer Cells. *Cancer Res.* **1997**, *57* (24), 5475-5479.

61. Cui, Y.; König, J.; Buchholz, U.; Spring, H.; Leier, I.; Keppler, D., Drug Resistance and ATP-Dependent Conjugate Transport Mediated by the Apical Multidrug Resistance Protein, MRP2, Permanently Expressed in Human and Canine Cells. *Mol. Pharmacol.* **1999**, *55* (5), 929-937.
62. Liedert, B.; Materna, V.; Schadendorf, D.; Thomale, J.; Lage, H., Overexpression of cMOAT (MRP2/ABCC2) Is Associated with Decreased Formation of Platinum-DNA Adducts and Decreased G2-Arrest in Melanoma Cells Resistant to Cisplatin. *J. Invest. Dermatol.* **2003**, *121* (1), 172-176.
63. Korita, P. V.; Wakai, T.; Shirai, Y.; Matsuda, Y.; Sakata, J.; Takamura, M.; Yano, M.; Sanpei, A.; Aoyagi, Y.; Hatakeyama, K.; Ajioka, Y., Multidrug resistance-associated protein 2 determines the efficacy of cisplatin in patients with hepatocellular carcinoma. *Oncol. Rep.* **2010**, *23* (4), 965-972.
64. Yamasaki, M.; Makino, T.; Masuzawa, T.; Kurokawa, Y.; Miyata, H.; Takiguchi, S.; Nakajima, K.; Fujiwara, Y.; Matsuura, N.; Mori, M.; Doki, Y., Role of multidrug resistance protein 2 (MRP2) in chemoresistance and clinical outcome in oesophageal squamous cell carcinoma. *Br. J. Cancer* **2011**, *104* (4), 707-713.
65. Lewis, A. D.; Hayes, J. D.; Wolf, C. R., Glutathione and glutathione-dependent enzymes in ovarian adenocarcinoma cell lines derived from a patient before and after the onset of drug resistance: intrinsic differences and cell cycle effects. *Carcinogenesis* **1988**, *9* (7), 1283-1287.
66. Chen, H. H.; Kuo, M. T., Role of glutathione in the regulation of Cisplatin resistance in cancer chemotherapy. *Met.-Based Drugs* **2010**, *2010*.
67. Kelley, S.; Basu, A.; Teicher, B.; Hacker, M.; Hamer, D.; Lazo, J., Overexpression of metallothionein confers resistance to anticancer drugs. *Science* **1988**, *241* (4874), 1813-1815.
68. Kasahara, K.; Fujiwara, Y.; Nishio, K.; Ohmori, T.; Sugimoto, Y.; Komiya, K.; Matsuda, T.; Saijo, N., Metallothionein Content Correlates with the Sensitivity of Human Small Cell Lung Cancer Cell Lines to Cisplatin. *Cancer Res.* **1991**, *51* (12), 3237-3242.
69. Vaisman, A.; Varchenko, M.; Umar, A.; Kunkel, T. A.; Risinger, J. I.; Barrett, J. C.; Hamilton, T. C.; Chaney, S. G., The Role of hMLH1, hMSH3, and hMSH6 Defects in Cisplatin and Oxaliplatin Resistance: Correlation with Replicative Bypass of Platinum-DNA Adducts. *Cancer Res.* **1998**, *58* (16), 3579-3585.
70. Kunkel, T. A.; Erie, D. A., DNA mismatch repair. *Annu. Rev. Biochem.* **2005**, *74*, 681-710.
71. Wood, R.; Araujo, S.; Ariza, R.; Batty, D.; Biggerstaff, M.; Evans, E.; Gaillard, P.-H.; Gunz, D.; Köberle, B.; Kuraoka, I. In *DNA damage recognition and nucleotide excision repair in mammalian cells*, Cold Spring Harbor symposia on quantitative biology, Cold Spring Harbor Laboratory Press: 2000; pp 173-182.
72. Shuck, S. C.; Short, E. A.; Turchi, J. J., Eukaryotic nucleotide excision repair: from understanding mechanisms to influencing biology. *Cell Res.* **2008**, *18* (1), 64-72.
73. Edwards, S. L.; Brough, R.; Lord, C. J.; Natrajan, R.; Vatcheva, R.; Levine, D. A.; Boyd, J.; Reis-Filho, J. S.; Ashworth, A., Resistance to therapy caused by intragenic deletion in BRCA2. *Nature* **2008**, *451* (7182), 1111-1115.

74. Narod, S. A.; Foulkes, W. D., BRCA1 and BRCA2: 1994 and beyond. *Nat. Rev. Cancer* **2004**, *4* (9), 665-676.
75. Vousden, K. H.; Lane, D. P., p53 in health and disease. *Nat. Rev. Mol. Cell Biol.* **2007**, *8* (4), 275-283.
76. Han, J.-Y.; Hong, E. K.; Choi, B. G.; Park, J. N.; Kim, K. W.; Kang, J. H.; Jin, J.-Y.; Park, S. Y.; Hong, Y. S.; Lee, K. S., Death receptor 5 and Bcl-2 protein expression as predictors of tumor response to gemcitabine and cisplatin in patients with advanced non-small-cell lung cancer. *Med. Oncol.* **2003**, *20* (4), 355-362.
77. Williams, J.; Lucas, P. C.; Griffith, K. A.; Choi, M.; Fogoros, S.; Hu, Y. Y.; Liu, J. R., Expression of Bcl-xL in ovarian carcinoma is associated with chemoresistance and recurrent disease. *Gynecol. Oncol.* **2005**, *96* (2), 287-295.
78. Erovic, B. M.; Pelzmann, M.; Grasl, M. C.; Pammer, J.; Kornek, G.; Brannath, W.; Selzer, E.; Thurnher, D., Mcl-1, vascular endothelial growth factor-R2, and 14-3-3 $\sigma$  expression might predict primary response against radiotherapy and chemotherapy in patients with locally advanced squamous cell carcinomas of the head and neck. *Clin. Cancer Res.* **2005**, *11* (24), 8632-8636.
79. Sakai, W.; Swisher, E. M.; Karlan, B. Y.; Agarwal, M. K.; Higgins, J.; Friedman, C.; Villegas, E.; Jacquemont, C.; Farrugia, D. J.; Couch, F. J.; Urban, N.; Taniguchi, T., Secondary mutations as a mechanism of cisplatin resistance in BRCA2-mutated cancers. *Nature* **2008**, *451* (7182), 1116-1120.
80. Michaud, W. A.; Nichols, A. C.; Mroz, E. A.; Faquin, W. C.; Clark, J. R.; Begum, S.; Westra, W. H.; Wada, H.; Busse, P. M.; Ellisen, L. W., Bcl-2 blocks cisplatin-induced apoptosis and predicts poor outcome following chemoradiation treatment in advanced oropharyngeal squamous cell carcinoma. *Clin. Cancer Res.* **2009**, *15* (5), 1645-1654.
81. Jain, H. V.; Meyer-Hermann, M., The molecular basis of synergism between carboplatin and ABT-737 therapy targeting ovarian carcinomas. *Cancer Res.* **2011**, *71* (3), 705-715.
82. Janson, V.; Johansson, A.; Grankvist, K., Resistance to caspase-8 and-9 fragments in a malignant pleural mesothelioma cell line with acquired cisplatin-resistance. *Cell Death Dis.* **2010**, *1* (9), e78-e78.
83. Wang, Y.; Nangia-Makker, P.; Balan, V.; Hogan, V.; Raz, A., Calpain activation through galectin-3 inhibition sensitizes prostate cancer cells to cisplatin treatment. *Cell Death Dis.* **2010**, *1* (11), e101-e101.
84. Galluzzi, L.; Senovilla, L.; Vitale, I.; Michels, J.; Martins, I.; Kepp, O.; Castedo, M.; Kroemer, G., Molecular mechanisms of cisplatin resistance. *Oncogene* **2012**, *31* (15), 1869-1883.
85. Kroemer, G.; Mariño, G.; Levine, B., Autophagy and the integrated stress response. *Mol. Cell* **2010**, *40* (2), 280-293.
86. Ren, J.-H.; He, W.-S.; Nong, L.; Zhu, Q.-Y.; Hu, K.; Zhang, R.-G.; Huang, L.-L.; Zhu, F.; Wu, G., Acquired cisplatin resistance in human lung adenocarcinoma cells is associated with enhanced autophagy. *Cancer Biother. Radiopharm.* **2010**, *25* (1), 75-80.
87. Yu, H.; Su, J.; Xu, Y.; Kang, J.; Li, H.; Zhang, L.; Yi, H.; Xiang, X.; Liu, F.; Sun, L., p62/SQSTM1 involved in cisplatin resistance in human ovarian cancer cells by clearing ubiquitinated proteins. *Eur. J. Cancer* **2011**, *47* (10), 1585-1594.

88. Friedman, E., Mirk/Dyrk1B in cancer. *J. Cell. Biochem.* **2007**, *102* (2), 274-279.
89. Deng, X.; Ewton, D. Z.; Friedman, E., Mirk/Dyrk1B Maintains the Viability of Quiescent Pancreatic Cancer Cells by Reducing Levels of Reactive Oxygen Species. *Cancer Res.* **2009**, *69* (8), 3317-3324.
90. Gao, J.; Zheng, Z.; Rawal, B.; Schell, M. J.; Bepler, G.; Haura, E. B., Mirk/Dyrk1B, a novel therapeutic target, mediates cell survival in non-small cell lung cancer cells. *Cancer Biol. Ther.* **2009**, *8* (17), 1671-1679.
91. Hu, J.; Friedman, E., Depleting Mirk kinase increases cisplatin toxicity in ovarian cancer cells. *Genes Cancer* **2010**, *1* (8), 803-811.
92. Yamamoto, K.; Okamoto, A.; Isonishi, S.; Ochiai, K.; Ohtake, Y., Heat shock protein 27 was up-regulated in cisplatin resistant human ovarian tumor cell line and associated with the cisplatin resistance. *Cancer Lett.* **2001**, *168* (2), 173-181.
93. Miyazaki, T.; Kato, H.; Faried, A.; Sohda, M.; Nakajima, M.; Fukai, Y.; Masuda, N.; Manda, R.; Fukuchi, M.; Ojima, H., Predictors of response to chemo-radiotherapy and radiotherapy for esophageal squamous cell carcinoma. *Anticancer Res.* **2005**, *25* (4), 2749-2755.
94. Zhang, Y.; Shen, X., Heat shock protein 27 protects L929 cells from cisplatin-induced apoptosis by enhancing Akt activation and abating suppression of thioredoxin reductase activity. *Clin. Cancer Res.* **2007**, *13* (10), 2855-2864.
95. Ren, A.; Yan, G.; You, B.; Sun, J., Down-regulation of Mammalian Sterile 20-Like Kinase 1 by Heat Shock Protein 70 Mediates Cisplatin Resistance in Prostate Cancer Cells. *Cancer Res.* **2008**, *68* (7), 2266-2274.
96. Johnstone, T. C.; Suntharalingam, K.; Lippard, S. J., The Next Generation of Platinum Drugs: Targeted Pt(II) Agents, Nanoparticle Delivery, and Pt(IV) Prodrugs. *Chem. Rev.* **2016**, *116* (5), 3436-3486.
97. Robins, A. B., The reaction of <sup>14</sup>C-labelled platinum ethylenediamine dichloride with nucleic acid constituents. *Chem. Biol. Interact.* **1973**, *6* (1), 35-45.
98. Conran, P. B., Pharmacokinetics of Platinum Compounds. In *Platinum Coordination Complexes in Cancer Chemotherapy*, Connors, T. A.; Roberts, J. J., Eds. Springer Berlin Heidelberg: Berlin, Heidelberg, 1974; pp 124-136.
99. Canetta, R.; Rozenzweig, M.; Carter, S. K., Carboplatin: the clinical spectrum to date. *Cancer Treat. Rev.* **1985**, *12*, 125-136.
100. Calvert, A. H.; Newell, D. R.; Gumbrell, L. A.; O'Reilly, S.; Burnell, M.; Boxall, F. E.; Siddik, Z. H.; Judson, I. R.; Gore, M. E.; Wiltshaw, E., Carboplatin dosage: prospective evaluation of a simple formula based on renal function. *J. Clin. Oncol.* **1989**, *7* (11), 1748-1756.
101. Pavelka, M.; Lucas, M. F. A.; Russo, N., On the Hydrolysis Mechanism of the Second-Generation Anticancer Drug Carboplatin. *Chem. Eur. J.* **2007**, *13* (36), 10108-10116.
102. Canetta, R.; Bragman, K.; Smaldone, L.; Rozenzweig, M., Carboplatin: current status and future prospects. *Cancer Treat. Rev.* **1988**, *15*, 17-32.
103. Knox, R. J.; Friedlos, F.; Lydall, D. A.; Roberts, J. J., Mechanism of cytotoxicity of anticancer platinum drugs: evidence that cis-diamminedichloroplatinum(II) and cis-

- diammine-(1,1-cyclobutanedicarboxylato)platinum(II) differ only in the kinetics of their interaction with DNA. *Cancer Res.* **1986**, *46* (4 Pt 2), 1972-9.
104. Connors, T. A.; Jones, M.; Ross, W. C. J.; Braddock, P. D.; Khokhar, A. R.; Tobe, M. L., New platinum complexes with anti-tumour activity. *Chem. Biol. Interact.* **1972**, *5* (6), 415-424.
105. Raymond, E.; Chaney, S. G.; Taamma, A.; Cvitkovic, E., Oxaliplatin: A review of preclinical and clinical studies. *Ann. Oncol.* **1998**, *9* (10), 1053-1071.
106. Butour, J. L.; Mazard, A. M.; Macquet, J. P., Kinetics of the reaction of cis-platinum compounds with DNA in vitro. *Biochem. Biophys. Res. Commun.* **1985**, *133* (1), 347-353.
107. Jennerwein, M. M.; Eastman, A.; Khokhar, A., Characterization of adducts produced in DNA by isomeric 1,2-diaminocyclohexaneplatinum(II) complexes. *Chem. Biol. Interact.* **1989**, *70* (1), 39-49.
108. Page, J. D.; Husain, I.; Sancar, A.; Chaney, S. G., Effect of the diamminocyclohexane carrier ligand on platinum adduct formation, repair, and lethality. *Biochemistry* **1990**, *29* (4), 1016-24.
109. Saris, C. P.; van de Vaart, P. M.; Rietbroek, R. C.; Bloramaert, F., In vitro formation of DNA adducts by cisplatin, lobaplatin and oxaliplatin in calf thymus DNA in solution and in cultured human cells. *Carcinogenesis* **1996**, *17* (12), 2763-2769.
110. Mamenta, E. L.; Poma, E. E.; Kaufmann, W. K.; Delmastro, D. A.; Grady, H. L.; Chaney, S. G., Enhanced Replicative Bypass of Platinum-DNA Adducts in Cisplatin-resistant Human Ovarian Carcinoma Cell Lines. *Cancer Res.* **1994**, *54* (13), 3500-3505.
111. Schmidt, W.; Chaney, S. G., Role of Carrier Ligand in Platinum Resistance of Human Carcinoma Cell Lines. *Cancer Res.* **1993**, *53* (4), 799-805.
112. Bruno, P. M.; Liu, Y.; Park, G. Y.; Murai, J.; Koch, C. E.; Eisen, T. J.; Pritchard, J. R.; Pommier, Y.; Lippard, S. J.; Hemann, M. T., A subset of platinum-containing chemotherapeutic agents kills cells by inducing ribosome biogenesis stress. *Nat. Med.* **2017**, *23* (4), 461-471.
113. Raymond, E.; Buquet-Fagot, C.; Djelloul, S.; Mester, J.; Cvitkovic, E.; Allain, P.; Louvet, C.; Gespach, C., Antitumor activity of oxaliplatin in combination with 5-fluorouracil and the thymidylate synthase inhibitor AG337 in human colon, breast and ovarian cancers. *Anticancer Drugs* **1997**, *8* (9), 876-885.
114. Shimada, M.; Itamochi, H.; Kigawa, J., Nedaplatin: a cisplatin derivative in cancer chemotherapy. *Cancer Manag. Res.* **2013**, *5*, 67-76.
115. Alberto, M. E.; Lucas, M. F. A.; Pavelka, M.; Russo, N., The Second-Generation Anticancer Drug Nedaplatin: A Theoretical Investigation on the Hydrolysis Mechanism. *J. Phys. Chem. B* **2009**, *113* (43), 14473-14479.
116. Ota, K.; Wakui, A.; Majima, H.; Niitani, H.; Inuyama, Y.; Ogawa, M.; Ariyoshi, Y.; Yoshida, O.; Taguchi, T.; Kimura, I.; et al., [Phase I study of a new platinum complex 254-S, cis-diammine (glycolato)-platinum (II)]. *Gan to Kagaku Ryoho* **1992**, *19* (6), 855-61.
117. Choi, C.-H.; Cha, Y.-J.; An, C.-S.; Kim, K.-J.; Kim, K.-C.; Moon, S.-P.; Lee, Z. H.; Min, Y.-D., Molecular mechanisms of heptaplatin effective against cisplatin-resistant cancer cell lines: less involvement of metallothionein. *Cancer Cell Int.* **2004**, *4* (1), 6.

118. Kim, D. K.; Kim, G.; Gam, J.; Cho, Y. B.; Kim, H. T.; Tai, J. H.; Kim, K. H.; Hong, W. S.; Park, J. G., Synthesis and antitumor activity of a series of [2-substituted-4,5-bis(aminomethyl)-1,3-dioxolane]platinum(II) complexes. *J. Med. Chem.* **1994**, *37* (10), 1471-85.
119. Lee, Y.-S.; Kang, K.-S.; Shin, D.-J.; Cho, J.-J.; Kim, H.-O.; Kim, B.-H.; Lim, Y.-K., Subacute toxicity of cis-malonato [(4R, 5R)-4, 5-bis (aminomethyl)-2-isopropyl-1, 3-dioxolane] platinum (II)(SKI 2053R) in beagle dogs. *Toxicol. Res.* **1992**, *8* (2), 235-253.
120. Ahn, J. H.; Kang, Y. K.; Kim, T. W., 386. Heptaplatin is more nephrotoxic than cisplatin. *Kidney* **2003**, *12* (3), 141.
121. Liu, W.; Chen, X.; Ye, Q.; Xu, Y.; Xie, C.; Xie, M.; Chang, Q.; Lou, L., A Novel Water-Soluble Heptaplatin Analogue with Improved Antitumor Activity and Reduced Toxicity. *Inorg. Chem.* **2011**, *50* (12), 5324-5326.
122. Gietema, J. A.; Veldhuis, G. J.; Guchelaar, H. J.; Willemse, P. H. B.; Uges, D. R. A.; Cats, A.; Boonstra, H.; van der Graaf, W. T. A.; Sleijfer, D. T.; de Vries, E. G. E.; Mulder, N. H., Phase II and pharmacokinetic study of lobaplatin in patients with relapsed ovarian cancer. *Br. J. Cancer* **1995**, *71* (6), 1302-1307.
123. McKeage, M. J., Lobaplatin: a new antitumour platinum drug. *Expert Opin. Invest. Drugs* **2001**, *10* (1), 119-128.
124. Yin, C.-Y.; Lin, X.-L.; Tian, L.; Ye, M.; Yang, X.-Y.; Xiao, X.-Y., Lobaplatin inhibits growth of gastric cancer cells by inducing apoptosis. *World J. Gastroenterol.* **2014**, *20* (46), 17426-17433.
125. Lobaplatin: D 19466. *Drugs in R&D* **2003**, *4* (6), 369-72.
126. Chen, Y.; Heeg, M. J.; Braunschweiger, P. G.; Xie, W.; Wang, P. G., A Carbohydrate-Linked Cisplatin Analogue Having Antitumor Activity. *Angew. Chem. Int. Ed.* **1999**, *38* (12), 1768-1769.
127. Haroutounian, S. A.; Georgiadis, M. P.; Bailar, J. C., Water soluble cis-platinum(II) complexes. *Inorg. Chim. Acta* **1986**, *124* (3), 137-139.
128. Liu, P.; Lu, Y.; Gao, X.; Liu, R.; Zhang-Negrerie, D.; Shi, Y.; Wang, Y.; Wang, S.; Gao, Q., Highly water-soluble platinum(ii) complexes as GLUT substrates for targeted therapy: improved anticancer efficacy and transporter-mediated cytotoxic properties. *Chem. Commun.* **2013**, *49* (24), 2421-2423.
129. Gabano, E.; Cassino, C.; Bonetti, S.; Prandi, C.; Colangelo, D.; Ghiglia, A.; Osella, D., Synthesis and characterisation of estrogenic carriers for cytotoxic Pt(II) fragments: biological activity of the resulting complexes. *Org. Biomol. Chem.* **2005**, *3* (19), 3531-9.
130. Descôteaux, C.; Provencher-Mandeville, J.; Mathieu, I.; Perron, V.; Mandal, S. K.; Asselin, É.; Bérubé, G., Synthesis of 17 $\beta$ -estradiol platinum(II) complexes: biological evaluation on breast cancer cell lines. *Bioorg. Med. Chem. Lett.* **2003**, *13* (22), 3927-3931.
131. Perron, V.; Rabouin, D.; Asselin, É.; Parent, S.; C.-Gaudreault, R.; Bérubé, G., Synthesis of 17 $\beta$ -estradiol-linked platinum(II) complexes and their cytotoxic activity on estrogen-dependent and -independent breast tumor cells. *Bioorg. Chem.* **2005**, *33* (1), 1-15.

132. Gagnon, V.; St-Germain, M.-È.; Descôteaux, C.; Provencher-Mandeville, J.; Parent, S.; Mandal, S. K.; Asselin, E.; Bérubé, G., Biological evaluation of novel estrogen-platinum(II) hybrid molecules on uterine and ovarian cancers—molecular modeling studies. *Bioorg. Med. Chem. Lett.* **2004**, *14* (23), 5919-5924.
133. Maeda, M.; Suga, T.; Takasuka, N.; Hoshi, A.; Sasaki, T., Effect of bis(bilato)-1,2-cyclohexanediammineplatinum(II) complexes on lung metastasis of B16-F10 melanoma cells in mice. *Cancer Lett.* **1990**, *55* (2), 143-7.
134. Larena, M. G.; Martinez-Diez, M. C.; Macias, R. I.; Dominguez, M. F.; Serrano, M. A.; Marin, J. J., Relationship between tumor cell load and sensitivity to the cytostatic effect of two novel platinum-bile acid complexes, Bamet-D3 and Bamet-UD2. *Journal of drug targeting* **2002**, *10* (5), 397-404.
135. Weitman, S. D.; Lark, R. H.; Coney, L. R.; Fort, D. W.; Frasca, V.; Zurawski, V. R., Jr.; Kamen, B. A., Distribution of the folate receptor GP38 in normal and malignant cell lines and tissues. *Cancer Res.* **1992**, *52* (12), 3396-401.
136. Gabano, E.; Ravera, M.; Cassino, C.; Bonetti, S.; Palmisano, G.; Osella, D., Stepwise assembly of platinum–folic acid conjugates. *Inorg. Chim. Acta* **2008**, *361* (5), 1447-1455.
137. Robillard, M. S.; van Alphen, S.; Meeuwenoord, N. J.; J. Jansen, B. A.; van der Marel, G. A.; van Boom, J. H.; Reedijk, J., Solid-phase synthesis of peptide-platinum complexes using platinum-chelating building blocks derived from amino acids. *New J. Chem.* **2005**, *29* (1), 220-225.
138. Robillard, M. S.; Valentijn, A. R. P. M.; Meeuwenoord, N. J.; van der Marel, G. A.; van Boom, J. H.; Reedijk, J., The First Solid-Phase Synthesis of a Peptide-Tethered Platinum(II) Complex. *Angew. Chem. Int. Ed.* **2000**, *39* (17), 3096-3099.
139. van Zutphen, S.; Stone, E. A.; van Rijt, S.; Robillard, M. S.; van der Marel, G. A.; Overkleeft, H. S.; den Dulk, H.; Brouwer, J.; Reedijk, J., Combinatorial discovery of new asymmetric cis platinum anticancer complexes is made possible with solid-phase synthetic methods. *J. Inorg. Biochem.* **2005**, *99* (10), 2032-2038.
140. Damian, M. S.; Hedman, H. K.; Elmroth, S. K. C.; Diederichsen, U., Synthesis and DNA Interaction of Platinum Complex/Peptide Chimera as Potential Drug Candidates (Eur. J. Org. Chem. 32/2010). *Eur. J. Org. Chem.* **2010**, *2010* (32).
141. Gibson, D., Platinum(IV) anticancer agents; are we en route to the holy grail or to a dead end? *J. Inorg. Biochem.* **2021**, *217*, 111353.
142. Gibson, D., Platinum(iv) anticancer prodrugs – hypotheses and facts. *Dalton Trans.* **2016**, *45* (33), 12983-12991.
143. Deeth, R. J.; Randell, K., Ligand Field Stabilization and Activation Energies Revisited: Molecular Modeling of the Thermodynamic and Kinetic Properties of Divalent, First-Row Aqua Complexes. *Inorg. Chem.* **2008**, *47* (16), 7377-7388.
144. Ang, W. H.; Pilet, S.; Scopelliti, R.; Bussy, F.; Juillerat-Jeanneret, L.; Dyson, P. J., Synthesis and Characterization of Platinum(IV) Anticancer Drugs with Functionalized Aromatic Carboxylate Ligands: Influence of the Ligands on Drug Efficacies and Uptake. *J. Med. Chem.* **2005**, *48* (25), 8060-8069.
145. Reubi, J. C., Peptide Receptors as Molecular Targets for Cancer Diagnosis and Therapy. *Endocr. Rev.* **2003**, *24* (4), 389-427.

146. Mukhopadhyay, S.; Barnés, C. M.; Haskel, A.; Short, S. M.; Barnes, K. R.; Lippard, S. J., Conjugated Platinum(IV)–Peptide Complexes for Targeting Angiogenic Tumor Vasculature. *Bioconjugate Chem.* **2008**, *19* (1), 39-49.
147. Mackay, F. S.; Woods, J. A.; Heringová, P.; Kašpárková, J.; Pizarro, A. M.; Moggach, S. A.; Parsons, S.; Brabec, V.; Sadler, P. J., A potent cytotoxic photoactivated platinum complex. *Proc. Natl. Acad. Sci.* **2007**, *104* (52), 20743-20748.
148. Dhar, S.; Lippard, S. J., Mitaplatin, a potent fusion of cisplatin and the orphan drug dichloroacetate. *Proc. Natl. Acad. Sci.* **2009**, *106* (52), 22199-22204.
149. Xue, X.; You, S.; Zhang, Q.; Wu, Y.; Zou, G.-z.; Wang, P. C.; Zhao, Y.-l.; Xu, Y.; Jia, L.; Zhang, X.; Liang, X.-J., Mitaplatin Increases Sensitivity of Tumor Cells to Cisplatin by Inducing Mitochondrial Dysfunction. *Mol. Pharmaceutics* **2012**, *9* (3), 634-644.
150. Phillips, A. M.; Pombeiro, A. J., Transition metal-based prodrugs for anticancer drug delivery. *Curr. Med. Chem.* **2019**, *26* (41), 7476-7519.
151. Li, X.; Liu, Y.; Tian, H., Current Developments in Pt(IV) Prodrugs Conjugated with Bioactive Ligands. *Bioinorg. Chem. Appl.* **2018**, *2018*, 8276139.
152. Petruzzella, E.; Sirota, R.; Solazzo, I.; Gandin, V.; Gibson, D., Triple action Pt(iv) derivatives of cisplatin: a new class of potent anticancer agents that overcome resistance. *Chem. Sci.* **2018**, *9* (18), 4299-4307.
153. Frei, A.; Zuegg, J.; Elliott, A. G.; Baker, M.; Braese, S.; Brown, C.; Chen, F.; G. Dowson, C.; Dujardin, G.; Jung, N.; King, A. P.; Mansour, A. M.; Massi, M.; Moat, J.; Mohamed, H. A.; Renfrew, A. K.; Rutledge, P. J.; Sadler, P. J.; Todd, M. H.; Willans, C. E.; Wilson, J. J.; Cooper, M. A.; Blaskovich, M. A. T., Metal complexes as a promising source for new antibiotics. *Chem. Sci.* **2020**, *11* (10), 2627-2639.
154. Brahimi-Horn, M. C.; Chiche, J.; Pouysségur, J., Hypoxia and cancer. *J. Mol. Med.* **2007**, *85* (12), 1301-1307.
155. Denny, W. A.; Wilson, W. R., Bioreducible mustards: a paradigm for hypoxia-selective prodrugs of diffusible cytotoxins (HPDCs). *Cancer Metastasis Rev.* **1993**, *12* (2), 135-151.
156. Wilson, W. R.; Tercel, M.; Anderson, R. F.; Denny, W. A., Radiation-activated prodrugs as hypoxia-selective cytotoxins: model studies with nitroarylmethyl quaternary salts. *Anti-Cancer Drug Des.* **1998**, *13* (6), 663-85.
157. Brown, J. M.; Wilson, W. R., Exploiting tumour hypoxia in cancer treatment. *Nat. Rev. Cancer* **2004**, *4* (6), 437-447.
158. Hall, M. D.; Failes, T. W.; Yamamoto, N.; Hambley, T. W., Bioreductive activation and drug chaperoning in cobalt pharmaceuticals. *Dalton Trans.* **2007**, (36), 3983-3990.
159. Hambley, T. W., Physiological Targeting to Improve Anticancer Drug Selectivity. *Aust. J. Chem.* **2008**, *61* (9), 647-653.
160. Chen, Y.; Hu, L., Design of anticancer prodrugs for reductive activation. *Med. Res. Rev.* **2009**, *29* (1), 29-64.
161. van Rijt, S. H.; Sadler, P. J., Current applications and future potential for bioinorganic chemistry in the development of anticancer drugs. *Drug Discovery Today* **2009**, *14* (23), 1089-1097.

162. Jungwirth, U.; Kowol, C. R.; Keppler, B. K.; Hartinger, C. G.; Berger, W.; Heffeter, P., Anticancer Activity of Metal Complexes: Involvement of Redox Processes. *Antioxid. Redox Signaling* **2011**, *15* (4), 1085-1127.
163. Wilson, W. R.; Hay, M. P., Targeting hypoxia in cancer therapy. *Nat. Rev. Cancer* **2011**, *11* (6), 393-410.
164. Graf, N.; Lippard, S. J., Redox activation of metal-based prodrugs as a strategy for drug delivery. *Adv. Drug Delivery Rev.* **2012**, *64* (11), 993-1004.
165. Heffern, M. C.; Yamamoto, N.; Holbrook, R. J.; Eckermann, A. L.; Meade, T. J., Cobalt derivatives as promising therapeutic agents. *Current Opinion in Chemical Biology* **2013**, *17* (2), 189-196.
166. Renfrew, A. K., Transition metal complexes with bioactive ligands: mechanisms for selective ligand release and applications for drug delivery. *Metallomics* **2014**, *6* (8), 1324-1335.
167. Patel, A.; Sant, S., Hypoxic tumor microenvironment: Opportunities to develop targeted therapies. *Biotechnol. Adv.* **2016**, *34* (5), 803-812.
168. Renfrew, A. K.; O'Neill, E. S.; Hambley, T. W.; New, E. J., Harnessing the properties of cobalt coordination complexes for biological application. *Coord. Chem. Rev.* **2018**, *375*, 221-233.
169. Zeng, Y.; Ma, J.; Zhan, Y.; Xu, X.; Zeng, Q.; Liang, J.; Chen, X., Hypoxia-activated prodrugs and redox-responsive nanocarriers. *Int. J. Nanomedicine* **2018**, *13*, 6551-6574.
170. Karmakar, S.; Maji, M.; Mukherjee, A., Modulation of the reactivity of nitrogen mustards by metal complexation: approaches to modify their therapeutic properties. *Dalton Trans.* **2019**, *48* (4), 1144-1160.
171. Sharma, A.; Arambula, J. F.; Koo, S.; Kumar, R.; Singh, H.; Sessler, J. L.; Kim, J. S., Hypoxia-targeted drug delivery. *Chem. Soc. Rev.* **2019**, *48* (3), 771-813.
172. Wang, X.; Wang, X.; Jin, S.; Muhammad, N.; Guo, Z., Stimuli-Responsive Therapeutic Metallodrugs. *Chem. Rev.* **2019**, *119* (2), 1138-1192.
173. Eaton, D. R.; O'Reilly, A., Oxidation of cobalt(II) amine complexes to mononuclear cobalt(III) complexes by dioxygen. *Inorg. Chem.* **1987**, *26* (25), 4185-4188.
174. Yang, L.; Crans, D. C.; Miller, S. M.; la Cour, A.; Anderson, O. P.; Kaszynski, P. M.; Godzala, M. E.; Austin, L. D.; Willsky, G. R., Cobalt(II) and Cobalt(III) Dipicolinate Complexes: Solid State, Solution, and in Vivo Insulin-like Properties. *Inorg. Chem.* **2002**, *41* (19), 4859-4871.
175. Teicher, B. A.; Abrams, M. J.; Rosbe, K. W.; Herman, T. S., Cytotoxicity, Radiosensitization, Antitumor Activity, and Interaction with Hyperthermia of a Co(III) Mustard Complex. *Cancer Res.* **1990**, *50* (21), 6971-6975.
176. Teicher, B. A.; Jacobs, J. L.; Cathcart, K. N.; Abrams, M. J.; Vollano, J. F.; Picker, D. H., Some complexes of cobalt (III) and iron (III) are radiosensitizers of hypoxic EMT6 cells. *Radiat. Res.* **1987**, *109* (1), 36-46.
177. Rockwell, S.; Dobrucki, I. T.; Kim, E. Y.; Marrison, S. T.; Vu, V. T., Hypoxia and radiation therapy: past history, ongoing research, and future promise. *Curr. Mol. Med.* **2009**, *9* (4), 442-458.

178. Guise, C. P.; Mowday, A. M.; Ashoorzadeh, A.; Yuan, R.; Lin, W.-H.; Wu, D.-H.; Smaill, J. B.; Patterson, A. V.; Ding, K., Bioreductive prodrugs as cancer therapeutics: targeting tumor hypoxia. *Chin. J. Cancer* **2014**, *33* (2), 80-86.
179. Harrison, L. B.; Chadha, M.; Hill, R. J.; Hu, K.; Shasha, D., Impact of Tumor Hypoxia and Anemia on Radiation Therapy Outcomes. *The Oncologist* **2002**, *7* (6), 492-508.
180. Wardman, P., Chemical radiosensitizers for use in radiotherapy. *Clin. Oncol. (R. Coll. Radiol.)* **2007**, *19* (6), 397-417.
181. Ware, D. C.; Wilson, W. R.; Denny, W. A.; Rickard, C. E. F., Design and synthesis of cobalt(III) nitrogen mustard complexes as hypoxia selective cytotoxins. The X-ray crystal structure of bis(3-chloropentane-2,4-dionato)(RS-N,N'-bis(2-chloroethyl)ethylenediamine)cobalt(III) perchlorate, [Co(Clacac)2(bce)]ClO<sub>4</sub>. *J. Chem. Soc., Chem. Commun.* **1991**, (17), 1171-1173.
182. Wilson, W. R.; Moselen, J. W.; Cliffe, S.; Denny, W. A.; Ware, D. C., Exploiting tumor hypoxia through bioreductive release of diffusible cytotoxins: The cobalt(III)-nitrogen mustard complex SN 24771. *Int. J. Radiat. Oncol. Biol. Phys.* **1994**, *29* (2), 323-327.
183. Ware, D. C.; Palmer, H. R.; Brothers, P. J.; Rickard, C. E. F.; Wilson, W. R.; Denny, W. A., Bis-tropolonato derivatives of Cobalt(III) complexes of bidentate aliphatic nitrogen mustards as potential hypoxia-selective cytotoxins. *J. Inorg. Biochem.* **1997**, *68* (3), 215-224.
184. Ware, D. C.; Palmer, H. R.; Pruijn, F. B.; Anderson, R. F.; Brothers, P. J.; Denny, W. A.; Wilson, W. R., Bis(dialkyl)dithiocarbamate cobalt(III) complexes of bidentate nitrogen mustards: synthesis, reduction chemistry and biological evaluation as hypoxia-selective cytotoxins. *Anti-Cancer Drug Des.* **1998**, *13* (2), 81-103.
185. Craig, P. R.; Brothers, P. J.; Clark, G. R.; Wilson, W. R.; Denny, W. A.; Ware, D. C., Anionic carbonato and oxalato cobalt(III) nitrogen mustard complexes. *Dalton Trans.* **2004**, (4), 611-618.
186. Ware, D. C.; Brothers, P. J.; Clark, G. R.; Denny, W. A.; Palmer, B. D.; Wilson, W. R., Synthesis, structures and hypoxia-selective cytotoxicity of cobalt(III) complexes containing tridentate amine and nitrogen mustard ligands. *J. Chem. Soc., Dalton Trans.* **2000**, (6), 925-932.
187. Downard, A. M.; Jane, R. T.; Polson, M. I. J.; Moore, E. G.; Hartshorn, R. M., Heterodinuclear ruthenium(ii)-cobalt(iii) complexes as models for a new approach to selective cancer treatment. *Dalton Trans.* **2012**, *41* (47), 14425-14432.
188. Campagna, S.; Puntoriero, F.; Nastasi, F.; Bergamini, G.; Balzani, V., Photochemistry and Photophysics of Coordination Compounds: Ruthenium. In *Photochemistry and Photophysics of Coordination Compounds I*, Balzani, V.; Campagna, S., Eds. Springer Berlin Heidelberg: Berlin, Heidelberg, 2007; pp 117-214.
189. Vos, J. G.; Kelly, J. M., Ruthenium polypyridyl chemistry; from basic research to applications and back again. *Dalton Trans.* **2006**, (41), 4869-4883.
190. Smith, S. L., War! What is it good for? Mustard gas medicine. *CMAJ* **2017**, *189* (8), E321-E322.

191. Gilman, A., The initial clinical trial of nitrogen mustard. *Am. J. Surg.* **1963**, *105* (5), 574-578.
192. Elmore, D. T.; Gulland, J. M.; Jordan, D. O.; Taylor, H. F. W., The reaction of nucleic acids with mustard gas. *Biochem. J* **1948**, *42* (2), 308-316.
193. Goldacre, R. J.; Loveless, A.; Ross, W. C. J., Mode of Production of Chromosome Abnormalities by the Nitrogen Mustards The Possible Role of Cross-Linking. *Nature* **1949**, *163* (4148), 667-669.
194. Kohn, K. W.; Spears, C. L.; Doty, P., Inter-strand crosslinking of DNA by nitrogen mustard. *J. Mol. Biol.* **1966**, *19* (2), 266-288.
195. Kohn, K. W.; Hartley, J. A.; Mattes, W. B., Mechanisms of DNA sequence selective alkylation of guanine-N7 positions by nitrogen mustards. *Nucleic Acids Res.* **1987**, *15* (24), 10531-10549.
196. Singh, R. K.; Kumar, S.; Prasad, D. N.; Bhardwaj, T. R., Therapeutic journey of nitrogen mustard as alkylating anticancer agents: Historic to future perspectives. *Eur. J. Med. Chem.* **2018**, *151*, 401-433.
197. Ahn, G. O.; Botting, K. J.; Patterson, A. V.; Ware, D. C.; Tercel, M.; Wilson, W. R., Radiolytic and cellular reduction of a novel hypoxia-activated cobalt(III) prodrug of a chloromethylbenzindoline DNA minor groove alkylator. *Biochem. Pharmacol.* **2006**, *71* (12), 1683-1694.
198. Lu, G.-L.; Stevenson, R. J.; Chang, J. Y.-C.; Brothers, P. J.; Ware, D. C.; Wilson, W. R.; Denny, W. A.; Tercel, M., N-alkylated cyclen cobalt(III) complexes of 1-(chloromethyl)-3-(5,6,7-trimethoxyindol-2-ylcarbonyl)-2,3-dihydro-1H-pyrrolo[3,2-f]quinolin-5-ol DNA alkylating agent as hypoxia-activated prodrugs. *Bioorg. Med. Chem.* **2011**, *19* (16), 4861-4867.
199. Itoh, Y.; Nagase, H., Matrix metalloproteinases in cancer. *Essays Biochem.* **2002**, *38*, 21-36.
200. Failes, T. W.; Cullinane, C.; Diakos, C. I.; Yamamoto, N.; Lyons, J. G.; Hambley, T. W., Studies of a Cobalt(III) Complex of the MMP Inhibitor Marimastat: A Potential Hypoxia-Activated Prodrug. *Chem. Eur. J.* **2007**, *13* (10), 2974-2982.
201. Sharma, S. V.; Bell, D. W.; Settleman, J.; Haber, D. A., Epidermal growth factor receptor mutations in lung cancer. *Nat. Rev. Cancer* **2007**, *7* (3), 169-181.
202. Karnthaler-Benbakka, C.; Groza, D.; Kryeziu, K.; Pichler, V.; Roller, A.; Berger, W.; Heffeter, P.; Kowol, C. R., Tumor-Targeting of EGFR Inhibitors by Hypoxia-Mediated Activation. *Angew. Chem. Int. Ed.* **2014**, *53* (47), 12930-12935.
203. Cressey, P. B.; Eskandari, A.; Bruno, P. M.; Lu, C.; Hemann, M. T.; Suntharalingam, K., The Potent Inhibitory Effect of a Naproxen-Appended Cobalt(III)-Cyclam Complex on Cancer Stem Cells. *ChemBioChem* **2016**, *17* (18), 1713-1718.
204. Duggan, K. C.; Walters, M. J.; Musee, J.; Harp, J. M.; Kiefer, J. R.; Oates, J. A.; Marnett, L. J., Molecular Basis for Cyclooxygenase Inhibition by the Non-steroidal Anti-inflammatory Drug Naproxen\*. *J. Biol. Chem.* **2010**, *285* (45), 34950-34959.
205. Boodram, J. N.; Mcgregor, I. J.; Bruno, P. M.; Cressey, P. B.; Hemann, M. T.; Suntharalingam, K., Breast Cancer Stem Cell Potent Copper (II)-Non-Steroidal Anti-Inflammatory Drug Complexes. *Angew. Chem.* **2016**, *128* (8), 2895-2900.

206. Heffern, M. C.; Kurutz, J. W.; Meade, T. J., Spectroscopic elucidation of the inhibitory mechanism of Cys2His2 zinc finger transcription factors by cobalt (III) Schiff base complexes. *Chem. Eur. J.* **2013**, *19* (50), 17043-17053.
207. Manus, L. M.; Holbrook, R. J.; Atesin, T. A.; Heffern, M. C.; Harney, A. S.; Eckermann, A. L.; Meade, T. J., Axial ligand exchange of N-heterocyclic cobalt (III) Schiff base complexes: molecular structure and NMR solution dynamics. *Inorg. Chem.* **2013**, *52* (2), 1069-1076.
208. Heffern, M. C.; Reichova, V.; Coomes, J. L.; Harney, A. S.; Bajema, E. A.; Meade, T. J., Tuning Cobalt(III) Schiff Base Complexes as Activated Protein Inhibitors. *Inorg. Chem.* **2015**, *54* (18), 9066-9074.
209. King, A. P.; Gellineau, H. A.; MacMillan, S. N.; Wilson, J. J., Physical properties, ligand substitution reactions, and biological activity of Co(III)-Schiff base complexes. *Dalton Trans.* **2019**, *48* (18), 5987-6002.
210. Garcia, C. V.; Parrilha, G. L.; Rodrigues, B. L.; Barbeira, P. J. S.; Clarke, R. M.; Storr, T.; Beraldo, H., Cobalt(III) complexes with 2-acetylpyridine-derived Schiff bases: Studies investigating ligand release upon reduction. *Polyhedron* **2017**, *124*, 86-95.
211. Śmiłowicz, D.; Metzler-Nolte, N., Bioconjugates of Co(III) complexes with Schiff base ligands and cell penetrating peptides: Solid phase synthesis, characterization and antiproliferative activity. *J. Inorg. Biochem.* **2020**, *206*, 111041.
212. Deng, J.; Li, T.; Su, G.; Qin, Q.-P.; Liu, Y.; Gou, Y., Co(III) complexes based on  $\alpha$ -N-heterocyclic thiosemicarbazone ligands: DNA binding, DNA cleavage, and topoisomerase I/II inhibitory activity studies. *J. Mol. Struct.* **2018**, *1167*, 33-43.
213. Lake, B. G., Coumarin Metabolism, Toxicity and Carcinogenicity: Relevance for Human Risk Assessment. *Food Chem. Toxicol.* **1999**, *37* (4), 423-453.
214. Jain, P.; Joshi, H., Coumarin: chemical and pharmacological profile. *J. Appl. Pharm. Sci.* **2012**, *2* (6), 236-240.
215. Chang, H.-T.; Chou, C.-T.; Lin, Y.-S.; Shieh, P.; Kuo, D.-H.; Jan, C.-R.; Liang, W.-Z., Esculetin, a natural coumarin compound, evokes Ca<sup>2+</sup> movement and activation of Ca<sup>2+</sup>-associated mitochondrial apoptotic pathways that involved cell cycle arrest in ZR-75-1 human breast cancer cells. *Tumor Biol.* **2016**, *37* (4), 4665-4678.
216. Kim, A. D.; Madduma Hewage, S. R. K.; Piao, M. J.; Kang, K. A.; Cho, S. J.; Hyun, J. W., Esculetin induces apoptosis in human colon cancer cells by inducing endoplasmic reticulum stress. *Cell Biochem. Funct.* **2015**, *33* (7), 487-494.
217. Pan, H.; Wang, B.-H.; Lv, W.; Jiang, Y.; He, L., Esculetin induces apoptosis in human gastric cancer cells through a cyclophilin D-mediated mitochondrial permeability transition pore associated with ROS. *Chem. Biol. Interact.* **2015**, *242*, 51-60.
218. Li, J.; Li, S.; Wang, X.; Wang, H., Esculetin induces apoptosis of SMMC-7721 cells through IGF-1/PI3K/Akt-mediated mitochondrial pathways. *Can. J. Physiol. Pharmacol.* **2017**, *95* (7), 787-794.
219. Areas, E. S.; de Assunção Paiva, J. L.; Ribeiro, F. V.; Pereira, T. M.; Kummerle, A. E.; Silva, H.; Guedes, G. P.; Cellis do Nascimento, A. C.; da Silva Miranda, F.; Neves, A. P., Redox-Activated Drug Delivery Properties and Cytotoxicity of Cobalt Complexes Based on a Fluorescent Coumarin- $\beta$ -Keto Ester Hybrid. *Eur. J. Inorg. Chem.* **2019**, *2019* (37), 4031-4039.

220. Silva, J. M.; Silva, E.; Reis, R. L., Light-triggered release of photocaged therapeutics - Where are we now? *J. Controlled Release* **2019**, *298*, 154-176.
221. Mello-Andrade, F.; Cardoso, C. G.; e Silva, C. R.; Chen-Chen, L.; de Melo-Reis, P. R.; de Lima, A. P.; Oliveira, R.; Ferraz, I. B. M.; Grisolia, C. K.; Almeida, M. A. P., Acute toxic effects of ruthenium (II)/amino acid/diphosphine complexes on Swiss mice and zebrafish embryos. *Biomed. and Pharmacother.* **2018**, *107*, 1082-1092.
222. Papageorgiou, P.; Katsambas, A.; Chu, A., Phototherapy with blue (415 nm) and red (660 nm) light in the treatment of acne vulgaris. *Br. J. Dermatol.* **2000**, *142* (5), 973-978.
223. Simons, J. R.; Bohnen, I. J. W. E.; Van Der Valk, P. G. M., A left-right comparison of UVB phototherapy and topical photochemotherapy in bilateral chronic hand dermatitis after 6 weeks' treatment. *Clin. Exp. Dermatol.* **1997**, *22* (1), 7-10.
224. Sidbury, R.; Davis, D. M.; Cohen, D. E.; Cordero, K. M.; Berger, T. G.; Bergman, J. N.; Chamlin, S. L.; Cooper, K. D.; Feldman, S. R.; Hanifin, J. M.; Krol, A.; Margolis, D. J.; Paller, A. S.; Schwarzenberger, K.; Silverman, R. A.; Simpson, E. L.; Tom, W. L.; Williams, H. C.; Elmets, C. A.; Block, J.; Harrod, C. G.; Begolka, W. S.; Eichenfield, L. F., Guidelines of care for the management of atopic dermatitis: Section 3. Management and treatment with phototherapy and systemic agents. *J. Am. Acad. Dermatol.* **2014**, *71* (2), 327-349.
225. Huo, M.; Chen, Y.; Shi, J., Triggered-release drug delivery nanosystems for cancer therapy by intravenous injection: where are we now? *Expert Opin. Drug Delivery* **2016**, *13* (9), 1195-1198.
226. Tuchin, V. V., Light scattering study of tissues. *Phys.-Usp.* **1997**, *40* (5), 495.
227. Simpson, C. R.; Kohl, M.; Essenpreis, M.; Cope, M., Near-infrared optical properties of ex vivo human skin and subcutaneous tissues measured using the Monte Carlo inversion technique. *Phys. Med. Biol.* **1998**, *43* (9), 2465.
228. Yang, Y.; Velmurugan, B.; Liu, X.; Xing, B., NIR photoresponsive crosslinked upconverting nanocarriers toward selective intracellular drug release. *Small* **2013**, *9* (17), 2937-2944.
229. Van Houten, J.; Watts, R., Photochemistry of tris (2, 2'-bipyridyl) ruthenium (II) in aqueous solutions. *Inorg. Chem.* **1978**, *17* (12), 3381-3385.
230. Pinnick, D. V.; Durham, B., Photosubstitution reactions of Ru(bpy)<sub>2</sub>XYn<sup>+</sup> complexes. *Inorg. Chem.* **1984**, *23* (10), 1440-1445.
231. Ahmed, I.; Fruk, L., The power of light: photosensitive tools for chemical biology. *Mol. BioSyst.* **2013**, *9* (4), 565-570.
232. Brieke, C.; Rohrbach, F.; Gottschalk, A.; Mayer, G.; Heckel, A., Light-controlled tools. *Angew. Chem. Int. Ed.* **2012**, *51* (34), 8446-8476.
233. Alvarez-Lorenzo, C.; Bromberg, L.; Concheiro, A., Light-sensitive intelligent drug delivery systems. *Photochem. Photobiol.* **2009**, *85* (4), 848-860.
234. Hufziger, K. T.; Thowfeik, F. S.; Charboneau, D. J.; Nieto, I.; Dougherty, W. G.; Kassel, W. S.; Dudley, T. J.; Merino, E. J.; Papish, E. T.; Paul, J. J., Ruthenium dihydroxybipyridine complexes are tumor activated prodrugs due to low pH and blue light induced ligand release. *J. Inorg. Biochem.* **2014**, *130*, 103-111.

235. Qu, F.; Park, S.; Martinez, K.; Gray, J. L.; Thowfeik, F. S.; Lundeen, J. A.; Kuhn, A. E.; Charboneau, D. J.; Gerlach, D. L.; Lockart, M. M.; Law, J. A.; Jernigan, K. L.; Chambers, N.; Zeller, M.; Piro, N. A.; Kassel, W. S.; Schmehl, R. H.; Paul, J. J.; Merino, E. J.; Kim, Y.; Papish, E. T., Ruthenium Complexes are pH-Activated Metallo Prodrugs (pHAMPs) with Light-Triggered Selective Toxicity Toward Cancer Cells. *Inorg. Chem.* **2017**, *56* (13), 7519-7532.
236. Matsumura, Y.; Ananthaswamy, H. N., Toxic effects of ultraviolet radiation on the skin. *Toxicol. Appl. Pharmacol.* **2004**, *195* (3), 298-308.
237. Barhoumi, A.; Liu, Q.; Kohane, D. S., Ultraviolet light-mediated drug delivery: Principles, applications, and challenges. *J. Controlled Release* **2015**, *219*, 31-42.
238. Weissleder, R., A clearer vision for in vivo imaging. *Nat. Biotechnol.* **2001**, *19* (4), 316-317.
239. Fan, N.-C.; Cheng, F.-Y.; Ho, J.-a. A.; Yeh, C.-S., Photocontrolled Targeted Drug Delivery: Photocaged Biologically Active Folic Acid as a Light-Responsive Tumor-Targeting Molecule. *Angew. Chem. Int. Ed.* **2012**, *51* (35), 8806-8810.
240. Tong, R.; Kohane, D. S., Shedding light on nanomedicine. *Wiley Interdiscip. Rev.: Nanomed. Nanobiotechnol.* **2012**, *4* (6), 638-662.
241. Zayat, L.; Calero, C.; Alborés, P.; Baraldo, L.; Etchenique, R., A New Strategy for Neurochemical Photodelivery: Metal–Ligand Heterolytic Cleavage. *J. Am. Chem. Soc.* **2003**, *125* (4), 882-883.
242. Filevich, O.; Etchenique, R., RuBiGABA-2: a hydrophilic caged GABA with long wavelength sensitivity. *Photochem. Photobiol.* **2013**, *12* (9), 1565-1570.
243. Garner, R. N.; Gallucci, J. C.; Dunbar, K. R.; Turro, C., [Ru(bpy)<sub>2</sub>(5-cyanouracil)<sub>2</sub>]<sup>2+</sup> as a Potential Light-Activated Dual-Action Therapeutic Agent. *Inorg. Chem.* **2011**, *50* (19), 9213-9215.
244. Porter, D. J.; Chestnut, W. G.; Merrill, B. M.; Spector, T., Mechanism-based inactivation of dihydropyrimidine dehydrogenase by 5-ethynyluracil. *J. Biol. Chem.* **1992**, *267* (8), 5236-5242.
245. Hidayatullah, A. N.; Wachter, E.; Heidary, D. K.; Parkin, S.; Glazer, E. C., Photoactive Ru(II) Complexes With Dioxinophenanthroline Ligands Are Potent Cytotoxic Agents. *Inorg. Chem.* **2014**, *53* (19), 10030-10032.
246. Havrylyuk, D.; Heidary, D. K.; Nease, L.; Parkin, S.; Glazer, E. C., Photochemical Properties and Structure–Activity Relationships of RuII Complexes with Pyridylbenzazole Ligands as Promising Anticancer Agents. *Eur. J. Inorg. Chem.* **2017**, *2017* (12), 1687-1694.
247. Li, A.; Turro, C.; Kodanko, J. J., Ru(II) Polypyridyl Complexes Derived from Tetradentate Ancillary Ligands for Effective Photocaging. *Acc. Chem. Res.* **2018**, *51* (6), 1415-1421.
248. Li, A.; Turro, C.; Kodanko, J. J., Ru(ii) polypyridyl complexes as photocages for bioactive compounds containing nitriles and aromatic heterocycles. *Chem. Commun.* **2018**, *54* (11), 1280-1290.
249. Kraft, S. S. n.; Bischof, C.; Loos, A.; Braun, S.; Jafarova, N.; Schatzschneider, U., A [4+2] mixed ligand approach to ruthenium DNA metallointercalators [Ru(tpa)(N–

- N)](PF<sub>6</sub>)<sub>2</sub> using a tris(2-pyridylmethyl)amine (tpa) capping ligand. *J. Inorg. Biochem.* **2009**, *103* (8), 1126-1134.
250. Joshi, T.; Pierroz, V.; Mari, C.; Gemperle, L.; Ferrari, S.; Gasser, G., A Bis(dipyridophenazine)(2-(2-pyridyl)pyrimidine-4-carboxylic acid)ruthenium(II) Complex with Anticancer Action upon Photodeprotection. *Angew. Chem. Int. Ed.* **2014**, *53* (11), 2960-2963.
251. Liu, Y.; Turner, D. B.; Singh, T. N.; Angeles-Boza, A. M.; Chouai, A.; Dunbar, K. R.; Turro, C., Ultrafast Ligand Exchange: Detection of a Pentacoordinate Ru(II) Intermediate and Product Formation. *J. Am. Chem. Soc.* **2009**, *131* (1), 26-27.
252. Respondek, T.; Garner, R. N.; Herroon, M. K.; Podgorski, I.; Turro, C.; Kodanko, J. J., Light Activation of a Cysteine Protease Inhibitor: Caging of a Peptidomimetic Nitrile with Ru(II)(bpy)<sub>2</sub>. *J. Am. Chem. Soc.* **2011**, *133* (43), 17164-17167.
253. Sharma, R.; Knoll, J. D.; Martin, P. D.; Podgorski, I.; Turro, C.; Kodanko, J. J., Ruthenium Tris(2-pyridylmethyl)amine as an Effective Photocaging Group for Nitriles. *Inorg. Chem.* **2014**, *53* (7), 3272-3274.
254. Guengerich, F. P., Cytochrome P450s and other enzymes in drug metabolism and toxicity. *AAPS J.* **2006**, *8* (1), E101-E111.
255. Laroche-Clary, A.; Morvan, V. L.; Yamori, T.; Robert, J., Cytochrome P450 1B1 Gene Polymorphisms as Predictors of Anticancer Drug Activity: Studies with *In vitro* Models. *Mol. Cancer Ther.* **2010**, *9* (12), 3315-3321.
256. Zamora, A.; Denning, C. A.; Heidary, D. K.; Wachter, E.; Nease, L. A.; Ruiz, J.; Glazer, E. C., Ruthenium-containing P450 inhibitors for dual enzyme inhibition and DNA damage. *Dalton Trans.* **2017**, *46* (7), 2165-2173.
257. Garten, A.; Schuster, S.; Penke, M.; Gorski, T.; de Giorgis, T.; Kiess, W., Physiological and pathophysiological roles of NAMPT and NAD metabolism. *Nat. Rev. Endocrinol.* **2015**, *11* (9), 535-546.
258. Olesen, U. H.; Christensen, M. K.; Björkling, F.; Jäätelä, M.; Jensen, P. B.; Sehested, M.; Nielsen, S. J., Anticancer agent CHS-828 inhibits cellular synthesis of NAD. *Biochem. Biophys. Res. Commun.* **2008**, *367* (4), 799-804.
259. von Heideman, A.; Berglund, Å.; Larsson, R.; Nygren, P., Safety and efficacy of NAD depleting cancer drugs: results of a phase I clinical trial of CHS 828 and overview of published data. *Cancer Chemother. Pharmacol.* **2010**, *65* (6), 1165-1172.
260. Ravaud, A.; Cerny, T.; Terret, C.; Wanders, J.; Bui, B. N.; Hess, D.; Droz, J.-P.; Fumoleau, P.; Twelves, C., Phase I study and pharmacokinetic of CHS-828, a guanidino-containing compound, administered orally as a single dose every 3 weeks in solid tumours: An ECRG/EORTC study. *Eur. J. Cancer* **2005**, *41* (5), 702-707.
261. Wei, J.; Renfrew, A. K., Photolabile ruthenium complexes to cage and release a highly cytotoxic anticancer agent. *J. Inorg. Biochem.* **2018**, *179*, 146-153.
262. Karaoun, N.; Renfrew, A. K., A luminescent ruthenium(II) complex for light-triggered drug release and live cell imaging. *Chem. Commun.* **2015**, *51* (74), 14038-14041.
263. Ho, Y.-S.; Wu, C.-H.; Chou, H.-M.; Wang, Y.-J.; Tseng, H.; Chen, C.-H.; Chen, L.-C.; Lee, C.-H.; Lin, S.-Y., Molecular mechanisms of econazole-induced toxicity on

- human colon cancer cells: G0/G1 cell cycle arrest and caspase 8-independent apoptotic signaling pathways. *Food Chem. Toxicol.* **2005**, *43* (10), 1483-1495.
264. Bolhuis, A.; Hand, L.; Marshall, J. E.; Richards, A. D.; Rodger, A.; Aldrich-Wright, J., Antimicrobial activity of ruthenium-based intercalators. *Eur. J. Pharm. Sci.* **2011**, *42* (4), 313-317.
265. Liu, X.; Sun, B.; Kell, R. E.; Southam, H. M.; Butler, J.; Li, X.; Poole, R. K.; Keene, F. R.; Collins, J. G., The antimicrobial activity of mononuclear ruthenium (II) complexes containing the dppz ligand. *ChemPlusChem* **2018**, *83* (7), 643-650.
266. Jain, A.; Garrett, N. T.; Malone, Z. P., Ruthenium-based Photoactive Metalloantibiotics. *Photochem. Photobiol.*
267. Gao, F.; Wang, F.; Nie, X.; Zhang, Z.; Chen, G.; Xia, L.; Wang, L.-H.; Wang, C.-H.; Hao, Z.-Y.; Zhang, W.-J.; Hong, C.-Y.; You, Y.-Z., Mitochondria-targeted delivery and light controlled release of iron prodrug and CO to enhance cancer therapy by ferroptosis. *New J. Chem.* **2020**, *44* (8), 3478-3486.
268. Ansari, K. I.; Kasiri, S.; Grant, J. D.; Mandal, S. S., Fe(III)-Salen and Salphen Complexes Induce Caspase Activation and Apoptosis in Human Cells. *J. Biomol. Screening* **2011**, *16* (1), 26-35.
269. Parker, L. L.; Lacy, S. M.; Farrugia, L. J.; Evans, C.; Robins, D. J.; O'Hare, C. C.; Hartley, J. A.; Jaffar, M.; Stratford, I. J., A novel design strategy for stable metal complexes of nitrogen mustards as bioreductive prodrugs. *J. Med. Chem.* **2004**, *47* (23), 5683-5689.
270. Levina, A.; McLeod, A. I.; Pulte, A.; Aitken, J. B.; Lay, P. A., Biotransformations of Antidiabetic Vanadium Prodrugs in Mammalian Cells and Cell Culture Media: A XANES Spectroscopic Study. *Inorg. Chem.* **2015**, *54* (14), 6707-6718.
271. Schatzschneider, U., PhotoCORMs: Light-triggered release of carbon monoxide from the coordination sphere of transition metal complexes for biological applications. *Inorg. Chim. Acta* **2011**, *374* (1), 19-23.
272. Ernst, R. J.; Song, H.; Barton, J. K., DNA Mismatch Binding and Antiproliferative Activity of Rhodium Metalloinsertors. *J. Am. Chem. Soc.* **2009**, *131* (6), 2359-2366.
273. Bruijninx, P. C. A.; Sadler, P. J., Controlling platinum, ruthenium, and osmium reactivity for anticancer drug design. In *Adv. Inorg. Chem.*, van Eldik, R.; Hubbard, C. D., Eds. Academic Press: 2009; Vol. 61, pp 1-62.
274. Zhao, Z.; Gao, P.; Ma, L.; Chen, T., A highly X-ray sensitive iridium prodrug for visualized tumor radiochemotherapy. *Chem. Sci.* **2020**, *11* (15), 3780-3789.
275. Horie, M.; Kato, H.; Endoh, S.; Fujita, K.; Nishio, K.; Komaba, L. K.; Fukui, H.; Nakamura, A.; Miyauchi, A.; Nakazato, T.; Kinugasa, S.; Yoshida, Y.; Hagihara, Y.; Morimoto, Y.; Iwahashi, H., Evaluation of cellular influences of platinum nanoparticles by stable medium dispersion. *Metallomics* **2011**, *3* (11), 1244-1252.
276. Moore, W.; Hysell, D.; Hall, L.; Campbell, K.; Stara, J., Preliminary studies on the toxicity and metabolism of palladium and platinum. *Environ. Health Perspect.* **1975**, *10*, 63-71.
277. Faroon, O.; Keith, S., Toxicological profile for cobalt. **2004**.

278. Kruszyna, H.; Kruszyna, R.; Hurst, J.; Smith, R. P., Toxicology and pharmacology of some ruthenium compounds: Vascular smooth muscle relaxation by nitrosyl derivatives of ruthenium and iridium. *Journal of Toxicology and Environmental Health* **1980**, *6* (4), 757-773.
279. Goldsmith, C. R., Aluminum and gallium complexes as homogeneous catalysts for reduction/oxidation reactions. *Coord. Chem. Rev.* **2018**, *377*, 209-224.
280. Chitambar, C. R., Gallium and its competing roles with iron in biological systems. *Biochim. Biophys. Acta* **2016**, *1863* (8), 2044-2053.
281. Shannon, R. D., Revised effective ionic radii and systematic studies of interatomic distances in halides and chalcogenides. *Acta Crystallogr. Sect. A: Found. Crystallogr.* **1976**, *32* (5), 751-767.
282. Collery, P.; Keppler, B.; Madoulet, C.; Desoize, B., Gallium in cancer treatment. *Crit. Rev. Oncol.* **2002**, *42* (3), 283-296.
283. Dudley, H. C.; Imirie, G. W., Jr.; Istock, J. T., Deposition of radiogallium (Ga72) in proliferating tissues. *Radiology* **1950**, *55* (4), 571-8.
284. Edwards, C. L.; Hayes, R. *Tumor Scanning with <sup>67</sup>Ga Citrate*; Oak Ridge Associated Universities, Tenn.: 1969.
285. Wylie, B. R.; Southee, A. E.; Joshua, D. E.; McLaughlin, A. F.; Gibson, J.; Hutton, B. F.; Morris, J. G.; Kronenberg, H., Gallium scanning in the management of mediastinal Hodgkin's disease. *Eur. J. Haematol.* **1989**, *42* (4), 344-347.
286. Hagemester, F. B.; Fesus, S. M.; Lamki, L. M.; Haynie, T. P., Role of the gallium scan in Hodgkin's disease. *Cancer* **1990**, *65* (5), 1090-1096.
287. van Amsterdam, J. H. G.; Kluin-Nelemans, J. C.; van Eck-Smit, B. L. F.; Pauwels, E. K. J., Role of <sup>67</sup>Ga scintigraphy in localization of lymphoma. *Ann. Haematol.* **1996**, *72* (4), 202-207.
288. Lavender, J. P.; Lowe, J.; Barker, J. R.; Burn, J. I.; Chaudhri, M. A., Gallium <sup>67</sup> citrate scanning in neoplastic and inflammatory lesions. *Br. J. Radiol.* **1971**, *44* (521), 361-366.
289. Littenberg, R. L.; Taketa, R. M.; Alazraki, N. P.; Halpern, S. E., Gallium-67 for Localization of Septic Lesions. *Ann. Intern. Med.* **1973**, *79* (3), 403-406.
290. Seam, P.; Juweid, M. E.; Cheson, B. D., The role of FDG-PET scans in patients with lymphoma. *Blood* **2007**, *110* (10), 3507-3516.
291. Ido, T.; Wan, C.-N.; Casella, V.; Fowler, J. S.; Wolf, A. P.; Reivich, M.; Kuhl, D. E., Labeled 2-deoxy-D-glucose analogs. <sup>18</sup>F-labeled 2-deoxy-2-fluoro-D-glucose, 2-deoxy-2-fluoro-D-mannose and <sup>14</sup>C-2-deoxy-2-fluoro-D-glucose. *J. Labelled Compd. Radiopharm.* **1978**, *14* (2), 175-183.
292. Wagner, H.; Burns, H.; Dannals, R.; Wong, D.; Langstrom, B.; Duelfer, T.; Frost, J.; Ravert, H.; Links, J.; Rosenbloom, S.; Lukas, S.; Kramer, A.; Kuhar, M., Imaging dopamine receptors in the human brain by positron tomography. *Science* **1983**, *221* (4617), 1264-1266.
293. Khan, M. U.; Khan, S.; El-Refaie, S.; Win, Z.; Rubello, D.; Al-Nahhas, A., Clinical indications for Gallium-68 positron emission tomography imaging. *Eur. J. Surg. Oncol.* **2009**, *35* (6), 561-567.

294. Loc'h, C.; Mazière, B.; Comar, D., A New Generator for Ionic Gallium-68. *J. Nucl. Med.* **1980**, *21* (2), 171-173.
295. Zimmerman, B. E.; Cessna, J. T.; Fitzgerald, R., Standardization of (68)Ge/(68)Ga Using Three Liquid Scintillation Counting Based Methods. *J. Res. Natl. Inst. Stand. Technol.* **2008**, *113* (5), 265-280.
296. Prata, I. M., Gallium-68: a new trend in PET radiopharmacy. *Curr. Radiopharm.* **2012**, *5* (2), 142-149.
297. Smith-Jones, P. M.; Stolz, B.; Bruns, C.; Albert, R.; Reist, H. W.; Fridrich, R.; Mäcke, H. R., Gallium-67/Gallium-68-[DFO]-Octreotide—A Potential Radiopharmaceutical for PET Imaging of Somatostatin Receptor-Positive Tumors: Synthesis and Radiolabeling In Vitro and Preliminary In Vivo Studies. *J. Nucl. Med.* **1994**, *35* (2), 317-325.
298. Govindan, S. V.; Michel, R. B.; Griffiths, G. L.; Goldenberg, D. M.; Mattes, M. J., Deferoxamine as a chelator for <sup>67</sup>Ga in the preparation of antibody conjugates. *Nucl. Med. Biol.* **2005**, *32* (5), 513-519.
299. Mathias, C. J.; Lewis, M. R.; Reichert, D. E.; Laforest, R.; Sharp, T. L.; Lewis, J. S.; Yang, Z.-F.; Waters, D. J.; Snyder, P. W.; Low, P. S.; Welch, M. J.; Green, M. A., Preparation of <sup>66</sup>Ga- and <sup>68</sup>Ga-labeled Ga(III)-deferoxamine-folate as potential folate-receptor-targeted PET radiopharmaceuticals. *Nucl. Med. Biol.* **2003**, *30* (7), 725-731.
300. Tsang, B. W.; Mathias, C. J.; Green, M. A., A gallium-68 radiopharmaceutical that is retained in myocardium: <sup>68</sup>Ga [(4, 6-MeO<sub>2</sub>sal) 2BAPEN]<sup>+</sup>. *J. Nucl. Med.* **1993**, *34* (7), 1127-1131.
301. Bergeron, R. J.; Wiegand, J.; Brittenham, G. M., HBED: the continuing development of a potential alternative to deferoxamine for iron-chelating therapy. *Blood* **1999**, *93* (1), 370-375.
302. Kostelnik, T. I.; Orvig, C., Radioactive Main Group and Rare Earth Metals for Imaging and Therapy. *Chem. Rev.* **2019**, *119* (2), 902-956.
303. Clarke, E. T.; Martell, A. E., Stabilities of the Fe(III), Ga(III) and In(III) chelates of N,N',N''-triazacyclononatriacetic acid. *Inorg. Chim. Acta* **1991**, *181* (2), 273-280.
304. Kubíček, V.; Havlíčková, J.; Kotek, J.; Tircsó, G.; Hermann, P.; Tóth, É.; Lukeš, I., Gallium(III) Complexes of DOTA and DOTA-Monoamide: Kinetic and Thermodynamic Studies. *Inorg. Chem.* **2010**, *49* (23), 10960-10969.
305. Ma, R.; Welch, M. J.; Reibenspies, J.; Martell, A. E., Stability of metal ion complexes of 1,4,7-tris(2-mercaptoethyl)-1,4,7-triazacyclonane (TACN-TM) and molecular structure of In(C<sub>12</sub>H<sub>24</sub>N<sub>3</sub>S<sub>3</sub>). *Inorg. Chim. Acta* **1995**, *236* (1), 75-82.
306. Prata, M. I. M.; Santos, A. C.; Geraldés, C. F. G. C.; Lima, J. J. P. d., Characterisation of <sup>67</sup>Ga<sup>3+</sup> complexes of triaza macrocyclic ligands: biodistribution and clearance studies. *Nucl. Med. Biol.* **1999**, *26* (6), 707-710.
307. Prata, M. I. M.; Santos, A. C.; Geraldés, C. F. G. C.; de Lima, J. J. P., Structural and in vivo studies of metal chelates of Ga(III) relevant to biomedical imaging. *J. Inorg. Biochem.* **2000**, *79* (1), 359-363.
308. P. André, J.; R. Maecke, H.; P. André, J.; Zehnder, M.; Macko, L.; G. Akyel, K., 1,4,7-Triazacyclononane-1-succinic acid-4,7-diacetic acid (NODASA): a new

- bifunctional chelator for radio gallium-labelling of biomolecules. *Chem. Commun.* **1998**, (12), 1301-1302.
309. Yang, C.-T.; Sreerama, S. G.; Hsieh, W.-Y.; Liu, S., Synthesis and Characterization of a Novel Macrocyclic Chelator with 3-Hydroxy-4-Pyrone Chelating Arms and Its Complexes with Medicinally Important Metals. *Inorg. Chem.* **2008**, *47* (7), 2719-2727.
310. de Sá, A.; Prata, M. I. M.; Geraldies, C. F. G. C.; André, J. P., Triaza-based amphiphilic chelators: Synthetic route, in vitro characterization and in vivo studies of their Ga(III) and Al(III) chelates. *J. Inorg. Biochem.* **2010**, *104* (10), 1051-1062.
311. Henze, M.; Schuhmacher, J.; Hipp, P.; Kowalski, J.; Becker, D. W.; Doll, J.; Mäcke, H. R.; Hofmann, M.; Debus, J.; Haberkorn, U., PET Imaging of Somatostatin Receptors Using [<sup>68</sup>Ga]DOTA-D-Phe<sup>1</sup>-Tyr<sup>3</sup>-Octreotide: First Results in Patients with Meningiomas. *J. Nucl. Med.* **2001**, *42* (7), 1053-1056.
312. Clarke, E. T.; Martell, A. E., Stabilities of trivalent metal ion complexes of the tetraacetate derivatives of 12-, 13- and 14-membered tetraazamacrocycles. *Inorg. Chim. Acta* **1991**, *190* (1), 37-46.
313. Heppeler, A.; Froidevaux, S.; Mäcke, H. R.; Jermann, E.; Béhé, M.; Powell, P.; Hennig, M., Radiometal-Labelled Macrocyclic Chelator-Derivatised Somatostatin Analogue with Superb Tumour-Targeting Properties and Potential for Receptor-Mediated Internal Radiotherapy. *Chem. Eur. J.* **1999**, *5* (7), 1974-1981.
314. Demmer, O.; Gourni, E.; Schumacher, U.; Kessler, H.; Wester, H.-J., PET Imaging of CXCR4 Receptors in Cancer by a New Optimized Ligand. *ChemMedChem* **2011**, *6* (10), 1789-1791.
315. Hennrich, U.; Benešová, M., [(68)Ga]Ga-DOTA-TOC: The First FDA-Approved (68)Ga-Radiopharmaceutical for PET Imaging. *Pharmaceuticals (Basel)* **2020**, *13* (3), 38.
316. Chauhan, A.; El-Khouli, R.; Waits, T.; Agrawal, R.; Siddiqui, F.; Tarter, Z.; Horn, M.; Weiss, H.; Oates, E.; Evers, B. M.; Anthony, L., Post FDA approval analysis of 200 gallium-68 DOTATATE imaging: A retrospective analysis in neuroendocrine tumor patients. *Oncotarget* **2020**, *11* (32), 3061-3068.
317. Ferreira, C. L.; Yapp, D. T.; Mandel, D.; Gill, R. K.; Boros, E.; Wong, M. Q.; Jurek, P.; Kiefer, G. E., <sup>68</sup>Ga small peptide imaging: comparison of NOTA and PCTA. *Bioconjugate Chem.* **2012**, *23* (11), 2239-2246.
318. Petrik, M.; Haas, H.; Dobrozemsky, G.; Lass-Flörl, C.; Helbok, A.; Blatzer, M.; Dietrich, H.; Decristoforo, C., <sup>68</sup>Ga-Siderophores for PET Imaging of Invasive Pulmonary Aspergillosis: Proof of Principle. *J. Nucl. Med.* **2010**, *51* (4), 639-645.
319. Petrik, M.; Umlaufova, E.; Raclavsky, V.; Palyzova, A.; Havlicek, V.; Haas, H.; Novy, Z.; Dolezal, D.; Hajduch, M.; Decristoforo, C., Imaging of Pseudomonas aeruginosa infection with Ga-68 labelled pyoverdine for positron emission tomography. *Sci. Rep.* **2018**, *8* (1), 15698.
320. Joaqui-Joaqui, M. A.; Pandey, M. K.; Bansal, A.; Raju, M. V. R.; Armstrong-Pavlik, F.; Dundar, A.; Wong, H. L.; DeGrado, T. R.; Pierre, V. C., Catechol-Based Functionalizable Ligands for Gallium-68 Positron Emission Tomography Imaging. *Inorg. Chem.* **2020**, *59* (17), 12025-12038.

321. Hart, M. M.; Adamson, R. H., Antitumor activity and toxicity of salts of inorganic group IIIa metals: aluminum, gallium, indium, and thallium. *Proc. Natl. Acad. Sci.* **1971**, 68 (7), 1623-1626.
322. Tajmir-Riahi, H.; Naoui, M.; Ahmad, R., A comparative study of calf-thymus DNA binding trivalent Al, Ga, Cr and Fe ions in aqueous solution. *Met. Ions Biol. Med.* **1992**, 2, 98-101.
323. Hedley, D. W.; Tripp, E. H.; Slowiaczek, P.; Mann, G. J., Effect of gallium on DNA synthesis by human T-cell lymphoblasts. *Cancer Res.* **1988**, 48 (11), 3014-3018.
324. Aoki, Y.; Lipsky, M. M.; Fowler, B. A., Alteration in protein synthesis in primary cultures of rat kidney proximal tubule epithelial cells by exposure to gallium, indium, and arsenite. *Toxicol. Appl. Pharmacol.* **1990**, 106 (3), 462-468.
325. Anghileri, L.; Thuvenot, P.; Brunotte, F.; Marchai, C.; Robert, J., Ionic competition and <sup>67</sup>Ga in vivo accumulation. *Nuklearmedizin* **1982**, 21 (03), 114-116.
326. Adamson, R.; Canellos, G.; Sieber, S., Studies on the antitumor activity of gallium nitrate (NSC-15200) and other group IIIa metal salts. *Cancer Chemother. Rep.* **1975**, 59 (3), 599-610.
327. Chitambar, C. R.; Matthaeus, W. G.; Antholine, W. E.; Graff, K.; O'Brien, W. J., Inhibition of leukemic HL60 cell growth by transferrin-gallium: effects on ribonucleotide reductase and demonstration of drug synergy with hydroxyurea. *Blood* **1988**, 72 (6), 1930-1936.
328. Berggren, M. M.; Burns, L. A.; Abraham, R. T.; Powis, G., Inhibition of protein tyrosine phosphatase by the antitumor agent gallium nitrate. *Cancer Res.* **1993**, 53 (8), 1862-1866.
329. Perchellet, E. M.; Ladesich, J. B.; Collery, P.; Perchellet, J.-P., Microtubule-disrupting effects of gallium chloride in vitro. *Anticancer Drugs* **1999**, 10 (5), 477-488.
330. Bedikian, A.; Valdivieso, M.; Bodey, G.; Burgess, M.; Benjamin, R.; Hall, S.; Freireich, E., Phase I clinical studies with gallium nitrate. *Cancer Treat. Rep.* **1978**, 62 (10), 1449-1453.
331. Hall, S. W.; Yeung, K.; Benjamin, R. S.; Stewart, D.; Valdivieso, M.; Bedikian, A. Y.; Loo, T. L., Kinetics of gallium nitrate, a new anticancer agent. *Clin. Pharmacol. Ther.* **1979**, 25 (1), 82-87.
332. Collery, P.; Millart, H.; Ferrand, O.; Jouet, J.; Dubois, J.; Barthes, G.; Pourny, C.; Pechery, C.; Choisy, H.; Cattan, A., Gallium chloride treatment of cancer patients after oral administration. A pilot study. *Chemotherapy* **1985**, 4, 1165-1166.
333. Collery, P.; Millart, H.; Lamiable, D.; Vistelle, R.; Rinjard, P.; Tran, G.; Gourdiere, B.; Cossart, C.; Bouana, J.; Pechery, C., Clinical pharmacology of gallium chloride after oral administration in lung cancer patients. *Anticancer Res.* **1989**, 9, 353-356.
334. Bernstein, L. R.; Tanner, T.; Godfrey, C.; Noll, B., Chemistry and pharmacokinetics of gallium maltolate, a compound with high oral gallium bioavailability. *Met.-Based Drugs* **2000**, 7 (1), 33-47.
335. Warrell, R.; Bockman, R.; Coonley, C.; Isaacs, M.; Staszewski, H., Gallium nitrate inhibits calcium resorption from bone and is effective treatment for cancer-related hypercalcemia. *J. Clin. Invest.* **1984**, 73 (5), 1487-1490.

336. Leyland-Jones, B., Treatment of cancer-related hypercalcemia: the role of gallium nitrate. *Semin. Oncol.* **2003**, *30* (2 Suppl 5), 13-19.
337. Zagzag, J.; Hu, M. I.; Fisher, S. B.; Perrier, N. D., Hypercalcemia and cancer: Differential diagnosis and treatment. *CA-Cancer J. Clin.* **2018**, *68* (5), 377-386.
338. Chitambar, C. R., Gallium-containing anticancer compounds. *Future Med. Chem.* **2012**, *4* (10), 1257-1272.
339. Gallium Nitrate for Acute Treatment of Cancer-Related Hypercalcemia. *Ann. Intern. Med.* **1988**, *108* (5), 669-674.
340. FDA Approves Ganite for Hypercalcemia. *Onco. Times* **2003**, *25* (20), 24.
341. Chitambar, C. R., Medical Applications and Toxicities of Gallium Compounds. *Int. J. Environ. Res. Public Health* **2010**, *7* (5), 2337-2361.
342. Pandey, A.; Savino, C.; Ahn, S. H.; Yang, Z.; Van Lanen, S. G.; Boros, E., Theranostic Gallium Siderophore Ciprofloxacin Conjugate with Broad Spectrum Antibiotic Potency. *J. Med. Chem.* **2019**, *62* (21), 9947-9960.
343. Sanderson, T. J.; Black, C. M.; Southwell, J. W.; Wilde, E. J.; Pandey, A.; Herman, R.; Thomas, G. H.; Boros, E.; Duhme-Klair, A.-K.; Routledge, A., A Salmochelin S4-Inspired Ciprofloxacin Trojan Horse Conjugate. *ACS Infect. Dis.* **2020**, *6* (9), 2532-2541.
344. Arivett, B. A.; Fiester, S. E.; Ohneck, E. J.; Penwell, W. F.; Kaufman, C. M.; Relich, R. F.; Actis, L. A., Antimicrobial Activity of Gallium Protoporphyrin IX against *Acinetobacter baumannii* Strains Displaying Different Antibiotic Resistance Phenotypes. *Antimicrob. Agents Chemother.* **2015**, *59* (12), 7657-7665.
345. Goss, C. H.; Kaneko, Y.; Khuu, L.; Anderson, G. D.; Ravishankar, S.; Aitken, M. L.; Lechtzin, N.; Zhou, G.; Czyz, D. M.; McLean, K.; Olakanmi, O.; Shuman, H. A.; Teresi, M.; Wilhelm, E.; Caldwell, E.; Salipante, S. J.; Hornick, D. B.; Siehnel, R. J.; Becker, L.; Britigan, B. E.; Singh, P. K., Gallium disrupts bacterial iron metabolism and has therapeutic effects in mice and humans with lung infections. *Sci. Trans. Med.* **2018**, *10* (460), eaat7520.
346. Banin, E.; Lozinski, A.; Brady, K. M.; Berenshtein, E.; Butterfield, P. W.; Moshe, M.; Chevion, M.; Greenberg, E. P.; Banin, E., The potential of desferrioxamine-gallium as an anti-*Pseudomonas* therapeutic agent. *Proc. Natl. Acad. Sci.* **2008**, *105* (43), 16761-16766.
347. Huayhuaz, J. A. A.; Vitorino, H. A.; Campos, O. S.; Serrano, S. H. P.; Kaneko, T. M.; Espósito, B. P., Desferrioxamine and desferrioxamine-caffeine as carriers of aluminum and gallium to microbes via the Trojan Horse Effect. *J. Trace Elem. Med. Biol.* **2017**, *41*, 16-22.
348. Ross-Gillespie, A.; Weigert, M.; Brown, S. P.; Kümmerli, R., Gallium-mediated siderophore quenching as an evolutionarily robust antibacterial treatment. *Evol. Med. Public Health* **2014**, *2014* (1), 18-29.
349. Ecker, D. J.; Matzanke, B. F.; Raymond, K. N., Recognition and transport of ferric enterobactin in *Escherichia coli*. *J. Bacteriol.* **1986**, *167* (2), 666-673.
350. JOH, T. H.; HWANG, O., Dopamine  $\beta$ -Hydroxylase: Biochemistry and Molecular Biology. *Ann. N.Y. Acad. Sci.* **1987**, *493* (1), 342-350.

351. Wise, R. A., Dopamine, learning and motivation. *Nat. Rev. Neurosci.* **2004**, *5* (6), 483-494.
352. Berke, J. D.; Hyman, S. E., Addiction, dopamine, and the molecular mechanisms of memory. *Neuron* **2000**, *25* (3), 515-532.
353. Levy, F., The dopamine theory of attention deficit hyperactivity disorder (ADHD). *Aust. N. Z. J. Psychiatry* **1991**, *25* (2), 277-283.
354. Delgado, P. L.; Moreno, F. A., Role of norepinephrine in depression. *Journal of Clinical Psychiatry* **2000**, *61*, 5-12.
355. Thomas D. Geraciotti, J., M.D. ; Dewleen G. Baker, M.D. ; Nosakhare N. Ekhatior, M.S. ; Scott A. West, M.D. ; Kelly K. Hill, M.D. ; Ann B. Bruce, M.D. ; Dennis Schmidt, Ph.D. ; Barbara Rounds-Kugler, R.N. ; Rachel Yehuda, Ph.D. ; Paul E. Keck, J., M.D. , and; John W. Kasckow, M.D., Ph.D., CSF Norepinephrine Concentrations in Posttraumatic Stress Disorder. *Am J. Psychiatry* **2001**, *158* (8), 1227-1230.
356. Tolosa, E.; Martí, M. J.; Valldeoriola, F.; Molinuevo, J. L., History of levodopa and dopamine agonists in Parkinson's disease treatment. *Neurology* **1998**, *50* (6 Suppl 6), S2-S10.
357. Borgman, R. J.; McPhillips, J. J.; Stitzel, R. E.; Goodman, I. J., Synthesis and pharmacology of centrally acting dopamine derivatives and analogs in relation to Parkinson's disease. *J. Med. Chem.* **1973**, *16* (6), 630-633.
358. Felix, A. M.; Winter, D. P.; Wang, S.-S.; Kulesha, I. D.; Pool, W. R.; Hane, D. L.; Sheppard, H., Synthesis and antireserpine activity of peptides of L-Dopa. *J. Med. Chem.* **1974**, *17* (4), 422-426.
359. Freitas, M. E.; Ruiz-Lopez, M.; Fox, S. H., Novel Levodopa Formulations for Parkinson's Disease. *CNS Drugs* **2016**, *30* (11), 1079-1095.
360. Davie, C. A., A review of Parkinson's disease. *Br. Med. Bull.* **2008**, *86* (1), 109-127.
361. Nutt, J. G.; Woodward, W. R.; Anderson, J. L., The effect of carbidopa on the pharmacokinetics of intravenously administered levodopa: The mechanism of action in the treatment of parkinsonism. *Ann. Neurol.* **1985**, *18* (5), 537-543.
362. Martorana, A.; Koch, G., "Is dopamine involved in Alzheimer's disease?". *Front. Aging Neurosci.* **2014**, *6* (252).
363. Nam, E.; Derrick, J. S.; Lee, S.; Kang, J.; Han, J.; Lee, S. J. C.; Chung, S. W.; Lim, M. H., Regulatory Activities of Dopamine and Its Derivatives toward Metal-Free and Metal-Induced Amyloid- $\beta$  Aggregation, Oxidative Stress, and Inflammation in Alzheimer's Disease. *ACS Chem. Neurosci.* **2018**, *9* (11), 2655-2666.
364. Simons, K. J.; Simons, F. E. R., Epinephrine and its use in anaphylaxis: current issues. *Curr. Opin. Allergy Clin. Immunol.* **2010**, *10* (4), 354-361.
365. Sneader, W., The discovery and synthesis of epinephrine. *Drug news & perspectives* **2001**, *14* (8), 491-494.
366. Lieberman, P., Use of epinephrine in the treatment of anaphylaxis. *Curr. Opin. Allergy Clin. Immunol.* **2003**, *3* (4), 313-318.

367. Krejci, V.; Hildebrand, L. B.; Sigurdsson, G. H., Effects of epinephrine, norepinephrine, and phenylephrine on microcirculatory blood flow in the gastrointestinal tract in sepsis. *Crit. Care. Med.* **2006**, *34* (5), 1456-1463.
368. De Backer, D.; Biston, P.; Devriendt, J.; Madl, C.; Chochrad, D.; Aldecoa, C.; Brasseur, A.; Defrance, P.; Gottignies, P.; Vincent, J.-L., Comparison of Dopamine and Norepinephrine in the Treatment of Shock. *N. Engl. J. Med.* **2010**, *362* (9), 779-789.
369. Day, N. P. J.; Phu, N. H.; Mai, N. T. H.; Bethell, D. B.; Chau, T. T. H.; Loc, P. P.; Van Chuong, L.; Sinh, D. X.; Solomon, T.; Haywood, G.; Hien, T. T.; White, N. J., Effects of dopamine and epinephrine infusions on renal hemodynamics in severe malaria and severe sepsis. *Crit. Care. Med.* **2000**, *28* (5), 1353-1362.
370. Ahmad, I.; Ahmed, S.; Anwar, Z.; Sheraz, M. A.; Sikorski, M., Photostability and Photostabilization of Drugs and Drug Products. *Int. J. Photoenergy* **2016**, *2016*, 8135608.
371. Hansen, L. D.; Lewis, E. A.; Eatough, D. J.; Bergstrom, R. G.; DeGraft-Johnson, D., Kinetics of drug decomposition by heat conduction calorimetry. *Pharm. Res.* **1989**, *6* (1), 20-27.
372. Won, C. M., Kinetics of Degradation of Levothyroxine in Aqueous Solution and in Solid State. *Pharm. Res.* **1992**, *9* (1), 131-137.
373. Mälkki, L.; Tammilehto, S., Decomposition of salbutamol in aqueous solutions. I. The effect of pH, temperature and drug concentration. *Int. J. Pharm.* **1990**, *63* (1), 17-22.
374. Bors, W.; Saran, M.; Michel, C.; Lengfelder, E.; Fuchs, C.; Spöttl, R., Pulse-radiolytic Investigations of Catechols and Catecholamines. *Int. J. Radiat. Biol. Relat. Stud. Phys., Chem. Med.* **1975**, *28* (4), 353-371.
375. McCord, J. M.; Fridovich, I., Superoxide Dismutase: An Enzymic Function For Erythrocyte (Hemocytin). *J. Biol. Chem.* **1969**, *244* (22), 6049-6055.
376. Misra, H. P.; Fridovich, I., The Role of Superoxide Anion in the Autoxidation of Epinephrine and a Simple Assay for Superoxide Dismutase. *J. Biol. Chem.* **1972**, *247* (10), 3170-3175.
377. Maier, G. P.; Bernt, C. M.; Butler, A., Catechol oxidation: considerations in the design of wet adhesive materials. *Biomater. Sci.* **2018**, *6* (2), 332-339.
378. Roberts, N. B.; Higgins, G.; Sargazi, M., A study on the stability of urinary free catecholamines and free methyl-derivatives at different pH, temperature and time of storage. *Clinical chemistry and laboratory medicine* **2010**, *48* (1), 81-7.
379. Walaas, E., The Chemical Transformation of the Catecholamines Induced by UV Irradiation. *Photochem. Photobiol.* **1963**, *2* (1), 9-24.
380. Mol, N. J. d.; Henegouwen, G. M. J. B. v.; Gerritsma, K. W., Photochemical Decomposition of Catecholamines—II. The Extend of Aminochrome Formation from Adrenaline, Isoprenaline and Noradrenaline Induced by Ultraviolet Light. *Photochem. Photobiol.* **1979**, *29* (3), 479-482.
381. Glickman, R.; Berry, J. C.; Kumar, N., Effect of Storage Temperature and Antioxidant Concentration on Catecholamine Stability. *Invest. Ophthalmol. Visual Sci.* **2013**, *54* (15), 6332-6332.
382. Miki, K.; Sudo, A., Effect of Urine pH, Storage Time, and Temperature on Stability of Catecholamines, Cortisol, and Creatinine. *Clin. Chem.* **1998**, *44* (8), 1759-1762.

383. Sánchez-Rivera, A. E.; Corona-Avenidaño, S.; Alarcón-Angeles, G.; Rojas-Hernández, A.; Ramírez-Silva, M. T.; Romero-Romo, M. A., Spectrophotometric study on the stability of dopamine and the determination of its acidity constants. *Spectrochim. Acta, Part A* **2003**, *59* (13), 3193-3203.
384. Zheng, J.; Mandal, R.; Wishart, D. S., A sensitive, high-throughput LC-MS/MS method for measuring catecholamines in low volume serum. *Anal. Chim. Acta* **2018**, *1037*, 159-167.
385. Hasegawa, T.; Wada, K.; Hiyama, E.; Masujima, T., Pretreatment and one-shot separating analysis of whole catecholamine metabolites in plasma by using LC/MS. *Anal. Bioanal. Chem.* **2006**, *385* (5), 814-820.
386. Church, W. H.; Hu, S. S.; Henry, A. J., Thermal degradation of injectable epinephrine. *Am. J. Emerg. Med.* **1994**, *12* (3), 306-309.
387. Shen, Y.; Ye, M. Y., Determination of the Stability of Dopamine in Aqueous Solutions by High Performance Liquid Chromatography. *J. Liq. Chromatogr.* **1994**, *17* (7), 1557-1565.
388. Ghanayem, N. S.; Yee, L.; Nelson, T.; Wong, S.; Gordon, J. B.; Marcdante, K.; Rice, T. B., Stability of dopamine and epinephrine solutions up to 84 hours. *Pediatr. Crit. Care Med.* **2001**, *2* (4), 315-317.
389. Tremblay, M.; Lessard, M. R.; Trepanier, C. A.; Nicole, P. C.; Nadeau, L.; Turcotte, G., Stability of norepinephrine infusions prepared in dextrose and normal saline solutions. *Can. J. Anesth.* **2008**, *55* (3), 163.
390. Carrera, V.; Sabater, E.; Vilanova, E.; Sogorb, M. A., A simple and rapid HPLC–MS method for the simultaneous determination of epinephrine, norepinephrine, dopamine and 5-hydroxytryptamine: Application to the secretion of bovine chromaffin cell cultures. *J. Chromatogr. B* **2007**, *847* (2), 88-94.
391. Larson, P. O.; Ragi, G.; Swandby, M.; Darcey, B.; Polzin, G.; Carey, P., Stability of Buffered Lidocaine and Epinephrine Used for Local Anesthesia. *J. Dermatol. Surg. Oncol.* **1991**, *17* (5), 411-414.
392. Stepensky, D.; Chorny, M.; Dabour, Z.; Schumacher, I., Long-term stability study of L-adrenaline injections: Kinetics of sulfonation and racemization pathways of drug degradation. *J. Pharm. Sci.* **2004**, *93* (4), 969-980.
393. Backe-Hansen, K.; Aarnes, E. D.; Venneröd, A. M.; Jensen, K. B., On the Stability of Adrenaline in Injections: A Comparison of Chemical and Bioassay Methods. *J. Pharm. Pharmacol.* **2011**, *15* (1), 804-809.
394. Willemsen, J. J.; Ross, H. A.; Jacobs, M. C.; Lenders, J. W.; Thien, T.; Swinkels, L. M.; Benraad, T. J., Highly sensitive and specific HPLC with fluorometric detection for determination of plasma epinephrine and norepinephrine applied to kinetic studies in humans. *Clin. Chem.* **1995**, *41* (10), 1455-1460.
395. Musso, N. R.; Vergassola, C.; Pende, A.; Lotti, G., Reversed-phase HPLC separation of plasma norepinephrine, epinephrine, and dopamine, with three-electrode coulometric detection. *Clin. Chem.* **1989**, *35* (9), 1975-1977.
396. Wu, D.; Xie, H.; Lu, H.; Li, W.; Zhang, Q., Sensitive determination of norepinephrine, epinephrine, dopamine and 5-hydroxytryptamine by coupling HPLC with

- [Ag(HIO<sub>6</sub>)<sub>2</sub>]<sup>5-</sup>–luminol chemiluminescence detection. *Biomed. Chromatogr.* **2016**, *30* (9), 1458-1466.
397. Kilts, C. D.; Anderson, C. M., The simultaneous quantification of dopamine, norepinephrine and epinephrine in micropunched rat brain nuclei by on-line trace enrichment HPLC with electrochemical detection: Distribution of catecholamines in the limbic system. *Neurochem. Int.* **1986**, *9* (3), 437-445.
398. Mishra, A. K.; Mishra, A.; Chattopadhyay, P., A reversed-phase high performance liquid chromatographic method for determination of Epinephrine in pharmaceutical formulation. *Arch. Appl. Sci. Res.* **2010**, *2*, 251-256.
399. Szulczewski, D. H.; Hong, W.-h., Epinephrine. In *Analytical Profiles of Drug Substances*, Florey, K., Ed. Academic Press: 1978; Vol. 7, pp 193-229.
400. Rawas-Qalaji, M.; Simons, F. E. R.; Collins, D.; Simons, K. J., Long-term stability of epinephrine dispensed in unsealed syringes for the first-aid treatment of anaphylaxis. *Ann. Allergy, Asthma, Immunol.* **2009**, *102* (6), 500-503.
401. Otto, C. W.; Yakaitis, R. W.; Blitt, C. D., Mechanism of action of epinephrine in resuscitation from asphyxial arrest. *Crit. Care. Med.* **1981**, *9* (4), 321-324.
402. Ellis, A. K.; Day, J. H., The role of epinephrine in the treatment of anaphylaxis. *Curr. Allergy Asthma Rep.* **2003**, *3* (1), 11-14.
403. Green, L. C., Anaphylactic shock and its implication for nurses. *Accid. Emerg. Nurs.* **1998**, *6* (2), 103-105.
404. Brustugun, J.; Kristensen, S.; Hjorth Tønnesen, H., Photostability of epinephrine - the influence of bisulfite and degradation products. *Pharmazie* **2004**, *59* (6), 457-463.
405. Heacock, R., The chemistry of adrenochrome and related compounds. *Chem. Rev.* **1959**, *59* (2), 181-237.
406. Shaker, M.; Bean, K.; Verdi, M., Economic evaluation of epinephrine auto-injectors for peanut allergy. *Ann. Allergy, Asthma, Immunol.* **2017**, *119* (2), 160-163.
407. Grubstein, B.; Milano, E., Stabilization of epinephrine in a local anesthetic injectable solution using reduced levels of sodium metabisulfite and edta. *Drug Dev. Ind. Pharm.* **1992**, *18* (14), 1549-1566.
408. Simons, F. E. R., First-aid treatment of anaphylaxis to food: Focus on epinephrine. *Journal of Allergy and Clinical Immunology* **2004**, *113* (5), 837-844.
409. Usach, I.; Martinez, R.; Festini, T.; Peris, J.-E., Subcutaneous Injection of Drugs: Literature Review of Factors Influencing Pain Sensation at the Injection Site. *Adv. Ther.* **2019**, *36* (11), 2986-2996.
410. Korenblat, P.; Lundie, M. J.; Dankner, R. E.; Day, J. H. In *A retrospective study of epinephrine administration for anaphylaxis: how many doses are needed?*, Allergy and asthma proceedings, OceanSide Publications; 1999: 1999; pp 383-386.
411. Creveling, C. R.; Daly, J. W.; Tokuyama, T.; Witkop, B., Labile lipophilic derivatives of norepinephrine capable of crossing the blood-brain barrier. *Experientia* **1969**, *25* (1), 26-27.
412. Borgman, R. J.; Baldessarini, R. J.; Walton, K. G., Diester derivatives as apomorphine prodrugs. *J. Med. Chem.* **1976**, *19* (5), 717-719.
413. Baldessarini, R. J.; Kula, N. S.; Walton, K. G.; Borgman, R. J., Hydrolysis of diester prodrugs of apomorphine. *Biochem. Pharmacol.* **1977**, *26* (19), 1749-1756.

414. Kuruma, I.; Bartholini, G.; Tissot, R.; Pletscher, A., The metabolism of L-3-O-methyldopa, a precursor of dopa in man. *Clin. Pharmacol. Ther.* **1971**, *12* (4), 678-682.
415. Saari, W. S.; Freedman, M. B.; Hartman, R. D.; King, S. W.; Raab, A. W.; Randall, W. C.; Engelhardt, E. L.; Hirschmann, R.; Rosegay, A., Synthesis and antihypertensive activity of some ester progenitors of methyldopa. *J. Med. Chem.* **1978**, *21* (8), 746-753.
416. Vickers, S.; Duncan, C. A.; White, S. D.; Breault, G. O.; Royds, R. B.; de Schepper, P. J.; Tempero, K. F., Evaluation of succinimidoethyl and pivaloyloxyethyl esters as progenitors of methyldopa in man, rhesus monkey, dog, and rat. *Drug Metab. Dispos.* **1978**, *6* (6), 640-646.
417. Lai, C. M.; Mason, W. D., New compounds: Synthesis of alkyl esters of D,L-dopa. *J. Pharm. Sci.* **1973**, *62* (3), 510-511.
418. Tejani-Butt, S. M.; Hauptmann, M.; D'Mello, A.; Frazer, A.; Marcoccia, J. M.; Brunswick, D. J., Evaluation of mono- and dibenzoyl esters of dopamine as potential prodrugs for dopamine in the central nervous system. *Naunyn-Schmiedeberg's Arch. Pharmacol.* **1988**, *338* (5), 497-503.
419. Bodor, N.; Sloan, K. B.; Higuchi, T.; Sasahara, K., Improved delivery through biological membranes. 4. Prodrugs of L-dopa. *J. Med. Chem.* **1977**, *20* (11), 1435-1445.
420. Cooper, D. R.; Marrel, C.; Testa, B.; van de Waterbeemd, H.; Quinn, N.; Jenner, P.; Marsden, C. D., L-Dopa Methyl Ester—A Candidate for Chronic Systemic Delivery of L-Dopa in Parkinson's Disease. *Clin. Neuropharmacol.* **1984**, *7* (1), 89-98.
421. Marrel, C.; Boss, G.; Testa, B.; Van de Waterbeemd, H.; Cooper, D., L-DOPA esters as potential prodrugs. II: Chemical and enzymatic hydrolysis. *Eur. J. Med. Chem.* **1985**, *20* (5), 467-470.
422. Garzon-Aburbeh, A.; Poupaert, J. H.; Claesen, M.; Dumont, P., A lymphotropic prodrug of L-dopa: synthesis, pharmacological properties and pharmacokinetic behavior of 1,3-dihexadecanoyl-2-[(S)-2-amino-3-(3,4-dihydroxyphenyl)propanoyl]propane-1,2,3-triol. *J. Med. Chem.* **1986**, *29* (5), 687-691.
423. Zhou, T.; Hider, R. C.; Jenner, P.; Campbell, B.; Hobbs, C. J.; Rose, S.; Jairaj, M.; Tayarani-Binazir, K. A.; Syme, A., Design, synthesis and biological evaluation of l-dopa amide derivatives as potential prodrugs for the treatment of Parkinson's disease. *Eur. J. Med. Chem.* **2010**, *45* (9), 4035-4042.
424. Atlas, D., DopAmide: Novel, Water-Soluble, Slow-Release l-dihydroxyphenylalanine (l-DOPA) Precursor Moderates l-DOPA Conversion to Dopamine and Generates a Sustained Level of Dopamine at Dopaminergic Neurons. *CNS Neurosci. Ther.* **2016**, *22* (6), 461-467.
425. De Caro, V.; Sutura, F. M.; Gentile, C.; Tutone, M.; Livrea, M. A.; Almerico, A. M.; Cannizzaro, C.; Giannola, L. I., Studies on a new potential dopaminergic agent: in vitro BBB permeability, in vivo behavioural effects and molecular docking evaluation. *J. Drug Targeting* **2015**, *23* (10), 910-925.
426. Giannola, L. I.; De Caro, V.; Giandalia, G.; Siragusa, M. G.; Lamartina, L., Synthesis and in vitro studies on a potential dopamine prodrug. *Die Pharmazie* **2008**, *63* (10), 704-10.

427. Pinnen, F.; Cacciatore, I.; Cornacchia, C.; Mollica, A.; Sozio, P.; Cerasa, L. S.; Iannitelli, A.; Fontana, A.; Nasuti, C.; Di Stefano, A., CNS delivery of l-dopa by a new hybrid glutathione–methionine peptidomimetic prodrug. *Amino Acids* **2012**, *42* (1), 261-269.
428. Peura, L.; Malmioja, K.; Huttunen, K.; Leppänen, J.; Hämäläinen, M.; Forsberg, M. M.; Rautio, J.; Laine, K., Design, Synthesis and Brain Uptake of LAT1-Targeted Amino Acid Prodrugs of Dopamine. *Pharm. Res.* **2013**, *30* (10), 2523-2537.
429. Denora, N.; Laquintana, V.; Lopedota, A.; Serra, M.; Dazzi, L.; Biggio, G.; Pal, D.; Mitra, A. K.; Latrofa, A.; Trapani, G.; Liso, G., Novel L-Dopa and Dopamine Prodrugs Containing a 2-Phenyl-imidazopyridine Moiety. *Pharm. Res.* **2007**, *24* (7), 1309-1324.
430. Giorgioni, G.; Claudi, F.; Ruggieri, S.; Ricciutelli, M.; Palmieri, G. F.; Stefano, A. D.; Sozio, P.; Cerasa, L. S.; Chiavaroli, A.; Ferrante, C.; Orlando, G.; Glennon, R. A., Design, synthesis, and preliminary pharmacological evaluation of new imidazolinones as l-DOPA prodrugs. *Bioorg. Med. Chem.* **2010**, *18* (5), 1834-1843.
431. Michaux, R.; Verly, W. G., Action cataleptique des éthers méthyliques des mono - et polyphenolamines. *Life Sci.* **1963**, *2* (3), 175-183.
432. Hussain, A.; Truelove, J., Prodrug approaches to enhancement of physicochemical properties of drugs IV: novel epinephrine prodrug. *J. Pharm. Sci.* **1976**, *65* (10), 1510-1512.
433. Huttunen, K. M., Identification of human, rat and mouse hydrolyzing enzymes bioconverting amino acid ester prodrug of ketoprofen. *Bioorg. Chem.* **2018**, *81*, 494-503.
434. Niemi, R.; Turhanen, P.; Vepsäläinen, J.; Taipale, H.; Järvinen, T., Bisphosphonate prodrugs: synthesis and in vitro evaluation of alkyl and acyloxymethyl esters of etidronic acid as bioreversible prodrugs of etidronate. *Eur. J. Pharm. Sci.* **2000**, *11* (2), 173-180.
435. Karpishin, T. B.; Stack, T. D. P.; Raymond, K. N., Stereoselectivity in chiral iron(III) and gallium(III) tris(catecholate) complexes effected by nonbonded weakly polar interactions. *J. Am. Chem. Soc.* **1993**, *115* (14), 6115-6125.
436. Kunkely, H.; Vogler, A., Optical properties of boron, gallium and gold complexes with salen ligands. Emission from intraligand excited states under ambient conditions. *Inorg. Chim. Acta* **2001**, *321* (1), 171-174.
437. Brumaghim, J. L.; Raymond, K. N., What Should Be Impossible: Resolution of the Mononuclear Gallium Coordination Complex, Tris(benzohydroxamato)gallium(III). *J. Am. Chem. Soc.* **2003**, *125* (40), 12066-12067.
438. Jackson, G. E., Aluminium, gallium and indium in biological fluids—a computer model of blood plasma. *Polyhedron* **1990**, *9* (2), 163-170.
439. Loomis, L. D.; Raymond, K. N., Kinetics of Gallium Removal from Transferrin and Thermodynamics of Gallium-Binding by Sulfonated Tricatechol Ligands. *J. Coord. Chem.* **1991**, *23* (1-4), 361-387.
440. Todd, P. A.; Fitton, A., Gallium Nitrate. *Drugs* **1991**, *42* (2), 261-273.
441. Seidman, A. D.; Scher, H. I.; Heinemann, M. H.; Bajorin, D. F.; Sternberg, C. N.; Dershow, D. D.; Silverberg, M.; Bosl, G. J., Continuous infusion gallium nitrate for

- patients with advanced refractory urothelial tract tumors. *Cancer* **1991**, 68 (12), 2561-2565.
442. Gómez, M.; Sánchez, D. J.; Domingo, J. L.; Corbella, J., Developmental toxicity evaluation of gallium nitrate in mice. *Arch. Toxicol.* **1992**, 66 (3), 188-192.
443. Straub, A. E.; Seitz, W. R., Fiber-optic temperature sensor based on the temperature dependence of the pKa of Tris. *Anal. Chem.* **1993**, 65 (10), 1491-1492.
444. Hacht, B., Gallium (III) ion hydrolysis under physiological conditions. *Bull. Korean Chem. Soc.* **2008**, 29 (2), 372-376.
445. García, C. R.; Angelé-Martínez, C.; Wilkes, J. A.; Wang, H. C.; Battin, E. E.; Brumaghim, J. L., Prevention of iron- and copper-mediated DNA damage by catecholamine and amino acid neurotransmitters, l-DOPA, and curcumin: metal binding as a general antioxidant mechanism. *Dalton Trans.* **2012**, 41 (21), 6458-6467.
446. Rehmann, J. P.; Barton, J. K., Proton NMR studies of tris (phenanthroline) metal complexes bound to oligonucleotides: characterization of binding modes. *Biochemistry* **1990**, 29 (7), 1701-1709.
447. Babushkin, D. E.; Semikolenova, N. V.; Zakharov, V. A.; Talsi, E. P., Mechanism of dimethylzirconocene activation with methylaluminumoxane: NMR monitoring of intermediates at high Al/Zr ratios. *Macromol. Chem. Phys.* **2000**, 201 (5), 558-567.
448. Ferreira, H.; Conradie, M. M.; Conradie, J., Cyclic voltammetry data of polypyridine ligands and Co(II)-polypyridine complexes. *Data Brief* **2019**, 22, 436-445.